Pathogen-Specific Adaptations to Conserved Signaling Pathways in *Cryptococcus neoformans*

by

Kyla Selvig Ost

University Program of Genetics and Genomics
Duke University

Date:_____

Approved:

_____
J. Andrew Alspaugh, Supervisor

_____
Joseph Heitman

_____
Meta Kuehn

_____
William Steinbach

_____
John Perfect, Chair

_____
Dennis Thiele

Dissertation submitted in partial fulfillment of
the requirements for the degree of Doctor of Philosophy
in the University Program in Genetics and Genomics
in the Graduate School
of Duke University

2016

ABSTRACT

Pathogen-Specific Adaptations to Conserved Signaling Pathways in *Cryptococcus neoformans*

by

Kyla Selvig Ost

University Program of Genetics and Genomics
Duke University

Date:_____

Approved:

_____
J. Andrew Alspaugh, Supervisor

_____
Joseph Heitman

_____
Meta Kuehn

_____
William Steinbach

_____
John Perfect, Chair

_____
Dennis Thiele

An abstract of a dissertation submitted in partial
fulfillment of the requirements for the degree
of Doctor of Philosophy in
the University Program in Genetics and Genomics
in the Graduate School of
Duke University

2016

Abstract

Cryptococcus neoformans is an opportunistic fungal pathogen that causes significant disease worldwide. Even though this fungus has not evolved specifically to cause human disease, it has a remarkable ability to adapt to many different environments within its infected host. *C. neoformans* adapts by utilizing conserved eukaryotic and fungal-specific signaling pathways to sense and respond to stresses within the host. Upon infection, two of the most significant environmental changes this organism experiences are elevated temperature and high pH.

Conserved Rho and Ras family GTPases are central regulators of thermotolerance in *C. neoformans*. Many GTPases require prenylation to associate with cellular membranes and function properly. Using molecular genetic techniques, microscopy, and infection models, I demonstrated that the prenyltransferase, geranylgeranyl transferase I (GGTase I) is required for thermotolerance and pathogenesis. Using fluorescence microscopy, I found that only a subset of conserved GGTase I substrates requires this enzyme for membrane localization. Therefore, the *C. neoformans* GGTase I may recognize its substrate in a slightly different manner than other eukaryotic organisms.

The alkaline response transcription factor, Rim101, is a central regulator of stress-response genes important for adapting to the host environment. In particular, Rim101 regulates cell surface alterations involved in immune avoidance. In other fungi, Rim101 is activated by alkaline pH through a conserved signaling pathway, but this pathway had yet been characterized in *C. neoformans*. Using molecular genetic

techniques, I identified and analyzed the conserved members of the Rim pathway. I found that it was only partially conserved in *C. neoformans,* missing the components that sense pH and initiate pathway activation. Using a genetic screen, I identified a novel Rim pathway component named Rra1. Structural prediction and genetic epistasis experiments suggest that Rra1 may serve as the Rim pathway pH sensor in *C. neoformans* and other related basidiomycete fungi.

To explore the relevance of Rim pathway signaling in the interaction of *C neoformans* with its host, I characterized the Rim101-regulated cell wall changes that prevent immune detection. Using HPLC, enzymatic degradation, and cell wall stains, I found that the *rim101*Δ mutation resulted in increased cell wall chitin exposure. In vitro co-culture assays demonstrated that increased chitin exposure is associated with enhanced activation of macrophages and dendritic cells. To further test this association, I demonstrated that other mutant strains with increased chitin exposure induce macrophage and dendritic cell responses similar to *rim101*Δ. We used primary macrophages from mutant mouse lines to demonstrate that members of both the Toll-like receptor and C-type lectin receptor families are involved in detecting strains with increased chitin exposure. Finally, in vivo immunological experiments demonstrated that the *rim101*Δ strain induced a global inflammatory immune response in infected mouse lungs, expanding upon our previous in vivo *rim101*Δ studies. These results demonstrate that cell wall organization largely determines how fungal cells are detected by the immune system.

Dedication

To Ryan, my greatest genetics experiment.

Contents

Abstract iv

List of Tables xii

List of Figures xiii

Acknowledgements xvi

1. Introduction 1

1.1 Cryptococcus neoformans: opportunistic fungal pathogen 1

1.2 Regulation of C. neoformans GTPases: potential drug targets 4

1.3 pH Response Pathways in Fungi: Adapting to Host-derived and Environmental Signals 6

1.3.1 Introduction 6

1.3.2 The Rim101/PacC transcription factors mediate pH responses in *Aspergillus nidulans* and *Saccharomyces cerevisiae* 7

1.3.3 *Candida albicans* 14

1.3.4 *Cryptococcus neoformans* 17

1.3.5 Other signaling pathways involved in the fungal pH response 22

1.4 The fungal cell wall 24

1.5 Summary of the work included in this thesis 26

1.5.1 Characterizing the *C. neoformans* geranylgeranyl transferase I 27

1.5.2 Mapping the *C. neoformans* alkaline response Rim pathway 28

1.5.3 Characterizing Rim101-regulated cell surface changes required for immune avoidance. 29

2. Restricted substrate specificity for the geranylgeranyl transferase-I enzyme in *Cryptococcus neoformans*: implications for virulence 32

2.1 Introduction 32

2.2 Materials and Methods 35

2.2.1 Strains, Media, and Growth conditions 35

2.2.2 Molecular biology 37

2.2.3 Microscopy 40

2.2.4 Animal and Macrophage experiments 40

2.3 Results 41

2.3.1 Identification of the *C. neoformans* Geranylgeranyltransferase-I 41

2.3.2 Cryptococcus neoformans Geranylgeranyltransferase-I is involved in high temperature growth and morphogenesis 42

2.3.3 *C. neoformans* Ggtase-I is required for virulence 44

2.3.4 Analysis of predicted geranylgeranyltransferase I substrates 46

2.3.5 Cdc42 function is dependent on prenylation 49

2.3.6 The cdc43Δ mutant does not exhibit cell wall defects 50

2.3.7 The cdc43Δ mutant has a mating defect 52

2.3.8 The cdc43Δ mutant is more susceptible to farnesyltransferase inhibitors. 53

2.4 Discussion 54

2.4.1 C. neoformans Ggtase-I Substrates 56

2.4.2 C. neoformans Ggtase-I role in mating 60

2.4.3 Disrupting *C. neoformans* Ggtase-I increases Ftase inhibitor efficacy 61

3. The *Cryptococcus neoformans* alkaline response pathway: Identification of novel a Rim pathway activator 63

3.1 Introduction 63

3.2 Results 67

3.2.1 Neutral/alkaline pH induces Rim101 proteolytic cleavage and nuclear localization. 67

3.2.3 Rim101 is not activated by high NaCl or iron limitation. 70

3.2.4 Identification and Characterization of *C. neoformans* Rim13 and Rim23 orthologs..... 70

3.2.5 ESCRT involvement in *C. neoformans* Rim pathway 74

3.2.6 Rim pathway membrane sensing complex components are not conserved in *C. neoformans.*..... 76

3.2.7 Identification of novel *C. neoformans* Rim pathway component..... 78

3.2.8 Rra1 is conserved throughout Basidiomycota. 81

3.2.9 The Rim pathway does not require Gα protein activity..... 84

3.2.10 pH-regulated Rim23-GFP localization requires Rra1 and ESCRT. 85

3.2.11 Rra1 localizes to punctate structures near the plasma membrane and endomembranes. 87

3.2.12 Rim23 does not co-localized with Rra1 under activating pH conditions. 90

3.2.13 Full-length Rra1-GFP is present in the membrane fraction 90

3.2.14 Membrane localization of the Rra1 C-terminus is regulated by pH. 91

3.2.15 The majority of the Rra1 C-terminus is dispensable for alkaline pH tolerance. 93

3.2.16 Rim pathway mutants induce an increased inflammatory response during infection. 96

3.3 Discussion..... 98

3.4 Materials and Methods 105

3.4.1 Strains, media, and growth conditions 105

3.4.2 Molecular Biology 109

3.4.3 Insertional Mutagenesis and assessment of mutants..... 116

3.4.4 Protein extraction, immunoprecipitation, and western blot 116

3.4.5 Microscopy..... 118

3.4.6 Virulence studies..... 118

4. Increased chitin exposure on the Cryptococcus neoformans cell wall is associated with increased immune recognition and inflammation 120

4.1 Introduction 120

4.2 Results 123

4.2.1 Analysis of chitin content and organization in the *rim101*Δ mutant cell wall 123

4.2.2 Identification of a Rim pathway-independent regulator of cell wall chitin during infection 127

4.2.3 The *rim101Δ* and *mar1Δ* cell surface defects are associated with increased recognition by macrophages and dendritic cells 130

*4.2.4 mar1*Δ and *rim101*Δ mutations increase recognition of acapsular *cap59Δ* mutant 132

4.2.5 Alteration in chitin synthesis and exposure increases recognition by BMMs. 133

4.2.6 In vitro response to *rim101Δ* and *mar1Δ* requires MyD88 and CARD9 136

4.2.7 In vitro response to the *rim101Δ* mutant does not require Dectin-1 139

*4.2.8 rim101*Δ induces a global increase in immune cell infiltration and inflammatory cytokine production in the lungs of infected mice. 140

4.3 Discussion..... 147

4.3.1 Role of chitin exposure in the immune detection of *C. neoformans*. 148

4.3.2 Other cell surface alteration that may contribute to *rim101*Δ and *mar1*Δ immune recognition..... 150

4.3.3 Characterization of the immune response to *rim101*Δ and *mar1*Δ in vivo. .. 151

4.3.4 Conclusion and future directions 153

4.4 Materials and Methods 154

4.4.1 Strains, media, and growth conditions 154

4.4.2 Molecular biology..... 154

4.4.3 Cell wall isolation and HPLC 155
4.4.4 Cell wall staining and Microscopy 155
4.4.5 In vitro macrophage and dendritic cell experiments 155
4.4.6 Animal experiments. 156
5. 5. Thesis conclusion 157
5.1 Future Directions 159
5.1.1 Defining the mechanism of Rim pathway activation 159
5.1.2 Expanding *C. neoformans* Rim pathway 161
5.1.3 Define role of Rim101 in titan cell formation and capsule attachment 162
5.1.4 Identify innate immune receptors that recognize *rim101*Δ 164
5.1.5 Determine whether the *rim101*Δ-induced immune response is protective... 165
References 167
Biography 185

List of Tables

Table 1: Chapter 2 Strains 36

Table 2: Chapter 2 Primers 38

Table 3: Chapter 3 Gene Loci 106

Table 4: Chapter 3 Strains 106

Table 5: Chapter 3 Primers 111

Table 6: Percent Leukocytes 142

Table 7: Chapter 4 Strains 154

List of Figures

Figure 1: Rim101/PacC pH response pathway.. 9

Figure 2: *C. neoformans* Rim101 and Rim20 proteins control capsule expression on the cell surface.. 21

Figure 3: Ggtase-I involvement in thermotolerance and fungal cell morphology. 43

Figure 4: Effect of *cdc43*Δ mutation on virulence. 45

Figure 5: Localization of Cdc42, Rac2, and Ras1..... 48

Figure 6: Cdc42 requires its prenylation motif for functionality. 50

Figure 7: Ggtase-I function is required for proper Rho10 localization but not for cell wall stress tolerance. 51

Figure 8: Role of Ggtase-I in mating. 53

Figure 9: *cdc43Δ* mutant is hypersensitive to Ftase inhibitors..... 54

Figure 10: A model of the canonical Rim pathway elucidated in ascomycete fungi 65

Figure 11: Rim101 proteolysis and nuclear localization are dependent on pH.. 699

Figure 12: Rim101 proteolysis complex components..... 71

Figure 13: Role of Rim13 and Rim23 orthologs in Rim101-regulated phenotypes. 73

Figure 14: ESCRT complex proteins, Vps23 and Snf7, are required for Rim101 activation. 76

Figure 15: Predicted arrestins and Rim9 orthologs are not required for Rim101-dependent phenotypes..... 77

Figure 16: The *rra1Δ* mutant is phenotypically identical to other Rim pathway mutants. 800

Figure 17: Rra1 is a membrane protein and is conserved through Basidiomycete fungi.. 82

Figure 18: Alignment of the conserved regions of the basidiomycete Rra1 orthologs... 833

Figure 19: Role of Gpa proteins in pH 8 and 1.5 M NaCl tolerance..... 844

Figure 20: Rim23-GFP forms plasma membrane-associated puncta under neutral/alkaline pH conditions.. 877

Figure 21: Rra1 localizes to plasma membrane and intracellular punctate structures that do no colocalize with Rim23..... 89

Figure 22: The Rra1 C-terminus displays pH dependent plasma membrane localization. 93

Figure 23: Rra1 C-terminus is dispensable for alkaline pH tolerance but not for concentrated NaCl tolerance..... 95

Figure 24: Effects of Rim pathway mutants on virulence..... 97

Figure 25: Model of *C. neoformans* Rim pathway.. 99

Figure 26: *rim101*Δ strain has increase chitin exposure.. 125

Figure 27: *MAR1* is required for capsule attachment and maintaining chitin levels/exposure in host-mimicking conditions..... 129

Figure 28: Mar1 function is independent of Rim101..... 130

Figure 29: *rim101*Δ and *mar1*Δ cells and cell walls increase TNF-α secretion from macrophages and dentritic cells.. 131

Figure 30: *rim101*Δ and *mar1*Δ mutations increase BMM TNF-α secretion independent of capsule. 133

Figure 31: Cell wall mutants with increased WGA induce more TNF-α secretion from BMMs. 135

Figure 32: MyD88 and CARD9 contribute to the TNF-α response to *rim101*Δ and *mar1*Δ.. 138

Figure 33: Dectin-1 is not required for the increased TNF-α response to *rim101*Δ..... 140

Figure 34: *rim101*Δ induces increased leukocyte recruitment to infected lungs. 143

Figure 35: *mar1*Δ has a significant growth defect in vivo. 144

Figure 36: *rim101*Δ elicits an inflammatory and Th1 cytokine response in infected lungs 147

Acknowledgements

First and foremost, I would like to thank Andy Alspaugh for welcoming me into his lab. Andy's mentorship and support have not only made me into a better scientist, but also into a better person. Joining his research group was one of the best decisions I have ever made.

I have to acknowledge the amazing people that I have had the privilege working with in the Alspaugh lab: Connie Nichols, Teresa O'Meara, Liz Ballou, Shannon Esher, Kaila Pianalto, Diana Norton, Maria Kohlbrenner, Jessie Narloch, Naureen Huda. These are some of the most intelligent, enthusiastic, and determined people I have ever met. Each has taught me what it means to be a strong woman in science.

I have to thank my family and friends for the love and support that has kept me motivated and happy throughout my many years as a student. My parent have always encouraged me to do my best in any everything I do and their support has been behind every one of my accomplishments.

Finally, I have to acknowledge my incredible husband for the love and support that has gotten me through this crazy graduate school experience.

1. Introduction

1.1 Cryptococcus neoformans: opportunistic fungal pathogen

Cryptococcus neoformans is an opportunistic pathogen that has emerged as a particularly dangerous pathogen during the last several decades. This organism primarily causes life-threatening megingioencephalitis in immunocompromised people, and it became a worldwide health issue during the HIV/AIDS pandemic. Increased use of immunosuppressive drugs, such as those given to organ transplant patients, has also expanded the population susceptible to *C. neoformans* infection [1]. According to the most recent report on the global incidence of cryptococcosis, over 1 million people suffer from *C. neoformans* infections each year, leading to more than 600,000 deaths [2]. While anti-retroviral HIV-treatment has reduced these figures since this 2009 study, the incidence and mortality rate of cryptococcosis remains high (in the hundreds of thousands), especially in resource-limited regions of the world, such as sub-Saharan Africa, where antifungal and antiretroviral treatments can be scarce [1].

C. neoformans is a member of the basidiomycete phylum, where it, and its sister species *Cryptococcus gattii*, are some of the only members known to cause disease in humans [3]. *C. neoformans* is found ubiquitously in the environment and is commonly isolated from bird, and specifically pigeon, droppings [4]. *C. neoformans* infections occur exclusively from the environment, and human to human transmission has never been reported. People residing in cities with large pigeon populations commonly encounter this organism, and one study demonstrated that the majority of children by age 5 in New York City are seropositive for *C. neoformans*, despite having no obvious immune

deficiencies [5]. This fungus has two morphotypes: a hyphal form that is produced during both sexual and asexual mating, and a more prevalent yeast form, which is the only morphotype that causes disease [6,7].

The primary route of *C. neoformans* inoculation is through the inhalation of desiccated yeast, or spores produced by mating [8]. In individuals with competent immune systems, the infection is either cleared from the lungs, or it can establish an asymptomatic latent infection [9,10]. Damage to the immune system, and specifically to cell-mediated immunity, allows fungal replication from either new or latent infections. *C. neoformans* can then escape the lung, and disseminate throughout the body, preferentially targeting the central nervous system, where the infection is universally fatal if left untreated [3,11]. Pulmonary infection can also lead to life-threatening cryptococcal pneumonia [12].

C. neoformans infection is also associated with a life-threatening inflammatory condition that develops during immune system recovery. Immune Reconstitution Inflammatory Syndrome, or IRIS, arises when the TH-1 cell-mediated arm of the immune system recovers after the initiation of HIV anti-retroviral treatment, or after stopping immunosuppressive drug treatment. This leads to an over-exuberant inflammatory response to latent or subclinical *C. neoformans* infection resulting in host damage [13][14]. The symptoms of IRIS resemble classical *C. neoformans* meningioencephalitis or pulmonary cryptococcosis, making misdiagnosis common and contributing to a high mortality rate [1].

While *C. neoformans* has not specifically evolved to cause human disease, it does have several virulence-associated phenotypes that make this fungus particularly

adapted to growth and survival in a mammalian host. First, *C. neoformans* is one of the rare fungi that is able to proliferate at temperatures as high as 39^{o}C, and this thermotolerance is vital for its ability to thrive at body temperature. In addition, *C. neoformans* produces several factors and phenotypes to combat stressors that it encounters during infection. The best known of these phenotypes is the protective polysaccharide capsule, which is widely considered the most important virulence phenotype and is almost always required for virulence. The capsule is comprised of a complex matrix of polysaccharides that is non-covalently bound to the cell surface. The primary components are glucuronoxylomannan (GXM) and glucuronoxylomannogalactan (GalXM) [15,16]. The capsule protects *C. neoformans* cells from immune cell detection and damage by a number of mechanisms that include: active suppression of immune cell activation and cytokine secretion by immune cells [17–19], shielding immune-stimulatory fungal cell wall components from immune detection [20,21], and protecting the cell from oxidative damage [22]. Several infection-relevant conditions induce capsule formation and include host pH, 5% CO_2, iron-limiting conditions, and tissue culture media [23–25]. The capsule is one of the defining features of *C. neoformans* and is used to diagnose *C. neoformans* infections.

Melanin production is another important *C. neoformans* virulence-associated phenotype that is often used to identify this fungal species and is important for pathogensis [26]. Melanin is an antoxidant that protects the cells from host-produced reactive oxygen species, in addition to providing some protection against antifungal drugs [3].

Both the capsule and melanin production are important protective measures that allow *C. neoformans* to survive inside the phagolysosme of macrophages. Macrophages are important niches for *C. neoformans* during infection, protecting the cells from further detection by the immune system and assisting their dissemination to the central nervous system. The ability to proliferate in macrophages in vitro is strongly correlated with virulence, and it is commonly used to predict the pathogenic potential of different *C. neoformans* strains [27].

Finally, *C. neoformans* produces a specialized type of giant cells, called titan cells, during infection. These cells are 5-10X larger than the typical yeast cells and have a thickened cell wall and a denser capsule, making them hyper-resistant to stressors and phagocytes encountered during infection [28,29]. Titan cells are polyploid, with up to 8 copies of the genome, facilitating their large size and also serving as a source of genetic diversity during infection [29,30]. Titan cells have also been shown to direct immune responses that favor *C. neoformans* survival and persistence [31,32].

1.2 Regulation of C. neoformans GTPases: potential drug targets

To sense and respond to its environment during infection, *C. neoformans* utilizes highly conserved Ras and Rho-family GTPase signaling proteins. These proteins regulate many central processes throughout eukaryotic organisms, including cell division, polarized growth, and general stress responses. In *C. neoformans*, many of these conserved GTPases are required for thermotolerance and responding to many host-relevant stressors. Mutant strains lacking one or more of these proteins are often

avirulent in animal models of infection. [33–36]. For this reason, GTPases make excellent candidates for drug inhibition.

The basic function of Ras and Rho-family GTPases is to propagate and amplify the signals from membrane receptors and sensors to downstream effector proteins. GTPases perform this function by interacting with downstream effectors and altering their function. GTPases are often referred to as molecular switches, that cycle between an active form, which is bound to the purine nucleoside triphosphate GTP, and an inactive, GDP-bound form. The exchange of GDP for GTP, which is facilitated by upstream activators, activate GTPases, while the hydrolysis of GTP to GDP inactivates them.

C. neoformans encodes two Ras paralogs in its genome, *RAS1* and *RAS2.* Ras1 serves as the primary Ras protein, and it is required for polarized growth, thermotolerance, mating, and many other cellular functions [33]. Ras1 regulates many of its downstream signaling pathways through the activity of the Rho-family GTPases: Cdc42, Cdc420, Rac1, and Rac2. Ras1 signals through Cdc42 to regulate thermotolerance responses, and the primary paralog, Cdc42, is completely required for virulence [34,37]. The Rac proteins regulate the Ras1-dependent processes necessary for polarized growth, such as hyphal formation during mating and bud-site selection during yeast growth. The Rac proteins serve redundant roles and are, together, essential for *C. neoformans* survival. [34–36].

C. neoformans also utilizes the Rho GTPases, Rho1, Rho10, and Rho11 to respond to thermal stress and cell wall stress. Rho1 is the most important of the three proteins, and is essential for *C. neoformans* viability. These Rho proteins signal through

the Mpk1 kinase pathway to regulate the thermal and cell wall stress responses. Rho1 also serves as an essential co-factor with Fks1 to synthesize the cell wall component β-1,3-glucan [38,39].

Rho and Ras GTPases must be physically associated with cellular membranes to interact with the appropriate signaling proteins. To associate with membranes, these proteins are posttranslationally modified with hydrophobic lipid moieties. In fungi and other eukaryotes, most Rho and Ras GTPases require modification with a prenyl group. Without this lipid modification, these proteins dissociate from membranes, and are almost always non-functional [40–42].

1.3 pH Response Pathways in Fungi: Adapting to Host-derived and Environmental Signals

This chapter was modified from a review article (of the same title) published in Mycobiology 39(4): 249-256 (2011). The authors were Kyla Selvig and J. Andrew Alspaugh. Since its publication, the model of Rim/Pal pathway activation and cellular localization has been updated. This chapter has been revised to reflect the current Rim/Pal pathway model.

1.3.1 Introduction

In order to survive, microorganisms must be able to sense and respond to their surroundings. These cells are frequently exposed to rapidly changing environmental stresses. However, microorganisms are remarkably resilient and have developed mechanisms to efficiently adapt to changes in their environment. Ambient pH is one extracellular condition to which these cells must be able to respond to in order to survive.

Changes in pH induce many stresses on cellular functions including altering micronutrient availability, protein function, and membrane potential.

Among microorganisms, fungi are often able to survive in a diverse range of environmental conditions. Those that live predominantly in the external environment must be able to propagate despite large variations in temperature, nutrient availability, and pH. Mammalian fungal pathogens are additionally able to survive the unique stresses of the various microenvironments within the infected host, where the pH can range from 2 to 10. Therefore, fungal signaling pathways responding to external pH signals are important components of their cellular machinery.

While many signaling pathways are directly or indirectly regulated by pH, one of the most specialized pH response pathways is the Pal/Rim alkaline response pathway. This pathway has been studied in multiple fungal species and is especially important for fungal pathogenesis. This review will focus primarily on how the Pal/Rim pathway stimulates changes in cellular processes as a response to alkaline ambient pH and how this pathway is utilized by fungal pathogens to colonize their host and cause disease.

1.3.2 The Rim101/PacC transcription factors mediate pH responses in *Aspergillus nidulans* and *Saccharomyces cerevisiae*

Ambient pH response signaling in fungi was first elucidated in *A. nidulans* and *S. cerevisiae.* The major effector, PacC in *A. nidulans* and Rim101 in *S. cerevisiae*, is a three Cys_2His_2 zinc finger transcription factor that mediates changes in gene expression in response to neutral or alkaline pH. Rim101/PacC is activated when a region of its C-terminus is proteolytically cleaved, allowing the processed protein to mediate gene regulation. This proteolysis is induced under alkaline or neutral conditions.

Activation of Rim101/PacC is stimulated by a highly conserved signaling pathway, referred to as the Pal pathway in filamentous fungi, and the Rim pathway in yeast-like fungi, involving interactions between signaling complexes on the plasma membrane. The Pal/Rim signal is initiated at the plasma membrane where a complex of proteins first senses neutral/alkaline pH. The activated complex recruits a non-canonical arrestin, Rim8/PalF, which then recruits the remaining pathway components. Rim101/PacC is then recruited and proteolytically processed [43–45] (Figure 1).

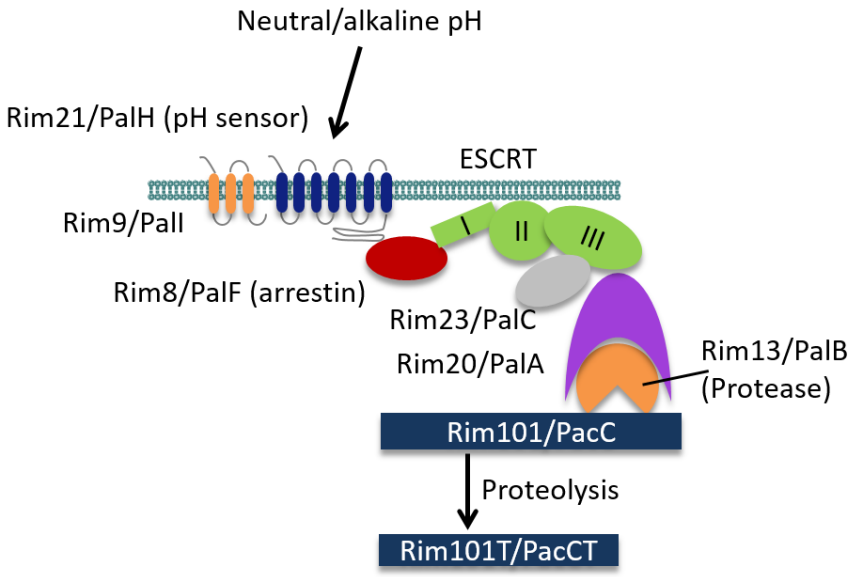

Figure 1: PacC/Rim101 pH response pathway. Neutral/alkaline pH signals are sensed at the cell surface by the 7 transmembrane-domain protein Rim21/PalH (blue). This extracellular signal leads to Rim8/PalF (red) ubiquitination and recruitment of the downstream Rim101 proteolysis complex. Prior to activation, Rim9/PalI (yellow) aids in the plasma membrane localization of the Rim21/PalH protein. At the plasma membrane, the Rim8/PalF arrestin-like protein interacts with the ESCRT complex, including ESCRT-I proteins that recruit and activate the ESCRT-II and –III proteins to this site. Rim23/PalC (grey) and PalA/Rim20 (purple) are then recruited to the ESCRT-III complex through their Bro domains, in turn recruiting both the calpain-like protease PalB/Rim13 (orange) and the transcription factor PacC/Rim101 (blue) into proximity. Proteolysis of PacC/Rim101 by the PalB/Rim13 protease results in the activation of this transcriptional regulator, and the resulting induction of alkaline response genes**.**

Sensing the external environment: Cell surface signaling events. In *A. nidulans*, the plasma membrane signaling complex is composed of a 7-transmembrane domain receptor, PalH, a 3-transmembrane domain protein, PalI, and an arrestin-related protein, PalF [46,47]. Orthologous proteins in *S. cerevisiae* have also been described (Figure 1).

It was previously hypothesized that the arrestin protein function in this pathway helps to internalize the pH signal from the cell surface receptor. It was recently demonstrated however, that Rim8/PalF does not induce endocytosis, and instead recruits downstream Pal/Rim proteins to the plasma membrane signaling complex [43–45]. Classically, arrestins mediate the downregulation of G protein-coupled receptor (GPCR) signaling by interacting with the cytosolic regions of GPCRs, preventing G-protein interaction, and mediating receptor endocytosis and degradation by the lysosome. However, arrestins can also serve as signaling scaffolds that mediate signaling from an endocytosed vesicle [48]. Since a G-protein does not appear to be involved in the Rim101/PacC signaling pathways, the arrestin-related Rim8/PalF appears to be mediating transcription factor processing through the latter arrestin function, but without induction of endocytosis. Also, the PalF and Rim8 arrestin proteins promote Rim101/PacC processing, which is not characteristic of the typically inhibitory behavior of arrestins [49–51]. Furthermore, *A. nidulans* PalF appears to interact with the C-terminal, cytosolic region of PalH regardless of ambient pH [51]; this interaction would theoretically inhibit any PalH/G-protein interaction. Therefore, the function of the PacF/Rim8 family of proteins is atypical for classical arrestin-like proteins.

The PalI protein is also a member of the plasma membrane signaling complex and functions by an unknown mechanism to promote proper PalH plasma membrane localization [46]. This hypothesized function is supported by the observation that PalH is located primarily on endosomal membranes in a *palI*Δ strain, rather than its typical localization to the plasma membrane [46]. *S. cerevisiae* Rim9 has a similar function in promoting Rim21 membrane localization [47].

Much of the plasma membrane signaling complex is conserved between *A. nidulans* and *S. cerevisiae;* however, there are several differences*. S. cerevisiae* has two 7 TMD receptors, Dgf16 and Rim21, both of which are homologous to PalH, and both required for Rim101 processing [52,53]. Dgf16 has recently been shown to interact directly with Rim21 and aid its membrane localization, similar to Rim9 [47]. In addition, unlike PalF, Rim8 ubiquitination is not dependent on pathway activation. It appears that a certain proportion of Rim8 molecules are always ubiquitinated regardless of ambient pH, and this ubiquitinated population is in complex with the ESCRT-I subunit Vps23 [50]. Neutral/alklaine pH conditions induce Rim8 association with Rim21, bringing together the ESCRT complex and the plasma membrane complex. This activation sequence appears to be different from the Pal pathway where PalF is already bound to PalH before pathway activation [49,51].

Assembly of the Rim101/PacC processing complex: In *A. nidulans*, neutral/alkaline pH induces PalF phosphorylation and ubiquitination, resulting the recruitment of the ESCRT machinery to the plasma membrane signaling complex [49,51]. The propagation of this signal requires the involvement of the recruitment of the ESCRT complex to the plasma membrane. The classical function of the ESCRT complex is to bind, sort, and transfer ubiquitinated cargo (often membrane proteins) into the multivesicular body (MVB) for degradation [54]. The ESCRT complex is also involved in retroviral budding, and cytokinetic abscission [54]. Formation of the ESCRT complex is initiated by ESCRT-0 binding to ubiquitinated cargo on endosomal membranes and the sequential recruitment of the other 3 complexes (ESCRT-I, -II, -III). The ESCRT –I, -II, and –III subunits Vps20-Snf7 were found to be required for *S. cerevisiae* Rim101

processing, and many members of the Pal/Rim signaling pathway have proven or predicted ESCRT subunit interaction domains [55].

After interacting with Rim21/PalH, Rim8/PalF recruits Vps23 (ESCRT-I subunit) which induces ESCRT complex assembly. PalC could also mediate interaction between the plasma membrane signaling complex and the ESCRT machinery. PalC is required for PacC activation and was found to localize to PalF/PalH endocytic vesicles after endocytosis. While its true function is unknown, PalC contains a Vps20-Snf7 interaction domain that may help the plasma membrane complex interact with downstream Pal proteins that also contain Vps20-Snf7 interaction domains [56].

The assembly of the ESCRT complex is likely induced by Rim8/PalF. Rim8, and possibly PalF, appears to be able to substitute for the ESCRT-0 protein Vps27 in binding to the ESCRT-I protein Vps23 to initiate ESCRT complex assembly [50,56,57]. The ESCRT complex then serves as a docking platform for the remaining Pal/Rim pathway components.

Transcription factor processing and activation. This pH-responsive signaling pathway ultimately results in the cleavage and activation of the Rim101/PacC transcription factors. The recruitment of the remaining ESCRT complex components leads to the recruitment of the Vps20-Snf7 interacting protein, Rim23/PalC and Rim20/PalA as well as the calpain-like protease Rim13/PalB. The exact function of Rim23/PalC is still unknown. One possible function is to stabilize the ESCRT complex, making it structurally more condusive for the recruitment of other Pal/Rim pathway members [44]. Rim20/PalA interacts with both the C-terminus of Rim101/PacC and Rim13/PalB, leading to the Rim13/PalB-mediated proteolysis and activation of

Rim101/PacC. For PacC, this proteolysis removes ~180 C-terminal amino acids, allowing this transcription factor it to relocate to the nucleus. In contrast, Rim101 is able to localize to the nucleus without Rim13 processing, but it is not able to mediate gene regulation without the removal of ~70 C-terminal amino acids [58,59]. One possibility for this observation is that Rim13-mediated cleavage may allow Rim101 to interact with other co-regulators that are necessary for gene regulation [59].

In *A. nidulans* once PacC is proteolytically processed, 245 C-terminal amino acids are further cleaved from this protein, presumably by the proteasome [56,60]. This second cleavage does not occur in *S. cerevisiae.* It has been hypothesized that both fully cleaved PacC and intermediate PacC are able to mediate gene regulation, with one form possibly acting as an activator and the other acting as a repressor. This may explain why *S. cerevisiae* Rim101 is believed to act only as a repressor but *A. nidulans* PacC can act as both an activator and repressor. However, it has yet to be definitively demonstrated if the intermediate form of PacC is functional.

Transcriptional response to Pal/Rim pathway. In neutral to alkaline conditions, activated PacC represses acid response genes while also inducing the expression of alkaline response genes. Most genes regulated by this transcription factor encode secreted enzymes (proteases and phosphatases) and permeases that function at either acidic or alkaline pH. PacC also regulates genes involved in the synthesis of secreted metabolites, such as penicillin and toxins. PacC induces its own expression, thereby serving in a positive feedback loop [60–62].

In *S. cerevisiae*, Rim101 promotes alkaline growth by repressing the expression of *NRG1*. Nrg1 is a transcription factor that inhibits the expression of ion transporters,

such as the Na^+-ATPase transporter Ena1, that are important for maintaining ion homeostasis during conditions of increased pH [59,63]. Expression of the low zinc-induced GPI-anchored protein Zps1 is also repressed by Nrg1, and its expression is induced when Rim101 is activated [59,63]. Smp1 is another transcription repressor that is direct target of Rim101, and is involved in the repression of haploid invasive growth, rough colony morphology, and sporulation. Its repression by Rim101 also induces *CTW1* expression, which has been shown to promote cell wall integrity [59]. Along with promoting growth in alkaline pH, Rim101 activity is involved in invasive growth, sporulation, and ion homeostasis [59,63].

1.3.3 *Candida albicans*

Candida albicans is a human commensal that commonly colonizes mucosal areas such as the oral-pharyngeal, gastrointestinal, and urogenital tracts. This organism is also able to cause invasive opportunistic infections at these mucosal surfaces, as well as systemic infections, potentially disseminating to almost any organ. The pH at these different anatomic areas ranges from quite acidic (GI tract and vaginal tract) to slightly alkaline (oral-pharyngeal tract and bloodstream). To survive pH changes of this magnitude, *C. albicans* must be able to sense these changes and drastically change its cellular functions in response to new environments. It is not surprising therefore, that *C. albicans* requires pH-sensing pathways, such as the Rim101 pathway, to survive within the infected host [64–67].

C. albicans is able to grow in both a yeast and a hyphal form. Transition from acidic to neutral/alkaline conditions stimulates *C. albicans* to switch from yeast to

filamentous growth [64–66]. This morphological change is important for virulence as filamentous growth has been found to be important for this organism's ability to cause systemic. Conversely, growth in the yeast form is needed for colonizing acidic environments like the vaginal tract [68].

The Rim101 pathway is important in pH-responsive morphological transitions, and therefore for *Candida* pathogenesis [64–67]. Like in *A. nidulans* and *S. cerevisiae*, the Rim101 pathway in *C. albicans* is activated by neutral to alkaline ambient pH, resulting in the proteolytic processing of the Rim101 transcription factor [66,67]. Many of the signaling components upstream of Rim101 activation are conserved in *C. albicans*, including homologs of Rim21/PalH, Dgf16; Rim8/PalF; Rim20/PalA; Rim13/PalB; and Rim9/PalI. All of these components were found to be required for proper alkaline response gene expression, proper processing of Rim101, and/or survival at high pH levels [52,65,66,69,70].

While much of the activation pathway seems to be similar to the Rim101/PacC pathways in *A. nidulans* and *S. cerevisiae*, the cleavage of *C. albicans* Rim101 is unique. In neutral to alkaline conditions, a ~10 kD C-terminal region is removed from the full length 85 kD Rim101p in a Rim13-dependent manner. However, Rim13 is also required for the cleavage of ~20 kD from the C-terminus of Rim101 in acidic conditions (pH 4). Rim8 and Rim20 were also found to be required for these processing events. It is hypothesized that the 75 kD form present in alkaline conditions functions to regulate alkaline response genes, while the 65 kD form present in acidic conditions regulates pH-independent genes [69]. C-terminally truncated forms of Rim101 are able to suppress mutations in genes encoding upstream components of Rim101 activation and restore

alkaline gene expression. However, it has not been demonstrated whether reconstitution with the 65kD-form of Rim101 present in acidic conditions would also rescue defects in alkaline-specific gene expression.

C. albicans Rim101 activation in alkaline conditions leads to the transcriptional induction of genes required for alkaline tolerance. Similar to *S. cerevisiae, C. albicans* Rim101 induces the expression of genes encoding ion pumps, such as *ENA1*, and iron acquisition genes, such as *FRP2*, *FRE2*, and *ARN1*. Along with increasing alkaline tolerance, the proteins encoded by these genes are important for high cation and low iron tolerance [67,71]. Unlike *S. cerevisiae*, *C. albicans* Rim101 appears to be able to act as both a transcriptional activator and repressor. Also, *C. albicans NRG1* is repressed under alkaline conditions, but in a Rim101-independent manner [66,67,72].

The *C. albicans* Rim101 pathway also regulates the expression of genes important for virulence. In addition to regulating genes necessary for hyphal growth, virulence-associated genes encoding adherence- and invasion-inducing proteins are also induced by the Rim101 pathway, such as the adhesin protein Als3 and the E-cadherin degrading protease Sap5p [73,74]. *The C. albicans* Rim101 pathway also regulates cell wall composition [62,67,73,74]. *PHR1* and *PHR2* were two of the first Rim101 regulated genes required for virulence. These β-1,3- and β-1,6-glucan crosslinking cell wall proteins are functionally homologous and are oppositely regulated by Rim101, with Rim101 inducing *PHR1* expression at alkaline pH while suppressing *PHR2* expression. Therefore, *PHR1* is required for infection of neutral to alkaline areas inside the host, while *PHR2* is required for infection of acidic areas [65,68,75]. In addition to controlling the expression of genes encoding cell surface proteins, Rim101 also

regulates the expression of genes encoding cell wall modifying enzymes. These modification enzymes, including a chitinase and a glucosidase, are induced by Rim101 and are important for interactions with endothelial cells [74].

Analysis of the *C. albicans* Rim101 pathway revealed that the components upstream of the transcription factor function in much the same way as their homologues in the *S. cerevisiae* Rim101 pathway or the *A. nidulans* PacC pathway. However, major differences are evident in the way *C. albicans* Rim101 is processed, the relative levels of transcriptional repression or activation attributed to this transcription factor, and the types of genes regulated by Rim101. Therefore, *C. albicans* has customized this conserved pH-signaling pathway to adapt to surviving in specific regions within the human host. In this environment, pH changes are not only stressors but also clues that this commensal organism uses to adapt to different locations within the human body.

1.3.4 *Cryptococcus neoformans*

The ascomycete Rim101/PacC signaling system has been studied in detail. Much less is known about this pathway in basidiomycetes. One such basidiomycete is the human opportunistic pathogen *Cryptococcus neoformans*. This organism causes fungal meningitis in immunocompromised individuals and has become a prevalent pathogen due to the HIV pandemic [76]. This organism grows in both yeast and hyphal form, and, similar to *C. albicans,* responds to pH signals to induce virulence factors. Unlike *C. albicans,* however, *C. neoformans* does not grow well above a pH of 8. It is able to grow inside macrophage phagolysosomes (pH 5) and in the slightly alkaline conditions of cerebrospinal fluid (CSF) and serum (pH 7.4) [77,78]. Melanin production,

polysaccharide capsule, and titan cell formation are all virulence factors that *C. neoformans* induces during infection, and each is regulated to some degree by the *C. neoformans* Rim101 transcription factor.

C. neoformans Rim101 was first characterized in a mutant library screen in which the *rim101*Δ mutant was found to have a slight melanin defect and also to survive better in mice compared to wild type strains [79]. The Rim101 protein was also identified in a bioinformatic search for transcription factors potentially regulated by the PKA pathway [80,81]. Discovering that the *C. neoformans* Rim101 has a functional PKA phosphorylation site was unexpected since this type of regulation was not appreciated for other PacC or Rim101 homologues.

Some of the processes regulated by the *C. neoformans* Rim101 protein are characteristic of the classical Rim pathway, suggesting that Rim101 is functionally conserved in *C. neoformans*. For example, similar to what is observed in *S. cerevisiae* and *C. albicans,* the *C. neoformans rim101*Δ strain is more susceptible to ion stress and alkaline growth conditions [81]. Along with these predicted functions, CnRim101 is also involved in species-specific functions, such as capsule attachment and titan cell formation [81,82]. The titan cell is a newly described *C. neoformans* morphotype that is 5-10 times larger than a regular cell, displaying a thickened capsule and increased resistance to oxidative and nitrosative stress [28,29].

Activation of *C. neoformans* Rim101 appears to be dependent on both classical upstream Rim/Pal activators and also by the PKA pathway. As in other organisms, activation of CnRim101 also requires proteolytic processing. When *C. neoformans* is incubated in non-capsule inducing conditions (rich medium at 30^{o}C), CnRim101 is

processed from its predicted 140 kD form to 120 kD. It is further processed to 70kD when the cells are incubated in capsule inducing conditions. This protein processing correlates with proper cellular localization. Rim101 is localized primarily to the nucleus in both capsule inducing and non-inducing conditions. This expected pattern of Rim101 localization is disrupted in conditions that disrupt proteolytic processing [81]. In the absence of activation by either Rim20 or PKA, CnRim101 remains in its full-length form and loses most of its nuclear localization, instead showing diffuse or punctate localization throughout the cell. Mutating the PKA phosphorylation site on CnRim101 also disrupts processing and nuclear localization [81].

Analysis of gene expression patterns regulated by CnRim101 under capsule inducing conditions reveal that this transcription factor primarily regulates genes associated with ion and metal homeostasis, cell wall modification, and capsule. For example, similar to *S. cerevisiae and C. albicans,* CnRim101 regulates the expression of the *ENA1* gene encoding a sodium pump important for ion homeostasis at increased pH [81]. Likely in response to altered metal ion availability in alkaline pH, CnRim101 also induces the expression of genes encoding an iron transporter and an iron permease (*SIT1* and *CFT1)*, and a copper transporter (*CTR4)*. Consistent with the capsule defect in the *C. neoformans rim101*Δ strain, CnRim101 appears to regulate genes known to be important for polysaccharide capsule biosynthesis, including, a glucose dehydrogenase (*UGD1),* a mannosyltransferase (*CMT1),* and a phosphomannomutase (*PMM).* Cell wall modification may also effect capsule attachment, which appears to be disrupted in the *rim101*Δ strain. Consistent with this hypothesis, CnRim101 regulates genes involved in cell wall production, including *AGS1* encoding an α-1,3-glucan synthase and α-glucan

1,3 beta-glucosidase protein [81]. *C. albicans* Rim101 was also found to regulate the expression of cell wall proteins, which were previously found to be important for virulence in an oral-pharyngeal infection model [74].

The *C. neoformans rim101* mutant strain is hypersusceptible to elevated pH and iron deprivation, two conditions known to exist in the host. Moreover, this strain has a dramatic defect in attachment of capsule, the main virulence factor for this pathogenic fungus (Figure 2). Therefore, one might have predicted that Rim101 would be required for pathogenesis. However, in two separate laboratories and two independent models of cryptococcosis, the CnRim101 mutant displayed preserved/enhanced virulence [79,81]. The mechanism behind this hypervirulence has yet to be elucidated. However, it was observed that the *rim101*Δ strain survived better than wild-type strains in macrophages, indicating that the mutant might be better adapted to grow in acidic conditions [81]. Therefore, CnRim101 may also be involved in the suppression of acid response genes. In a separate study, a *rim101*Δ mutant strain was noted to be engulfed by macrophages better than wild type [83]. However, because the level of phagocytosis was determined after 24hr incubation with macrophages, it is unclear if the higher number macrophage cells containing *rim101*Δ cells was due to increased phagocytosis or to better survival/replication inside the macrophages. Nevertheless, these data suggest that the *rim101*Δ strain may interact with its host's immune system differently than wild type *C. neoformans*, perhaps in part offering initial insight into the mechanism for the enhanced virulence of this mutant strain.

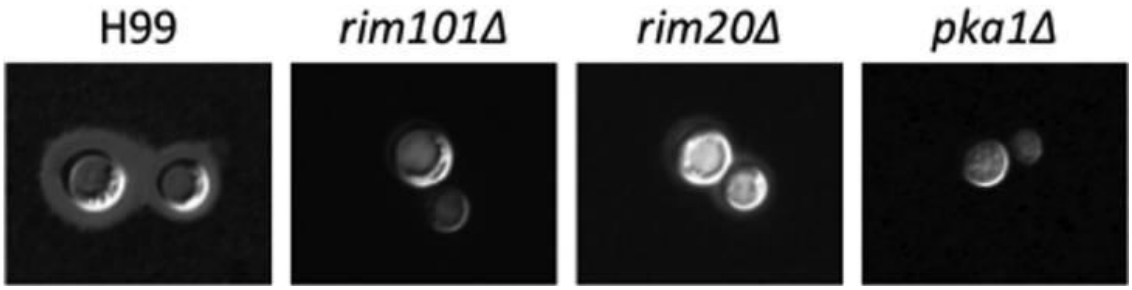

Figure 2: *C. neoformans* Rim101 and Rim20 proteins control capsule expression on the cell surface. The indicated strains were incubated at 37°C and 5% CO_2 in DMEM for 3 days and stained with India ink to visualize the polysaccharide capsule.

Studies on the Rim101 pathway in *C. neoformans* have already revealed significant differences in the way it is regulated. However, little is currently known about how CnRim101 is activated or the specific proteins mediating its activation. Genes encoding Rim13/PalB, Rim9/PalI, and PalC homologues are present in the *C. neoformans* genome. These homologues, along with a Rim101/PacC and Rim20/PalA homologues, were also found in the related basidiomycete *Ustilago maydis.* In this plant fungal pathogen, all of these Rim pathway components, except Rim9/PalI, are required for ion stress tolerance and growth in alkaline conditions [84,85]. Interestingly, homologues of the cell surface signaling proteins Rim21/PalH, Rim8/PalF, or Dgf16 are not immediately recognizable in either the *U. maydis* or the *C. neoformans* genomes [84,85]. Proteins with homologous functions could be present but without sufficient conservation of sequence to be detected by homology searches. For example, the predicted 7-trasnmembrane G-protein coupled receptor Grp5 was previously found to be important for titan cell formation. However, this protein did not readily interact with known G-alpha proteins in a modified yeast two-hybrid assay. Because Rim101 is also required for titan cell formation, it is interesting to speculate if Gpr5 or a related protein is acting

as the pH-responsive sensor protein, similar to Rim21/PalH or Dgf16. Alternatively, it is possible that the Pal/Rim pathway is regulated in a unique way in basidiomycetes, such as the unexpected PKA regulation of Rim101 in *C. neoformans.*

In addition to identifying the proteins responsible for activating Rim101 in *C. neoformans,* further studies will also define the active form of CnRim101. While this transcriptional regulator is minimally proteolytically processed in YPD (yeast-peptone-dextrose medium) which has a pH of 6.5 [81], it is unknown how the protein is processed in more acidic conditions, such as a macrophage phagolysosome. Also, there appears to be a second processing even that occurs under host relevant conditions [81]. Does this protein processing occur in response to increases in pH or to another host-derived environmental cue, such as alterations in temperature, iron levels, or CO_2 levels? Finally, defining the role of the Rim pathway in *C. neoformans* capsule attachment and immune activation will likely provide important insight into how this fungal pathogen avoids immune recognition and establishes long-lived infections in the human host.

1.3.5 Other signaling pathways involved in the fungal pH response

The Pal/Rim pH response pathway acts together and in parallel with other signaling pathways to modulate cellular functions in response to changes in pH. Because pH changes create such widespread changes to cellular functions, these interacting signaling pathways are involved in diverse cellular processes, such as nutrient acquisition and carbonic anhydrase activity.

The calcineurin pathway acts in parallel with the Rim pathway in *S. cerevisiae* and *C. albicans* [86–88]. In response to alkaline pH signals, the cytoplasmic Ca^{2+}

concentration increases, activating the calcium-responsive phosphatase calcineurin. This important signaling protein activates the transcription factor Crz1, which in turn controls the expression of pH response genes, such as that encoding the sodium pump Ena1 that is also regulated by the Rim101 pathway.

The PKA pathway is also involved in fungal pH response. In *S. cerevisiae*, PKA activation correlates with decreased alkaline tolerance [89]. PKA activity may increase alkaline sensitivity through phosphorylation and inhibition of Crz1, as mentioned above. Therefore, PKA acts in opposition to calcineurin in the pH response [88]. In contrast, the *C. neoformans* PKA pathway is involved in increasing alkaline tolerance [81]. Therefore, the PKA pathway may be utilized for both inducing and repressing the alkaline response in different fungal species.

The concentration of intracellular bicarbonate (HCO_3^-) changes with pH and CO_2 levels. Carbonic anhydrase is the enzyme responsible for accelerating the conversion of CO_2 into bicarbonate [90]. In *C. neoformans,* alterations in carbonic anhydrase activity and resulting shifts in bicarbonate levels regulate adenylyl cyclase activity in a pH-dependent manner [91]. Therefore, fungi such as *C. neoformans* use multiple, interacting proteins and signaling pathways (carbonic anhydrase, PKA, Rim 101, calcineurin) to modulate the cellular response to the environmental pH signal.

Finally, changes in pH levels result in changes in nutrient availability. The nutrient sensing TOR pathway negatively regulates the alkaline-induced yeast-to-hyphal transition in *C. albicans.* Mds3 is involved in inhibiting TOR in response to alkaline pH, allowing for morphologic changes [92]. Interestingly, *C. albicans* may be able to locally regulate is pH in low glucose conditions. Metabolism of amino acids during glucose

starvation leads to the secretion of ammonia, which sufficiently increases the pH surrounding the *C. albicans* cells to induce a yeast-to-hyphal transition [93].

In summary, both pathogenic and non-pathogenic fungal species have adapted intricate mechanisms to respond to common environmental signals such as changes in ambient pH. Species-specific alterations in conserved signaling paradigms indicate ways in which these distantly related organisms have adapted these pathways to survive in their unique environmental niches. In particular, fungal pathogens of humans have linked the expression of virulence-associated phenotypes to host-derived pH cues in order to effectively colonize and survive within their host.

1.4 The fungal cell wall

The fungal cell wall serves as an essential barrier against the environment. During infection, the cell wall interacts directly with immune cells, and the cell wall components and structure often dictate how the immune system responds to a particular fungal pathogen.

The typical fungal cell wall is composed of interlinked layers made up of carbohydrates and proteins. The innermost layer is usually made up of chitin and glucans, that include β-1,3- and β -1,6-glucan, which give the cell wall strength and rigidity. The outer layer often contain glucans, including β -1,3- and α-1,4- glucans, and glycoproteins and serves an important role in interacting with the environment. Fungal cell walls also contain chitosan, a deacetylated form of chitin. [94]

The structure and relative levels of each component vary significantly from one fungal species to another. *C. neoformans*, for example, has significantly more cell wall β

-1,6-glucan, chitin, and chitosan than *C. albicans* and *S. cerevisiae* [95]. This structure is also highly dynamic and changes substantially during morphological transitions. For instance, *A. fumigatus* hyphae have proportionally more α -1,3-glucan and chitin than spores in addition to containing a hyphal-specific extracellular matrix [96]. Alterations in nutrient availability and other environmental conditions can also significantly alter the cell surface. It was recently demonstrated that the *C. albicans* cell wall structure and composition significantly changes when grown in different carbon sources [97]. There is also spatial heterogeneity in the composition of the cell wall within individual cells. Chitin and chitosan are often concentrated at bud necks and hyphal septa in most fungi [94]. The dynamic nature makes it challenging to define a “typical” cell wall for any given species.

Many of the cell wall components are not found in humans or other mammals. Therefore, this structure marks invading fungi as “foreign” to the immune system, and there are several cell wall carbohydrates that are directly detected by innate immune sensors. β-1,3-glucan is the best studies pathogen-associated molecular pattern (PAMP) and is directly detected by the receptor Dectin-1 to induce inflammatory cytokine production and promote fungal clearing [98,99]. β -1,6-glucan has also recently been demonstrated to induce inflammatory immune responses, though the specific immune sensors have not been identified [100]. Fungal mannoproteins elicit protective immune responses and are recognized primarily by the C-type lectin receptors [99]. Chitin and chitosan are also detected by host immune receptors and secreted chitinases, though the resulting immune responses range from immune suppressive to inflammatory depending the specific structure and source of this carbohydrate [101–105].

Successful fungal pathogens often have mechanisms to shield immune activating cell wall components from immune detection. *Histoplasm capulatum* shields its β -1,3-glucan layer with a layer of the immunologically inert molecule α 1-3-glucan [106,107]. The hydrophobic protein rodlet layer on *Aspergillus* spores prevent detection of β -1,3-glucan and other cell wall components by immune receptors [108,109]. In addition, the mannoprotein layer on *C. albicans* has been shown to hide more immune stimulatory molecules during infection [110]. *C. neoformans* is perhaps that best at shielding its cell wall from detection, by forming the immune suppressive polysaccharide capsule. The capsule coating makes this fungal pathogen remarkably difficult to detect by innate immune cells in vitro and in vivo [20,25]. On the other hand, capsule components can elicit a protective adaptive immune response [111].

1.5 Summary of the work included in this thesis

The work presented in this thesis focuses on two *C. neoformans* signaling modules important for responding to host infection conditions. The Ras/Rho GTPases had been studied extensively for their function in *C. neoformans* mating, polarized growth, and thermotolerance. In Chapter 2, I describe my work to characterize an important posttranslational modification, called geranylgeranylation, in the localization and function of Rho and Ras-family GTPases. Also, the alkaline response Rim pathway regulates the expression of several virulence-associated phenotypes required for adapting the host environment. In particular, the Rim pathway regulates cell surface attributes required for avoiding immune detection. Chapter 3 describes how we identified and characterized the proteins that make up the *C. neoformans* Rim pathway. Finally, I

describe my work exploring the Rim101-regulated cell surface changes that prevent detection by the immune system.

1.5.1 Characterizing the *C. neoformans* geranylgeranyl transferase I

Many Rho and Ras GTPases are posttranslationally modified with a lipid prenyl groups to facilitate membrane interaction. Most eukaryotes have two prenyltransferase enzyme, the farnesyl transferase and the geranylgeranyl transferase. Prior to this study, *C. neoformans* Ras1 was shown to require its prenylation site to function [112], and the farnesyl transferase was found to be required for thermotolerance and mating [113]. However, the geranylgeranyl transferase I had not yet been characterized in *C. neoformans.*

Both prenylatransferases are heterodimers, containing a common α subunit and a distinct β subunit. I identified the *C neoformans* gene encoding the geranylgeranyl transferase I β subunit, *CDC43.* Disruption of *CDC43* led to temperature sensitivity, cytokinesis defects, and reduced virulence in a mouse inhalation model of infection. By analyzing the localization of several predicted GGTase I substrates, I identify Cdc42, Cdc420, and Rho10 as GGTase I substrates. However, I found that several other predicted GGTase I substrates do not require this prenyltransferase enzyme for membrane localization. These findings suggest that there may be significant overlap between GGTase I and FTase substrates. This study also suggests that the protein motif specifiying GGTase I vs. FTase substrates is may be different in *C. neoformans.*

1.5.2 Mapping the *C. neoformans* alkaline response Rim pathway

Rim101 is a conserved fungal transcription factor that regulates the response to alkaline pH stress. At the beginning of this project, our lab had identified Rim101 as a key transcription factor responsible for sensing and responding to stresses during infection. This includes the responses to alkaline pH and low iron conditions. While we had a detailed understanding of Rim101-regulated processes we had a limited understanding of the proteins and signals that activate the Rim101. The Rim pathway is conserved throughout most fungi and we had evidence that at least on component of the canonical pathway was required for Rim101 activation. However, the cAMP/PKA pathway was also found to regulate Rim101 activity and it was unclear whether it had functionally replaced much of the Rim pathway [81,114].

To define the Rim pathway, I first identified and characterized the conserved components of the canonical ascomycete Rim pathway. I found that members of the Rim101 proteolysis complex, Rim23, Rim20, and Rim13, were required for Rim101 activaiton. Around the same time, the Kronstad lab demonstrated that the ESCRT complex was also a conserved component of this pathway [115,116] . Interestingly, I was unable to identify any functional orthologs for components of the membrane sensing complex in *C. neoformans* or any other basidiomycete genome. This suggested that the basidiomycete Rim pathway may respond to pH in a different way than the ascomycete pathway.

To identify the missing members of the *C. neoformans* Rim pathway, I designed an insertional mutagenesis screen to specifically identify Rim pathway activators. From this screen, I identified one mutant that was unable to activate Rim101 and was

phenotypically identical to other Rim pathway mutants. This mutant had an insertion in a novel, basidiomycete specific, gene that we name *RRA1* (Required for Rim101 Activation 1). The Rra1 protein contains 7 predicted transmembrane domains, suggesting that it is structurally similar to the Rim21/PalH ascomycete pH sensor. In addition, Rra1 was required for Rim101 proteolysis complex assembly, suggesting that Rra1 functions upstream of this complex. These data suggest that Rra1 is the pH sensor for the Rim pathway. However, I recently found that unlike Rim21/PalH, Rra1 localizes primarily to intracellular membrane structures. Moreover, Rra1 does not appear to interact with the Rim101 proteolysis complex. Together, these data suggest that Rra1 may serve as a pH sensor for the *C. neoformans* Rim pathway, but likely senses pH and activates downstream Rim pathway components in a very different manner than Rim21/PalH. This study describes the most comprehensive analysis of the Rim pathway in any basiciomycete fungus, and significantly advances our understanding of how *C. neoformans* senses and responds to environmental pH.

1.5.3 Characterizing Rim101-regulated cell surface changes required for immune avoidance.

Prior to this project, we had identified Rim101 as an important regulator of fungal cell surface properties during infection. Without Rim101 regulation, the cell wall became thick and disordered and could no longer attach the capsule to its cell surface [117]. The aberrant cell surface properties were associated with a dramatic and detrimental immune response in a mouse lung model of infection. Initial characterization of *rim101*Δ cell wall defects revealed that this mutant bound significantly more of the chitin-binding lectin, wheat germ agglutinin (WGA).

The goal of this project was to determine the cell surface alterations that lead to the dramatic immune response to the *rim101*Δ mutant. We started by analyzing the *rim101*Δ cell wall changes in more detail. Using HPLC, enzymatic digestion, and cell wall staining, we found that the *rim101*Δ did not have a dramatic alteration in major cell wall carbohydrate levels. Instead, we found that *rim101*Δ has a dramatic increase in the exposure of chitin molecules on its cell wall. We identify another regulator of chitin exposure and capsule attachment, Mar1, which regulates these processes independently from Rim101.

Using both the *rim101*Δ and *mar1*Δ mutant strains, we found that their cell surface alterations are more readily recognized by macrophages and dendritic cells in vitro. We demonstrated that their cell wall alterations increase immune cell activation independent of capsule. We have begun to identify the specific immune receptors required for increased recognition of *rim101*Δ and *mar1*Δ and preliminary experiments demonstrated that multiple pathogen recognition receptors in the Toll-like receptor and C-type lectin receptor families are required for this response. Finally, we analyzed the immune response to both mutant strains in a mouse inhalation model of infection. In this model, *rim101*Δ induces a dramatic immune response, characterized by increased levels of most leukocytes and cytokines measured. The *rim101*Δ infected lungs had particularly high levels of neutrophils and inflammatory and Th1-driving cytokines. These results expand on our previous analysis of the lung immune response to *rim101*Δ, where we also observed a dramatic influx of neutrophils. On the other hand, the *mar1*Δ mutant appeared to be cleared from the lungs early during the infection, suggesting that the

immune response to this mutant was effective in clearing the organism and preventing disease.

This study demonstrated that chitin exposure is strongly associated with increased immune recognition, and *C. neoformans* may actively suppress chitin exposure during infection. Our results also demonstrate that the same immune responses measured in vitro can have dramatically different outcomes in vivo depending on the strength and duration of the infection.

2. Restricted substrate specificity for the geranylgeranyl transferase-I enzyme in *Cryptococcus neoformans*: implications for virulence

This chapter was modified from a manuscript (of the same title) published in Eukaryotic Cell 12(11) : 1462-71 (2013). The authors are Kyla Selvig, Elizabeth R. Ballou, Connie B. Nicholes, and J. Andrew Alspaugh.

2.1 Introduction

In eukaryotic cells, Ras-like GTPases perform vital signaling roles necessary for cell growth, differentiation, and morphogenesis. The majority of their functions are performed at cellular membranes, but their protein sequences alone are not sufficient for membrane interaction. Instead, these proteins must be post-translationally modified with lipid moieties that facilitate membrane association. Most commonly, these GTPases are modified by the addition of an isoprenoid group in a process known as protein prenylation.

Many members of the Ras-like GTPase family have a characteristic C-terminal CaaX-box motif, which designates them as prenyltransferase substrates. This motif consists of a cysteine followed by two aliphatic amino acids and variable amino acid. A prenyltransferase can bind to this motif and covalently attach an isoprenoid group onto the CaaX-box cysteine. This modification is irreversible and is often essential for stable membrane localization [41,42,118].

The two prenyltransferase enzymes that catalyze this type of prenylation are farnesyltransferase (Ftase) and geranylgeranyl transferase-I (Ggtase-I). These are structurally similar, dimeric enzyme complexes that share a common α-subunit and are

differentiated by their distinct β-subunits. Prenyl pyrophosphates (farnesyl pyrophosphate or geranylgeranyl pyrophosphate) interact with specific β-subunits, giving the prenyltransferase donor group specificity. The β-subunit typically interacts with certain CaaX-box sequences to allow for target substrate specificity. In general, substrates for Ftase or Ggtase-I enzymes are differentiated by the identity of the variable amino acid (X) of the CaaX-box. Although there is overlapping specificity between Ftase and Ggtase-I substrates, CaaX-box proteins terminating in leucine or other hydrophobic amino acids are typically geranylgeranylated, while Ftase substrates can terminate in one of several different amino acids [119–121].

Once prenylated, the C-termini of these proteins are further modified in the endoplasmic reticulum prior to plasma membrane localization. First, the terminal aaX amino acids are cleaved by the CaaX specific protease Rce1 [122–125]. The remaining terminal cysteine is then carboxymethylated by the Ste14/Icmt methyltransferase [124,126]. These modifications are important for full membrane association of the prenylated protein but are not absolutely required for protein function.

Because prenylation substrates are involved in a variety of cellular processes, inhibition of this process is often lethal. For this reason, there have been many prenyltransferase inhibitors developed to target cancer cells. More recently, a number of these prenyltransferase inhibitors have been repurposed to inhibit eukaryotic pathogens. Prenyltransferase inhibitors have been shown to be effective against two pathogenic parasites, Trypanosoma brucei and Plasmodium falciparum, in mouse models of infection [127–129]. Additionally, prenyltransferases have been shown to be important for fungal pathogen virulence and virulence-associated phenotypes. In the opportunistic

pathogen *Candida albicans*, the shared Ftase and Ggtase-I α subunit is essential [130]. In addition, *C. albicans* Ras1 requires its predicted prenylation site to mediate hyphal growth, a phenotype important for *C. albicans* virulence [131].

Cryptococcus neoformans is a pathogenic fungus that causes life-threating disease in immunocompromised individuals. *C. neoformans* has emerged as a significant global health problem due to rising numbers of immunocompromised patients caused by the HIV pandemic and the increased use of immunosuppressive drugs following organ transplants. This environmental fungus establishes a primary infection in the lungs before disseminating to the brain in immunocompromised patients. Worldwide, over 600,000 deaths are caused by *C. neoformans* infections each year, primarily as a result of meningoencephalitis [2].

Previous work has documented that protein farnesylation plays an important role in *C. neoformans* growth, differentiation, and virulence [113]. Furthermore, the CnRas1 GTPase, which is a predicted target protein for prenylation, loses all detectable function after disruption of its C-terminal CaaX motif [112]. Interestingly, while Ras proteins are typically farnesylated, the C-terminal amino acid sequences of *C. neoformans* Ras1 and Ras2 proteins suggest that they are Ggtase-I substrates. To date, no studies have documented the role of the Ggtase-I in *C. neoformans* virulence.

Typical Ggtase-I substrates include Rho-family proteins (Rho, Rac, and Cdc42). In many eukaryotes, these and other predicted Ggtase-I substrates play central roles in cell polarity and stress response. In the model yeast *S. cerevisiae*, the Ggtase-I β-subunit is essential, likely due to the role of Ggtase-I in modifying Cdc42 and Rho1, both essential proteins in this yeast [132]. Many of these predicted Ggtase-I substrates are

conserved in *C. neoformans*; in particular, the Rho-family GTPases have been shown to be extremely important in high temperature growth and virulence. For example, the duplicate *C. neoformans* Cdc42 and Cdc420 paralogs help to direct septin protein localization and cytokinesis [37]. The Rac proteins, Rac1 and Rac2, play a more specialized role in cell polarity, reactive oxygen species localization, and endocytic vesicular trafficking [35,36,133]. *C. neoformans* Rho proteins are important for cell wall synthesis and integrity [39].

In this study, we define the role of the *C. neoformans* Ggtase-I by disrupting the Ggtase-I β-subunit and show that the Ggtase-I enzyme plays a role in high temperature growth, virulence, and mating. We also explore several predicted Ggtase-I substrates that reveal potential plasticity in prenyltransferase specificity in *C. neoformans*.

2.2 Materials and Methods

2.2.1 Strains, Media, and Growth conditions

The strains used in this study are listed in Table 1. All mutants and fluorescent-fusion expressing strains were created in the *C. neoformans* H99 MATα background. Unless otherwise stated, strain were cultured on YPD (yeast extract 1%, peptone 2%, dextrose 2%) [134] plates or in YPD liquid media. Mating experiments were conducted on MS mating medium [135]. The cell wall and membrane stress plates were made by adding indicated concentrations of Congo Red, Calcofluor White, SDS, or caffeine to YPD prior to autoclaving. To create strain KS41 (cdc43Δ (MATa)), the CH9 (cdc43Δ (MATα) strain was crossed with KN99a (MATa), and recombinant spores were isolated by microdissection. To analyze morphogenesis, overnight liquid YPD cultures grown at

30oC with 150 rpm shaking were diluted 1:10 in fresh YPD pre-warmed to 30oC or 37oC. These cultures were incubated at the indicated temperature with shaking (150 rpm) for 18 hr. prior to imaging.

Table 1: Chapter 2 Strains

Strain	**Genotype**	**Source**
H99	*MAT α*	(53)
KN99	*MAT a*	(54)
CH9	MAT α *cdc43::nat*	this study
KS41	*MAT a cdc43Δ::nat*	this study
KS37	*MAT α cdc43Δ::nat CDC43*	this study
ERB016	*MAT α pHIS-GFP-CDC42-nat*	this study
KS8	*MAT α cdc43Δ::nat pHIS-GFP-CDC42-neo*	this study
KS13	*MAT α pHIS-GFP-cdc42(C190A)*	this study
ERB010	*MAT α cdc42::nat*	(21)
ERB011	*MAT α cdc42::nat cdc420::neo*	(21)
ERB013	*MAT α cdc42::nat CDC42-neo*	(21)
KS13	*MAT α cdc42::nat cdc42(C190A)-neo*	this study
KS14	*MAT α cdc42::nat cdc42(C190A)-neo*	this study
KS15	*MAT α cdc42::nat cdc42(C190A)-neo*	this study
ERB053	*MAT α rac2::neo + pHIS-GFP-RAC2-nat*	this study
KS49	*MAT α rac2::neo pHIS-GFP-rac2(C195A)*	this study

KS84	*MAT α rac2::neo cdc43::nat pHIS-GFP-RAC2-neo*	this study
CBN55	*MAT*α *ras1*::*neo ras1*(*C207A*)-*nat*	(19)
KS44	*MAT α cdc43Δ::nat pHIS-mCherry-RAS1-neo*	this study
CBN116	*MAT α pHIS-mCherry-Ras1-neo*	this study
KS126	*MAT α pHIS-GFP-RHO1-neo*	this study
KS129	*MAT α cdc43Δ::nat pHIS-GFP-RHO1-neo*	this study
KS132	*MAT α pHIS-GFP-RHO10-neo*	this study
KS135	*MAT α cdc43Δ::nat pHIS-GFP-RHO10-neo*	this study
KS138	*MAT α pHIS-GFP-RHO11-neo*	this study
KS141	*MAT α cdc43Δ::nat pHIS-GFP-RHO11-neo*	this study

2.2.2 Molecular biology

Primers used to create each strain are listed in Table 2. The cdc43Δ mutant was created by replacing the entire open reading frame in H99 strain with the dominant nourseothricin (NAT) resistance gene [136]. As previously described [137], PCR overlap extension was used to create a *cdc43*Δ::nat disruption construct, which was integrated into the genome using biolistic transformation as previously described [138]. The *cdc43*Δ::nat construct was created using the following primers (Table 2): *CDC43* 3' Flank: AA3014 and AA1996; *CDC43* 5' Flank: AA1999 and AA3015; NAT resistance marker: AA1997 and AA1998. Primers AA3014 and AA3045 were used to amplify the final disruption construct. The *cdc43*Δ mutant was confirmed by Southern blot. The AA3210 and AA3211 primers were used to create the Southern blot probe.

Table 2: Chapter 2 Primers

Primer	Sequence
AA1510	5'-CGGGATCCCGGGAGATTATGCTGCGGATGT-3'
AA1519	5'-CGGGATCCCGAGAAGGGGGAGTCTGGAAC-3'
AA1638	5'-CGCGGATCCATGCAGACAATCAAGTGTG-3'
AA1928	5'-GGGCCCAGATCTATGGCCATGCAGAGTATC-3'
AA1996	5'GCTAGTTTCTACATCTCTTCCGTGTGTGTGGGTGCATGGTGA3'
AA1997	5'-TCACCATGCACCCACACACACGGAAGAGATGTAGAAACTAGC-3'
AA1998	5'-GGTGATCTCTCTTTGCAGCCTTGCTAGGCTGCGAGGAT-3'
AA1999	5'-ATCCTCGCAGCCTAGCAAGGCTGCAAAGAGAGATCACC-3'
AA3014	5'-TTCGCGGGAAAGTAAGTCTC-3'
AA3015	5'-AAATGTCGGACAGGACAAGG-3'
AA3045	5'-TCGGCCTTTCTCCAAAACTA-3'
AA3184	5'-GTCTAAAAAGGCCCTCATCCTTTGAAGAC-3'
AA3185	5'-GTCTTCAAAGGATGAGGGCCTTTTTAGAC-3'
AA3188	5'-GGGCCCGGATCCTATGGGCACAGACAGACAGC-3'
AA3189	5'-GGGCCCGGATCCATGGCTCCTCTCGACTCTCC-3'
AA3210	5'-ACCAATGCGAGAGGAAGAGA-3'
AA3211	5'-TCTGCGTCCTTCAAATACCC-3'
AA3404	5'-GGGCCCAGATCTTCAGAGAATCAAAGCCTG-3'
AA3767	5'-CCTATAGGATCCCTCAATCCTCATCCACGCCA-3'
AA3768	5'-GTTGGAGGATCCTAACGATCCACTCCGGAAAC-3'

AA3769	5'-AACGACGGATCCATGTCTGTAAGTGCTGGGAC-3'
AA3770	5'-AAGCTCGGATCCAAATTATCACGCGGCAACTC-3'
AA3771	5'-CCAAGATCTGCGGCCCACCACCTCTTTTCC-3'
AA3772	5'-TATGAAGATCTTTCCGGCGGG-3'

To reconstitute the *cdc43*Δ mutant, primers AA3189 and AA3188 were used to amplifythe *CDC43* locus, promoter and terminator. The PCR product was cloned into the TOPO TA vector pCR2.1 (Invitrogen), digested with BamHI, and ligated into BamHI digested pJAF1 [137] vector to create pKS1. This plasmid was transformed into the cdc43Δ mutant and transformants were screened for Neomycin resistance and rescued thermotolerance.

To create the GFP-tagged *cdc42*C190A (pKS3) and rac2C195A (pKS12) fusion proteins, PCR overlap extension was performed to introduce the appropriate base pair changes in addition to adding restriction sites. The primers used to generate the *cdc42*C190A point mutations were: Flank 1: AA1638 and AA3184 (mutation primer), Flank 2: AA3185 (mutation primer) and AA1519; the full length product was amplified using AA1638 and AA1519. For GFP-*rac2*C195A: AA1928 and AA3404 (mutation primer with BglII restriction site. These point mutants were then cloned into pCN50 [81] containing the neomycin resistance marker, His3 promoter, and GFP.

The GFP-tagged Rho1, Rho10, and Rho11 plasmids were created by amplifying each gene and terminator sequence from H99 genomic DNA and cloning them into the single BamHI site in pCN50. The following primer pairs were used: RHO1: AA3767 and AA3768, RHO10: AA3769 and AA3770, RHO11: AA3771 and AA3772.

To create the pKS4 plasmid, which contains the cdc42C190A under its endogenous promoter, PCR overlap extension was performed and the resulting fragment was cloned into the BamHI site in pJAF1 [137]. Primers used: Flank 1:AA1510 and AA3184; Flank 2: AA3185 and AA1519; the full length product was amplified using AA1510 and AA1519.

2.2.3 Microscopy

Morphology and mating images were obtained using differential interference microscopy (DIC); fluorescent mating images were captured using a Zeiss Axio Imager A1 fluorescent microscope equipped with an AxioCam MRM digital camera. The high resolution fluorescent images were captured using the DeltaVision Elite deconvolution microscope equipped with a Coolsnap HQ2 high resolution CCD camera.

For images of mating structures, samples were fixed with 70% ethanol and permeabilized with 1% TritonX-100. The cell wall was visualized using Calcofluor White and nuclei were stained with SYTOX Green (Molecular Probes S7020).

2.2.4 Animal and Macrophage experiments

As previously described [139] J774.1 murine macrophage-like cells were used to assess survival within macrophages. J774.1 cells (1X105 cells/well) were plated in a 96-well plate and incubated for 18 hr. J774.1 cells were then activated for 1 hr. in 10 nM phorbol myristate acetate (PMA) diluted in DMEM (Dulbecco's Modified Eagles Medium). *C. neoformans* cells were washed two times with PBS and opsonized for 1 hr. at 37oC in DMEM containing 1 µg/ml anti-GXM MAb 18b7 [140,141]. The PMA was removed from the J774.1 cells, and 1X105 opsonized *C. neoformans* cells were added

to each well (MOI of 1). After 1 hr. of co-incubation, the non-engulfed/adherent *C. neoformans* cells were removed by washing 3 times with 200 µl PBS. DMEM was then added to each well and incubated for 24 hr. To release phagocytosed *C. neoformans* cells, sterile dH2O was added to each well, and the macrophages were lysed by vigorous pipetting. Wells were washed 2 more times with sterile dH2O and combined. Quantitative culturing was used to assess the number of viable *C. neoformans* cells.

Virulence was tested using the inhalation model of infection describe in [142]. Briefly, 10 female A/Jcr mice were anesthetized with 140 µl of 12 mg/ml ketamine HCl and 1 mg/ml xylazine in PBS. Each mouse was then intranasally inoculated with 1X105 cells in 25ul of PBS. The mice were monitored and sacrificed based on predetermined symptoms that predict imminent death. Groups were compared using the log-rank test (JMP software; SAS Institute, Cary, NC). All studies were performed in compliance with institutional guidelines for animal experimentation.

2.3 Results

2.3.1 Identification of the *C. neoformans* Geranylgeranyltransferase-I

In *S. cerevisiae* and *C. albicans*, the Ggtase-I β-subunit is encoded by *CDC43*. One potential Cdc43 ortholog (CNAG_02756) was identified in the *C. neoformans* genome by reciprocal BLAST searches using the *S. cerevisiae* and *C. albicans* Cdc43 protein sequences. The *CnCDC43* gene encodes a 259 amino acid protein with 24% and 32.5% sequence similarity to the ScCdc43 and CaCdc43 proteins, respectively.

2.3.2 Cryptococcus neoformans Geranylgeranyltransferase-I is involved in high temperature growth and morphogenesis.

To elucidate the role of the *C. neoformans* Ggtase-I, we created a *C. neoformans cdc43*Δ mutant by replacing the entire ORF with a drug resistance marker. The *CDC43* locus was completely deleted in several isolates, and Southern blot analysis showed that each had a single integration event removing the entire *CDC43* coding region. Therefore, unlike *S. cerevisiae*, the *C. neoformans CDC43* gene is not essential.

Ggtase-I activity is required for proper cell proliferation and differentiation in other eukaryotes, especially under conditions of cell stress [143–146]. Therefore, we tested the *cdc43*Δ mutant for growth defects under high temperature stress, which is one of the major cell stresses this organism encounters during infection. While the *C. neoformans cdc43*Δ mutant grew equally well as wild type at 30ºC, it displayed a marked growth defect at 37ºC and a more severe defect at 39ºC (Figure 3A).

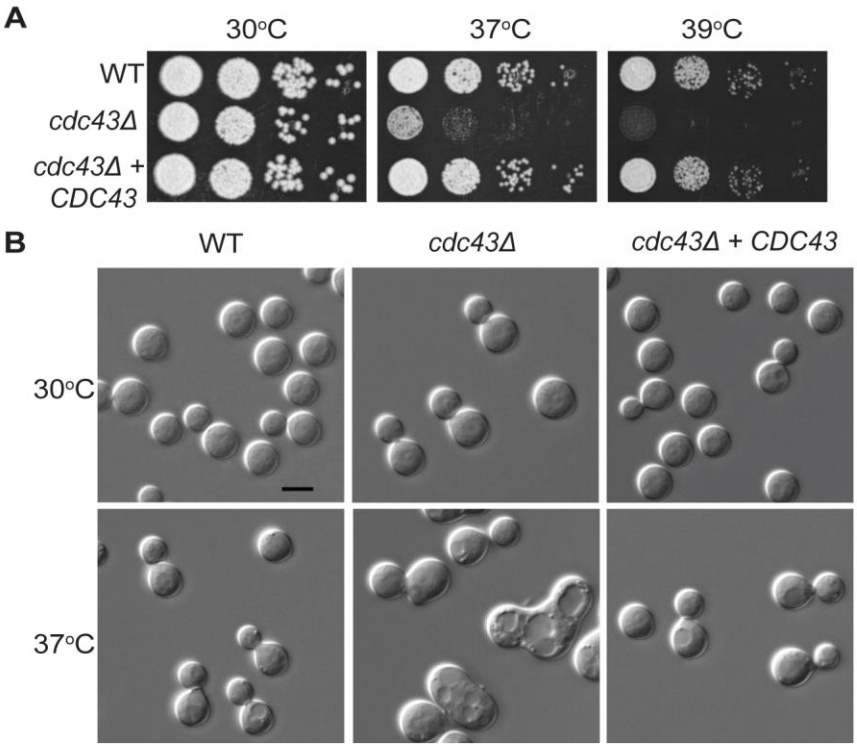

Figure 3: Ggtase-I involvement in thermotolerance and fungal cell morphology. (A) The *cdc43*Δ mutant has a growth defect at 37ºC and 39ºC. 5-fold serial dilutions of the indicated strains were spotted onto YPD medium and incubated for 48 hr. at the indicated temperatures. **(B)** The *cdc43*Δ mutant displayed apparent cytokinesis defects when grown at 37ºC. Cells were incubated in YPD medium to mid-logarithmic phase at 30ºC and shifted to preheated medium at 37ºC for 18hr. Cell morphology was assessed by photomicroscopy.

Temperature sensitivity often results from dysregulation of the cell cycle at high temperature, leading to specific morphological defects in *C. neoformans* cells [33,35,147,148]. Consistent with this hypothesis, there were notable morphological changes in the *cdc43*Δ cells compared to wild type when incubated at 37ºC (Figure 3B). At this elevated temperature, the majority of the *cdc43*Δ cells displayed wide bud necks and chains of multiple budding cells, indicative of a cytokinesis defect. As expected, the

morphology of the *cdc43*Δ mutant was indistinguishable from wild type when grown at 30ºC. Importantly, both the temperature sensitivity and the morphological defects of the *cdc43*Δ mutant were completely rescued by the reintroduction of the wild-type *CDC43* allele in the *cdc43*Δ +*CDC43* complemented strain.

2.3.3 *C. neoformans* Ggtase-I is required for virulence

Because *C. neoformans* must be able to grow at high temperatures to cause disease, we hypothesized that the temperature-sensitive *cdc43*Δ mutant would have a defect in virulence. *C. neoformans* is a facultative intracellular pathogen, and the ability to replicate within macrophages is strongly correlated with the ability to cause disease [149]. Therefore, we tested the *cdc43*Δ strain by co-culturing J774A.1 murine macrophages with opsonized *C. neoformans* cells at a multiplicity of infection of 1:1 for 1 hour. At this point, unengulfed cells were removed by gentle washing. After 24 hours, the macrophages were lysed, and the intracellular fungal replication/survival rate was determined by quantitative culture. The cdc43Δ mutant had a significant growth/survival defect in macrophages, with an output:input viable cell ratio that was 41% lower than wild type *C. neoformans* (Figure 4A). This indicates that Cdc43, and therefore Ggtase-I activity, is required for full growth in association with macrophages.

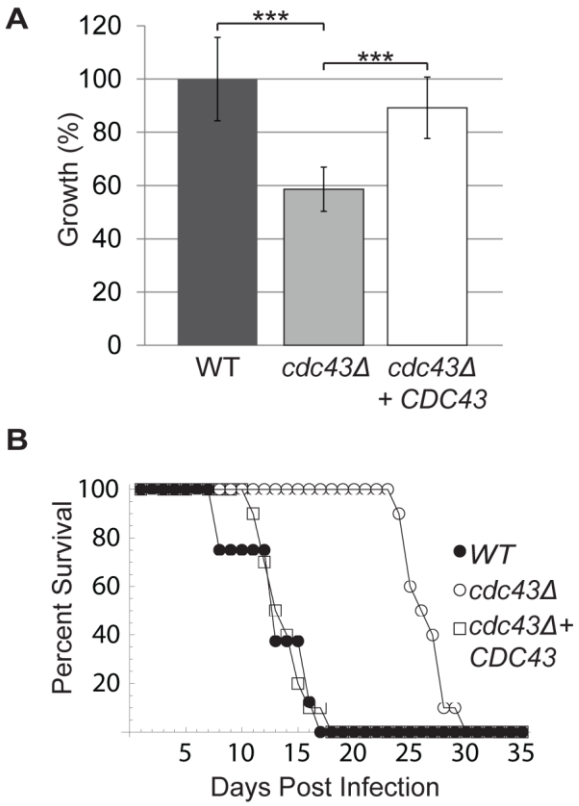

Figure 4: Effect of *cdc43*Δ mutation on virulence. (A) *cdc43*Δ has a relative growth defect compared wild type and reconstituted strains in murine macrophages. *C. neoformans* cells were opsonized with anticapsular antibody (18B7) and co-incubated with J774.1 murine macrophage-like cells that had been activated in PMA. After 1 hr, unphagocytosed *Cryptococcus* cells were washed away, and phagocytosed cells were co-incubated with macrophages for 24 hr. Macrophages were lysed and surviving fungal cells were quantitatively cultured. The viable output/input cell number was calculated for each strain and normalized to wild type. (***) stars indicate a p<0.001 **(B)** *cdc43*Δ has a delayed virulence in mice. 10 A/J mice were intranasally infected with 1X10^5 cells for each strain and monitored for survival.

We then extended our analysis of the *cdc43*Δ strain by assessing virulence in a mouse inhalation model of cryptococcal infection. We intranasally inoculated 10 female AJ mice with $5X10^5$ cryptococcal cells of the wild type, *cdc43*Δ, and *cdc43*Δ + *CDC43* strains. There was no statistically significant difference in survival of mice infected with the wild type or reconstituted strain, with all mice succumbing to the infection by day 17.

In contrast, mice infected with the *cdc43*Δ mutant displayed significantly longer survival until day 30 (p=<0.0001) (Figure 4B). These results demonstrate that the Cdc43 protein is required for full virulence in a physiologically relevant model of *C. neoformans* infection, likely due to its role in growth at elevated temperature.

2.3.4 Analysis of predicted geranylgeranyltransferase I substrates

We hypothesized that the *cdc43*Δ mutant phenotypes were due to mislocalization of one or more Ggtase-I substrates. Small GTPases constitute an important group of prenylated proteins that require membrane localization to be fully functional [118,150]. In *C. neoformans*, growth and morphology are maintained at elevated temperatures by the coordinated action of several GTPases. In other eukaryotes, Cdc42 and Rac proteins are classical Ggtase-I substrates, defined by C-terminal CaaX-box motifs ending in leucine. In *C. neoformans*, Ras1 also terminates in a leucine, designating it as a potential Ggtase-I substrate, even though Ras proteins are generally farnesylated in other eukaryotes [112]. These three GTPases are required for mating, morphology, and high temperature growth in *C. neoformans* [33,35,37,112]. Since Ras, Rac, and Cdc42 proteins in *C. neoformans* regulate different aspects of morphogenesis, mating, and stress responses, elucidating their roles in the *cdc43*Δ mutant phenotype could potentially provide insight into which of these proteins require geranylgeranylation for their full activity.

To explore the interaction between protein localization and activity for Ras, Rac, and Cdc42 proteins, we examined the effect of cdc43Δ mutation on their localization. To do this, we utilized fluorescent-fusion proteins and chose to initially examine Rac2,

Cdc42, and Ras1 as the representative paralogs. In *C. neoformans*, mCherry-Ras1 is primarily localized to the plasma membrane [112], while GFP-Rac2 localizes to both the plasma membrane and endomembranes [35]. Similarly, we observed GFP-Cdc42 localized to the plasma membrane and endomembranes in *CDC43* competent cells (Figure 3). Despite the presence of the CaaL geranylgeranylation motif in Ras1 and Rac2, these proteins maintained wild-type membrane localization in the *cdc43*Δ mutant background. However, the GFP-Cdc42 protein, which has the same CaaL motif as Rac2, was mislocalized primarily in the cytoplasm in the cdc43Δ mutant. Together, these results suggest that Cdc42 requires Cdc43 and geranylgeranylation for full membrane association. Additionally, the lack of mislocalization of the Ras1 and Rac2 proteins in the cdc43Δ mutant strain suggests that the CaaL motif is insufficient for determining prenylation specificity (Figure 5).

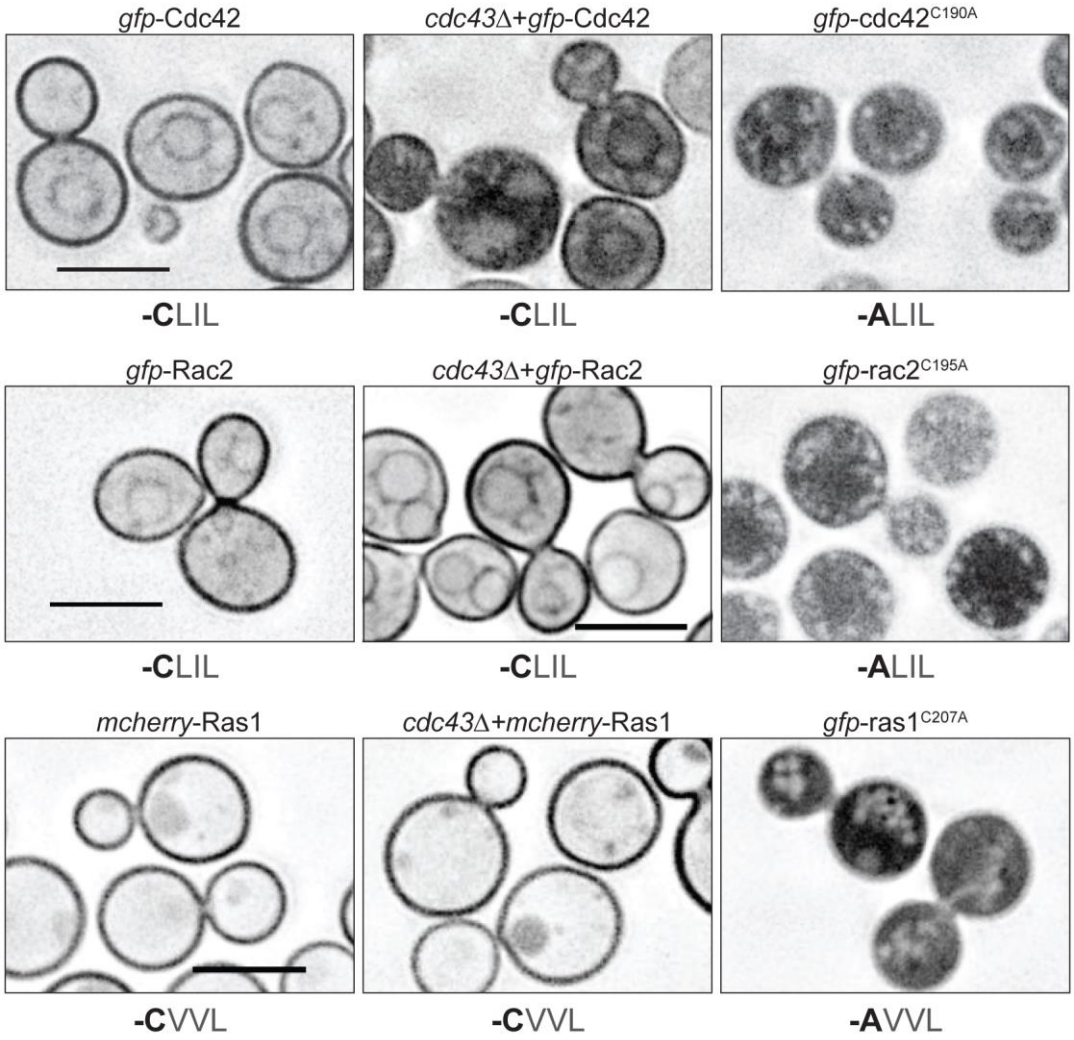

Figure 5: Localization of Cdc42, Rac2, and Ras1. Wild type and *cdc43Δ* strains expressing the indicated GFP-fusion proteins were grown in YPD medium at 30°C and imaged by Delta Vision microscopy. Scale bars = 5 μm

Previously, we demonstrated that *C. neoformans* Ras1 requires its prenylation site (the CaaX-box cysteine) for membrane localization [112], and mutating this site completely disrupts protein localization and function ([112] and Figure 5). Both Rac2 and Cdc42 contain poly-basic regions that potentially aid in membrane localization. To confirm that the Rac2 and Cdc42 also require prenylation for appropriate membrane

localization, we mutated the CaaX-box cysteine to an alanine in both proteins. Both the rac2C195A and cdc42C190A non-prenylatable mutants localized diffusely throughout the cytoplasm and showed no membrane localization. Therefore, both Rac2 and Cdc42 require their predicted prenylation sites for membrane interaction. These data suggest that, despite containing identical CaaX motifs, the Ras1, Rac2, and Cdc42 proteins are differentially targeted by prenyltransferases in *C. neoformans*.

2.3.5 Cdc42 function is dependent on prenylation

In concordance with the altered localization of Cdc42, the *cdc43*Δ mutant has several phenotypes that mimic disrupted Cdc42 activity, including temperature sensitivity and cytokinesis defects [37]. The phenotypic similarities between *cdc42*Δ and *cdc43*Δ mutants, combined with the finding that GFP-Cdc42 is unable to fully interact with membranes in the *cdc43*Δ mutant, suggest that Cdc42 function is dependent on geranylgeranylation. To explore the role of prenylation in Cdc42 function, we examined whether the *cdc42*C190A point mutant would be able to complement a *cdc42*Δ null mutant. We introduced the *cdc42*C190A mutant allele into the *cdc42*Δ strain. In contrast to full phenotypic complementation of the *cdc42*Δ strain with the wild type Cdc42 allele, two independent *cdc42*Δ+Cdc42C190A isolates demonstrated no restoration of *cdc42*Δ mutant phenotypes, including failed growth at 37^{o}C (Figure 6). We confirmed wild type levels of expression in these strains using semi-quantitative PCR with primers specific to *CDC42* mRNA (data not shown). We also sequenced the mutant allele to confirm there were no additional mutations in the *CDC42* coding sequence. These results are

consistent with a requirement for geranylgeranylation-dependent membrane localization for full Cdc42 activity.

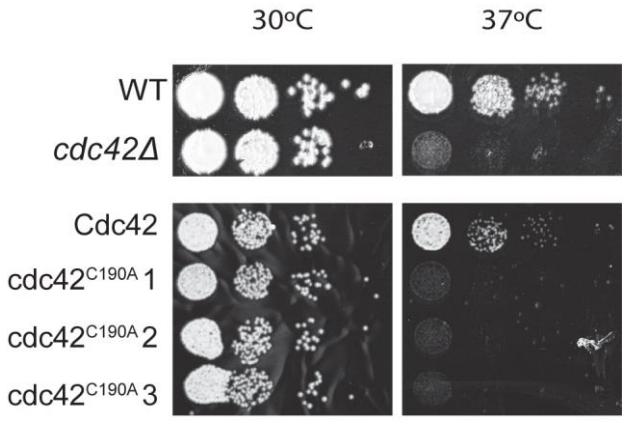

Figure 6: Cdc42 requires its prenylation motif for functionality. The WT, *cdc42Δ* mutant, *cdc42Δ*+Cdc42 reconstituted strain and the prenylation defective *cdc42Δ*+ Cdc42^{C190A} strains were serially diluted and incubated on YPD medium for 48 hr. at 30°C or 37°C

2.3.6 The cdc43Δ mutant does not exhibit cell wall defects

In *S. cerevisiae*, Rho1, another member of the Rho-GTPase family, is geranylgeranylated [132]. Like Cdc42, Rho1 geranylgeranylation is required for full protein function. In *C. neoformans*, there are 3 paralogs of Rho1: Rho1, Rho10, and Rho11. Lam et al. defined the role of each of these paralogs and found that while Rho1 is essential in *C. neoformans*, each of the paralogs is involved in the cell wall stress response to varying degrees. All three Rho proteins contain C-terminal CaaX motifs, with Rho1 and Rho10 containing CaaL sequences. While Rho10 was previously predicted to lack a CaaX motif, analysis of the Rho10 transcript sequence using RNA sequencing data revealed that one splice site was mis-annotated; the corrected sequence contains a CLIL C-terminal motif ([39] FungiDB.org). To determine whether any of the Rho paralogs

require geranylgeranylation for localization, we analyzed the localization of GFP-Rho fusion proteins in wild type and *cdc43*Δ cells. Of the 3 Rho paralogs, only GFP-Rho10 localized to cellular membranes in wild type cells (Figure 7A and data not shown). This membrane localization was slightly disrupted in the cdc43Δ mutant, indicating that the Rho10 protein is likely a Ggtase-I substrate.

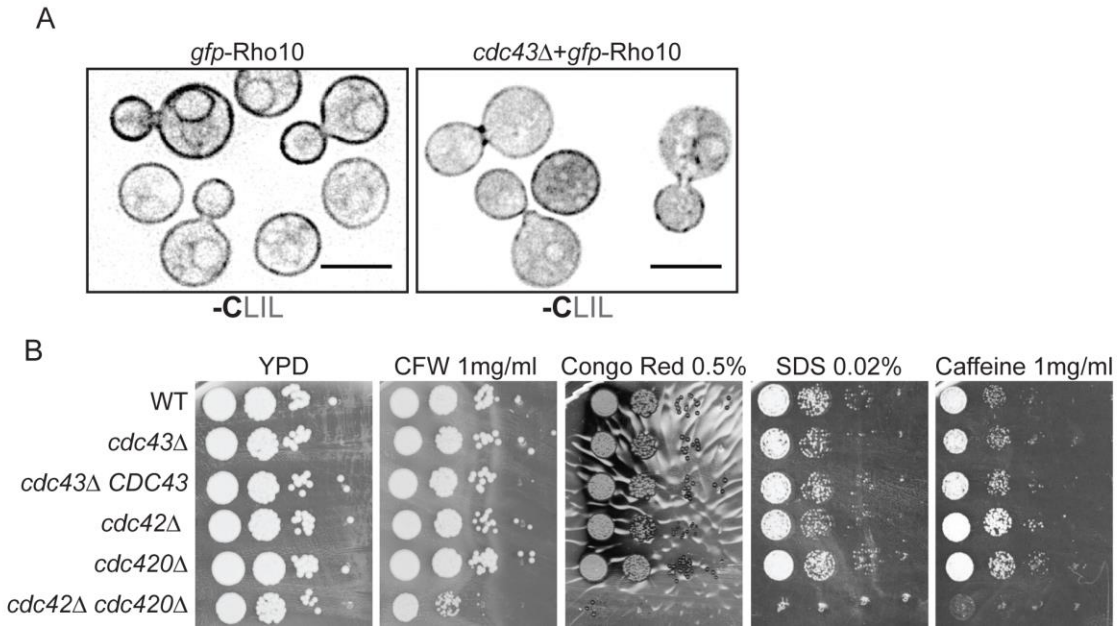

Figure 7: Ggtase-I function is required for proper Rho10 localization but not for cell wall stress tolerance. (A) Wild type and *cdc43Δ* cells expressing GFP-Rho10 were cultured in YPD at 30ºC and imaged using DeltaVision microscopy. Scale bar = 5 µm 10-fold serial dilutions of each strain was spotted onto YPD containing the indicated cell wall stressor. Plates were incubated at 30ºC for sufficient time to visualize colonies.

The rho10Δ mutant is sensitive to several cell wall and cell membrane stresses, including caffeine, calcofluor white, and SDS. If the function of Rho10 is significantly disrupted in the cdc43Δ mutant, we hypothesized that the *cdc43*Δ mutant would be sensitive to cell wall and cell membrane stresses [39]. To confirm that any cell wall sensitivities would be due specifically to Rho10 defects, we also examined the growth of

the cdc42Δ, cdc42Δ, and cdc42Δ cdc420Δ mutant strains on the same cell wall stressors. We found that the *cdc42*Δ *cdc420*Δ double mutant had dramatic growth defects compared to wild type on all stresses tested, with particular sensitivity to SDS. However, we found that the *cdc43*Δ mutant grew as well as wild type on all cell wall and cell membrane stressors (Figure 7B). These results indicate that Cdc43, and therefore Ggtase-I activity, is not required for Rho10 function. Additionally, these results indicate that while Cdc43 is required for Cdc42 and Cdc420 localization and functions in high temperature growth, it is not required for their full protein function in cell wall integrity.

2.3.7 The cdc43Δ mutant has a mating defect

To determine whether the Ggtase-I mutant has a mating defect similar to *cdc42*Δ, we analyzed the hyphae and spore formation in cdc43Δ crosses. The unilateral mating between cdc43Δ MATα and an isogenic wild type strain of the opposite mating type (MATa) produced filaments and spores indistinguishable from a wild type cross (data not shown). In contrast, the *cdc43*Δ MATα / *cdc43*Δ MATa bilateral mutant cross resulted in delayed mating hyphae production (Figure 8A). Instead of being evenly distributed around the mating reaction, as was observed for the wild type mating, the *cdc43*Δ MATα / *cdc43*Δ MATa hyphae are sporadically distributed, with noticeable gaps between each grouping of hyphae. While there is a notable decrease in mating hyphae production at early time points in a *cdc43*Δ mutant bilateral cross, these mating mixtures eventually produced wild type levels of mating structures and viable spores (Figure 8B). Additionally, each hyphal segment maintained two nuclei as observed in wild type crosses (Figure 8C).

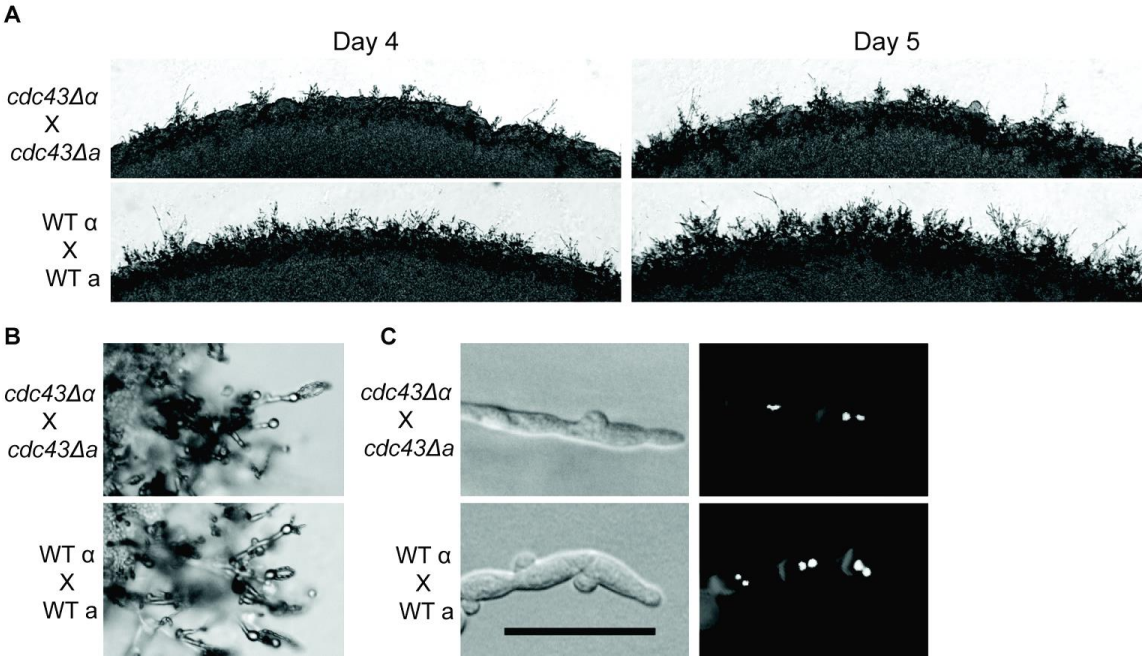

Figure 8: Role of Ggtase-I in mating. **(A)** The indicated strains were co-incubated in the dark on MS media. The same location on each plate was imaged for 4 and 5 days. **(B)** Basidia and spore structures were imaged from matings shown in (A). **(C)** Mating plugs were cut, permeabilized, and stained with calcofluor to visualize the cell wall and Sytox green to visualize nuclei. Scale bar = 20 μm

2.3.8 The cdc43Δ mutant is more susceptible to farnesyltransferase inhibitors.

In other eukaryotes, the Ftase enzyme can partially compensate for a cdc43Δ mutation by farnesylating Ggtase-I substrates [132]. Therefore, we hypothesized that Ftase inhibition may be more detrimental to cell survival in the absence of a partially redundant prenyltransferase. To test this possibility, we performed antifungal drug susceptibility testing in wild type and *cdc43*Δ strains using tipifarnib and manumycin A, two Ftase inhibitors [151]. Standard disk diffusion assays revealed enhanced antifungal effect for both of these compounds in the *cdc43*Δ mutant compared to the isogenic wild

type strain. Additionally, assessment of the minimal inhibitory concentration (MIC) for these strains in liquid media revealed that the *cdc43*Δ strain was 4-fold more sensitive to tipifarnib and 2-fold more sensitive to manumycin A compared to the wild type (Figure 9). Therefore, some degree of cross-prenylation may be protective for basic growth parameters in *C. neoformans*, even in the absence of significant cell stress.

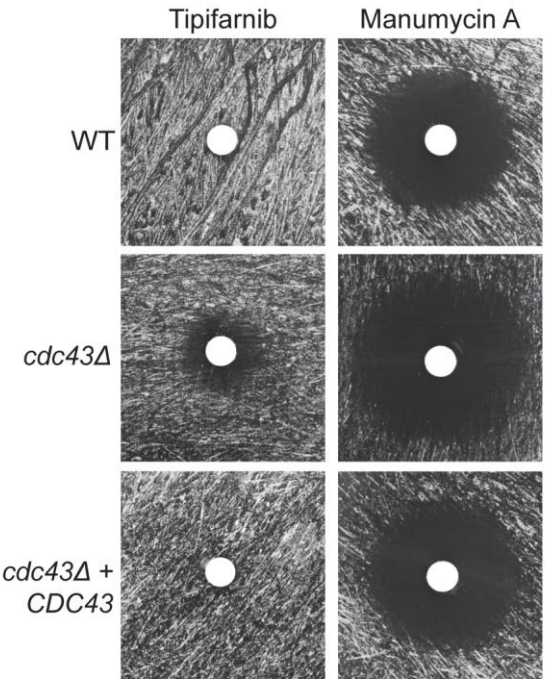

Figure 9: *cdc43Δ* mutant is hypersensitive to Ftase inhibitors. Wild type and *cdc43Δ* cells were incubated at 37°C on YNB plates with sterile cotton disk containing 10ul of 20μM tipifarnib or 20μM manumycin A.

2.4 Discussion

In this study, we identified and characterized the role of the putative geranylgeranyltransferase-I enzyme in the pathogenic fungus *C. neoformans*. Our lab has previously explored the importance of prenylation for *C. neoformans* survival during

infection. Pharmacological inhibition of the Ftase enzyme inhibited mating and also resulted in increased susceptibility to the calcineurin inhibitor FK506 [113]. In a subsequent study, the *C. neoformans* Ras1 protein was shown to require its predicted prenylated cysteine to be functional [112]. Appropriate Ras1 membrane localization is absolutely required for adaptation to the elevated temperatures of the host; therefore, Ras1 prenylation is likely essential for *C. neoformans* virulence.

Previous work on the *C. neoformans* Ram1 Ftase protein revealed that this enzyme is required for Ras1 localization and function. While Ras1 is a conserved Ftase substrate in most eukaryotes, the *C. neoformans* Ras1 protein contains a CaaX-box motif normally found on Ggtase-I substrates. Classically, the variable (X) amino acid of the CaaX-box determines whether the protein will be an Ftase or a Ggtase-I substrate [119]. While this paradigm may represent an oversimplification of prenyltransferase specificity, it is generally accepted that proteins containing CaaL (leucine) motifs are primarily Ggtase-I substrates. Interestingly, *C. neoformans* Ras1 terminates in a leucine residue, despite being farnesylated by Ftase in vitro and losing membrane localization after Ftase inhibition. Due to the importance of Ftase in *C. neoformans* infections, we hypothesized that the Ftase may be the major CaaX prenyltransferase in *C. neoformans*.

To more fully explore the role of prenyltransferases in *C. neoformans* biology, we identified the gene encoding the predicted Ggtase-I β-subunit and characterized its role in cellular proliferation and virulence. We generated several *cdc43*Δ mutants, demonstrating that in *C. neoformans*, Ggtase-I activity is not essential. However, this mutant displayed growth defects and morphological abnormalities at elevated temperatures. These results indicate that, while *C. neoformans* Ggtase-I activity may not

be completely required for cellular proliferation, Ggtase-I substrates likely regulate many important stress-related processes in the fungal cell.

These phenotypes are in contrast to studies in *S. cerevisiae*, where the Ftase is dispensable but the Ggtase-I enzyme is essential [152]. However, the relative importance of these prenyltransferases appears to vary from species to species, as the *C. albicans CDC43* gene is not essential and the *cdc43*Δ mutant displays only a mild morphological defects [146].

2.4.1 C. neoformans Ggtase-I Substrates

The phenotypes that result from disrupting prenylation are likely to be consequences of altered function in their substrate proteins. While we have no biochemical evidence that the *C. neoformans* protein is acting as a component of the Ggtase-I complex, our data strongly indicates that this highly conserved protein is required for Ggtase-I function. The commonly studied Ggtase-I substrates belong to the Rho GTPase family, which is comprised of Rho, Cdc42, and Rac proteins. In *C. neoformans*, these proteins regulate cellular polarity, morphogenesis, and cell wall integrity. *C. neoformans* encodes two Cdc42 proteins, three Rho proteins, and two Rac proteins. Each of these GTPases contains C-terminal CaaX motifs, and all but Rho11 and Rac1 have CaaL domains and are therefore predicted to be typical Ggtase-I substrates. Therefore, to test the hypothesis that each of these proteins requires geranylgeranylation for appropriate localization, we examined the localization of each via GFP-fusion constructs in the background of a *cdc43*Δ mutant strain that lacks Ggtase-I function. We additionally examined an mCherry-Ras1 fusion protein, as the *C.*

neoformans Ras1 also contains a CaaL motif. Although most of these Rho-family proteins were predicted Ggtase-I substrates based on their CaaX motifs, and have been shown to be geranylgeranylated in other eukaryotes [132,146,153], only Cdc42, Cdc420, and Rho10 required the Cdc43 Ggtase-I β subunit for membrane localization in *C. neoformans*.

We also demonstrated that Cdc42 absolutely requires its prenylation site for both membrane localization and function. It is therefore likely that the *cdc43*Δ mutant phenotypes result from decreased Cdc42 protein function. In fact, both the *cdc42*Δ temperature sensitivity and cytokinesis defects are shared phenotypes of *cdc42*Δ and *cdc42*Δ *cdc420*Δ mutants [37]. However, the *cdc42*Δ mutations cause much more severe temperature sensitivity and virulence defects compared to the *cdc43*Δ mutant. Furthermore, the *cdc43*Δ mutant displays appropriately structured clamp cells during mating, which are abnormal in *cdc42*Δ *cdc420*Δ mutants. Finally, the *cdc43*Δ mutant was not sensitive to cell wall or membrane stresses while the *cdc42*Δ *cdc420*Δ mutant was highly sensitive to each of these stresses. Taken together, these results indicate that Cdc42 and Cdc420 activity are only partially disrupted in the *cdc43*Δ mutant. A close examination of GFP-Cdc42 localization in the *cdc43*Δ mutant shows that membrane localization is not completely abolished in the *cdc43*Δ mutant, providing some explanation for the intermediate *cdc43*Δ phenotypes. Potentially, the intact farnesyltransferase may compensate in the absence of Ggtase-I activity. Additionally, it is possible that some of Cdc42/Cdc420 functions are independent of membrane localization and are thus not affected when this localization is disrupted.

The *C. neoformans* Rho1, Rho10, and Rho11 proteins function in cell wall maintenance, stress response, and high temperature growth. Rho1 is the only Rho protein in *C. neoformans* that appears to be essential. Mutating these proteins dramatically reduces *C. neoformans* adaptations to cell wall stresses [39]. Even though Rho10 membrane localization was mildly disrupted in the *cdc43*Δ mutant, the *cdc43*Δ mutant displayed no increased sensitivity to calcofluor white, Congo red, SDS, or caffeine. Therefore, Rho10 activity appears to be sufficient to support cell wall integrity in spite of incomplete membrane localization.

In contrast to commonly accepted models, GFP-Rho1 and GFP-Rho11 proteins were not localized primarily to the plasma membrane in wild type cells. Membrane localization of Rho proteins has been established in *S. cerevisiae*, *S. pombe*, *and C. albicans* [132,144,146]. There are several possibilities as to why these proteins are not obviously localized to the plasma membrane. First, perhaps only a small percentage of the cellular Rho1 and Rho11 protein population is membrane localized, making it difficult to visualize membrane association. Additionally, we used a histone H3 promoter to drive constitutive expression of the GFP constructs. It is possible that overexpression of Rho1 or Rho11 is detrimental to *C. neoformans* cells, and we may have inadvertently selected for transformants in which there is decreased membrane localization in order to decrease their activity. Supporting this model, Lam et al. found that Rho1 is detrimental to *C. neoformans* cells when constitutively active [39]. However, there is no increase in membrane staining in strains with lower GFP-Rho1 or GFP-Rho11 expression. Therefore, it is also possible that the proteins are sequestered into the cytoplasm via inhibitory proteins, such as guanosine nucleotide dissociation inhibitors (GDIs). These

GDIs decrease the effective activity of small GTPases by binding to their prenyl groups and removing these proteins from membranes [154].

In addition to their predicted prenylation sites, most prenylated proteins contain at least one additional membrane-targeting domain. The *C. neoformans* Ras1 protein is also palmitoylated, and each of the *C. neoformans* Rho family GTPases contains a polybasic domain upstream from the CaaX box motif. These domains are also important for membrane localization, but they are rarely sufficient for membrane interaction [155,156]. Therefore, even though Cdc42 and Rac2 both contain polybasic regions, both lose all membrane localization when their prenylation sites are disrupted (Figure 3), similar to Ras1 [112]. Therefore, membrane localization signals distant from the CaaX motif are insufficient to direct membrane localization of these proteins in the absence of prenylation.

The results of this paper demonstrate that the *C. neoformans* Ggtase-I plays a conserved role in Cdc42 and Rho10 protein localization, but that it is not likely to be the major CaaX prenyltransferase in this species. The only clear Ggtase-I substrates were the Cdc42 proteins and Rho10, even though there are several other important GTPases that are predicated to be Ggtase-I substrates. We hypothesize that many of the classical Ggtase-I substrates, such as the Rac proteins, are instead Ftase substrates in *C. neoformans*. Furthermore, the CaaL motif is clearly not a sufficiently conserved Ggtase-I recognition sequence in *C. neoformans*, which implies that there may be an unknown mechanism for prenyltransferase substrate recognition. These studies, and our previous work, suggest that the Ftase prenyltransferase has assumed many of the canonical Ggtase-I substrates in this microbial pathogen. Supporting this hypothesis, biochemical

analysis of the *C. neoformans* Ftase revealed a uniquely high affinity for CaaL domains in vitro [151]. This is a clear deviation from a similar study on human prenyltransferase substrate specificity, which demonstrated that the hydrophobic X-amino acids, primarily leucine, specify Ggtase-I substrates [119].

Although the Rho proteins analyzed here are some of the most studied Ggtase-I substrates, there are other potential substrates that may contribute to the *cdc43*Δ mutant phenotypes. The chitin synthase regulator (Csr1-3) proteins, which are involved in chitin and chitosan synthesis, all contain CaaX motifs and likely require membrane localization for their function [157].

2.4.2 C. neoformans Ggtase-I role in mating

In addition to affecting high temperature growth and morphology in *C. neoformans*, many of the prenylation substrates are required for efficient mating [33,37]. In *C. neoformans*, the Cdc42 and Rac proteins act downstream of Ras1 to regulate septin localization and the establishment of polarized growth, both of which are central processes in the complex mating reaction [35–37]. In addition, both a and α pheromones contain CaaX box domains, suggesting that, as in *S. cerevisiae*, prenylation is required for pheromone function in *C. neoformans* [40]. We found that the *cdc43*Δ mutant had a very subtle defect during mating filament formation. This phenotype is also similar to *cdc42*Δ and *cdc420*Δ mutants; therefore, we hypothesized that this *cdc43*Δ phenotype was primarily due to decreased Cdc42 protein function. However, the *cdc43*Δ mating filaments had normal clamp cell morphology and dikaryotic nuclear transport, which are normally disrupted when the Cdc42 proteins are mutated. Therefore, as suggested by

our studies in fungal cell growth and morphogenesis, Cdc42 protein activity in mating is reduced but not abolished in the absence of the Cdc43 Ggtase-I protein.

2.4.3 Disrupting *C. neoformans* Ggtase-I increases Ftase inhibitor efficacy

While some classical Ggtase-I substrates appeared to be fully functional in the Ggtase-I deficient *cdc43*Δ mutant, this mutation still resulted in decreased *C. neoformans* virulence, both in macrophages and in a mouse inhalation model of *C. neoformans* infection. This decreased virulence is likely due to the *cdc43*Δ thermosensitivity.

While Cdc43 is required for full virulence, all mice infected with the *cdc43*Δ mutant eventually succumbed to the infection. Therefore, *C. neoformans* Ggtase-I alone would not be an ideal antifungal drug target. However, previous investigations have shown that farnesyltransferase inhibitors dramatically impair *C. neoformans* growth. In addition, the results presented in this paper indicate that there may be an unexpected degree of overlap between Ggtase-I and Ftase substrate specificity. Therefore, we studied the concept of cross-prenylation using Ftase inhibitors in strains with disrupted Ggtase-I function. The *cdc43*Δ mutant was significantly more sensitive to both Ftase inhibitors tested. These results indicate that while Ggtase-I inhibitors are not likely to be effective antifungal agents on their own, they could be combined with Ftase inhibitors to increase their efficacy.

In conclusion, these studies demonstrate that the *C. neoformans* Ggtase-I performs a conserved role in the prenylation and localization of the Cdc42 proteins and Rho10. This activity is important for allowing growth of this pathogenic fungus at host

physiological temperatures. In fact, disruption of Ggtase-I function results in impaired virulence in an animal model of *C. neoformans* infection. However, these studies also suggest that the CaaX motif is not sufficient to determine the specificity of farnesylation versus geranylgeranylation; some degree of compensatory farnesylation appears to occur with proteins classically predicted to be Ggtase-I substrates. Moreover, between the two types of prenyltransferases, the Ftase is likely more directly required for virulence-associated function. Single or dual prenylation inhibition strategies are therefore promising tools to explore the pathogenesis and drug inhibition of this important pathogen.

3. The *Cryptococcus neoformans* alkaline response pathway: Identification of novel a Rim pathway activator

This chapter was modified from a manuscript (of the same title) published in PLOS Genetics 11(4):e100159. doi10.1371/journal.pgen.1005159 (2015). The authors are Kyla S Ost, Teresa R O'Meara, Naureen Huda, Shannon K Esher, J. Andrew Alspaugh. Figures 21, 22, and 23 show unpublished results.

3.1 Introduction

To survive the harsh environment of the infected host, microorganisms must be able to sense their external environment and adaptively alter their cellular processes. For example, microorganisms often encounter changes in extracellular pH when moving between different microenvironments. For fungal pathogens, the alkaline-response transcription factor Rim101 plays a central role in adapting to changing environmental and host conditions.

Rim101 was first implicated in fungal pathogenesis in the human fungal pathogen *Candida albicans* in which the *rim101*Δ mutant was demonstrated to be defective in the yeast to hyphal transition, and therefore unable to cause disseminated infection [64]. More recently, Bertuzzi and Schrettl et al. demonstrated that the opportunistic pathogen *Aspergillus fumigatus* requires the Rim101 ortholog PacC for virulence in a murine model of infection [158]. Since then, several investigators have demonstrated that other human, insect, and plant fungal pathogens require this conserved alkaline response pathway to cause disease [114,159–162].

More recently, the physiological role of Rim101 has been defined in the opportunistic fungal pathogen, *Cryptococcus neoformans*. *C. neoformans* is a basidiomycete yeast that causes life-threatening meningitis in immunocompromised individuals. Due to the emergence of HIV and the increased use of immunosuppressive therapies, this once-rare pathogen has become a significant global health problem, with over 1 million new infections estimated each year [2]. In *C. neoformans*, Rim101 is required for the proper formation of the protective polysaccharide capsule, as well as growth under several stress conditions such as low iron, elevated salt concentrations, and alkaline pH [81,163]. In addition, Rim101 mediates cell wall modifications that allow for capsule attachment and the masking/repression of cell surface pathogen associated molecular patterns (PAMPs). In the *rim101Δ* mutant strain, failed cell wall masking of immunogenic PAMPs results in a dramatic hyper-inflammatory response and immune-mediated host damage in a mouse inhalation model of cryptococcal infection [117].

The signaling pathway responsible for sensing and activating Rim101 has been defined in model ascomycetes, such as *Aspergillus nidulans* and *Saccharomyces cerevisiae,* and it is highly conserved throughout other members of this phylum (Fig. 10). In these species, initial activation of the Rim/Pal pathway involves extracellular sensing of pH by the 7-transmembrane domain receptor, Rim21/PalH [45,47,49]. This protein is a component of the membrane sensing complex, also comprised of the arrestin-like proteins Rim8/PalF, as well as the chaperone Rim9/PalI proteins [46,47,49]. Several ascomycete fungi require an additional component of the membrane signaling complex, Dfg16, which may serve as a Rim21/PalH chaperone [52]. Rim8/PalF recruitment to the sensing complex results in activation of part of the ESCRT complex, proteins also

involved in endosome function [43,54,55]. Rim8/PalF binding to the ESCRT-I protein Vps23 induces the assembly of the ESCRT-II and –III complexes as a scaffolding platform for Rim pathway activation [43,50]. On this platform, the Rim proteolysis complex forms, composed of Rim23/PalC, Rim20/PalA, and the Rim13/PalB protease [44]. The intact Rim proteolysis complex catalyzes cleavage and activation of its target, the Rim101/PalC transcription factor [164,165].

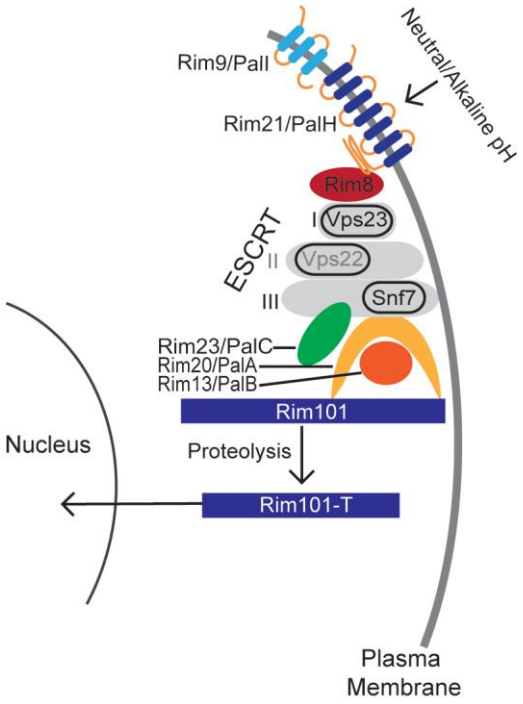

Figure 10: A model of the canonical Rim pathway elucidated in ascomycete fungi [44,67]

This Rim/Pal signaling pathway has only recently been analyzed in basidiomycetes, a diverse group of fungi including some human and animal pathogens [81,84]. In the maize pathogen *Ustilago maydis*, the ESCRT-interacting complex (Rim23/PalC Rim20/PalA, and Rim13/PalB) was conserved and required for Rim101/PacC activation.

However, elements of the membrane receptor complex (Rim9/PalI, Rim21/PalH, and Rim8/PalF) were either missing from the genome or not required for Rim101 processing [85]. In *C. neoformans,* there are several differences in the mechanism of Rim101 activation from established signaling paradigms in other fungal species. First, similar to *U. maydis,* the Rim/Pal membrane sensing complex proteins are not evident by homology searches. Also, we previously observed a novel connection between Rim101 and the cAMP/Protein Kinase A pathway [81,114]. The connection between these two conserved pathways reveals that the processes leading to Rim101 activation in this fungal species may occur in a somewhat distinct manner from that in distantly related ascomycetes. However, *C. neoformans* Rim101 activation also appears to require members of the canonical Rim activation pathway because deletion of the *RIM20* ortholog resulted in phenotypes identical to a *rim101Δ* mutation [81]. This observation implicated the involvement of both the cAMP and the classical pH response pathway in the activation of *C. neoformans* Rim101 [81,114]. While the *C. neoformans* cAMP/PKA signaling pathway has been extensively characterized, comparatively little is known about the *C. neoformans* Rim pathway

In this study, we determined that *C. neoformans* encodes functional orthologs of the major components of the Rim101 proteolysis complex, Rim13/PalB, Rim23/PalC, and Rim20/PalA. In contrast to these highly conserved distal components of Rim101 activation, the surface pH-responsive proteins, Rim8/PalF and Rim21/PalH, could not be identified using sequence or domain-based searches. Utilizing a random mutagenesis screen specifically designed to find *C. neoformans* Rim101 activators, we identified a previously unrecognized membrane protein required for *C. neoformans* Rim101

activation, which we named *RRA1* (Required for Rim101 Activation 1). While the Rra1 protein lacks significant sequence similarity to any component of the ascomycete Rim/Pal pathway, its predictive protein structure, containing 7-transmembrane domains, is similar to the Rim21/PalH sensors in ascomycetes. Moreover, predicted orthologs for Rra1 were found only in basidiomycetes. We also observe that Rim pathway signaling likely occurs in punctate regions on the plasma membrane. The recruitment of Rim23 to these puncta requires components of the ESCRT complex in addition to Rra1, suggesting that Rra1 functions upstream of other *C. neoformans* Rim pathway components. These findings suggest fundamental biological differences between the ways in which ascomycetes and basidiomycetes have developed cell surface signaling units to respond to common environmental signals.

3.2 Results

3.2.1 Neutral/alkaline pH induces Rim101 proteolytic cleavage and nuclear localization.

As modeled in Fig. 1, the Ascomycete Rim101/PacC transcription factor is activated by Rim13/PalB-mediated proteolytic cleavage in response to elevated pH signals. Previously, we demonstrated that the GFP-Rim101 fusion protein, when overexpressed by the histone *HIS3* promoter, was proteolytically cleaved from a 120 kDa form to a 70 kDa form in response to incubation in tissue culture medium [81]. To dissect the role of pH in Rim101 activation, we created a strain expressing GFP-Rim101 from its endogenous locus instead of the highly active histone3 promoter. The endogenously expressed *GFP-RIM101* allele fully rescued all *rim101Δ* mutant phenotypes. Using this strain, we assessed GFP-Rim101 proteolysis in defined media at

pH 4, 6, and 8. At pH 4 we exclusively observed the intact 140 kDa form of the GFP-Rim101 protein, suggesting that this is a non-inducing condition for Rim101 proteolysis and activation. In a dose-response relationship with increasing pH, we observed increased proteolytic processing of GFP-Rim101 resulting in a predominant 100 kDa processed form as well as lower molecular weight forms that either represent further processing or proteolytic degradation (Fig. 11A). In addition, GFP-Rim101 proteolytic processing correlated with increased nuclear localization (Fig. 11B). Together, this demonstrates that the *C. neoformans* Rim101 protein is activated by increasing pH.

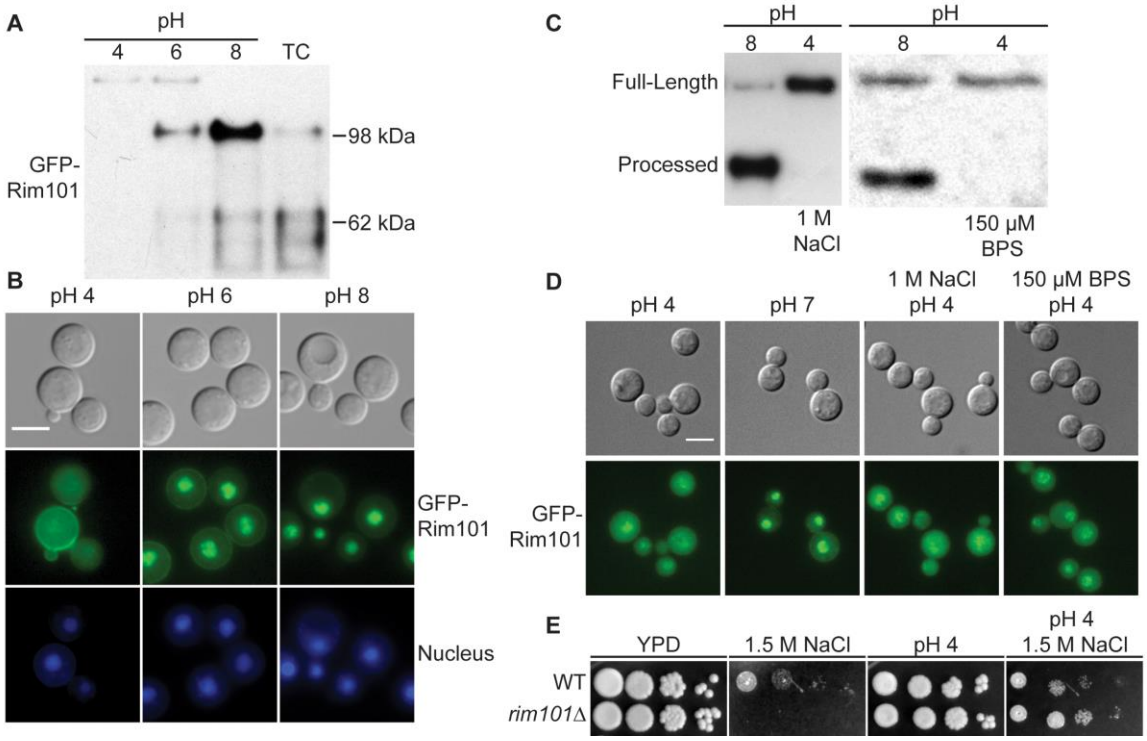

Figure 11: Rim101 proteolysis and nuclear localization are dependent on pH. (A) GFP-Rim101 is proteolytically processed from 140 kDa to ~100 kDa in response to increasing pH. GFP-Rim101 was immunoprecipitated from wild-type cells after incubating for 5 hr at the indicated pH 8 (SC medium buffered with McIlvaine's buffer). Protein processing was determined by western blotting using an α-GFP antibody. **(B)** GFP-Rim101 nuclear localization increases in response to increasing pH. Cells were cultured in the same way as in (A). GFP signal was assessed by epifluorescence microscopy. Nuclei were stained using Hoechst 33342 live nuclei stain. Scale bar = 5 µm. **(C)** GFP-Rim101 proteolysis is not induced by 1 M NaCl or 150 µM BPS. Cells were cultured in each indicated condition for 3 hr. GFP-Rim101 was analyzed by western blot. **(D)** GFP-Rim101 localization in response to pH 7 SC (McIlvaine's) or pH 4 SC (McIlvaine's) with 1 M NaCl or 150 µM BPS. Cell assessed epifluorescence microscopy after 30 min incubation in each condition. Scale bar = 5 µm **(E)** *rim101Δ* is not NaCl sensitive at pH 4. Strains spotted onto YPD, YPD 150mM HEPES pH 4 1.5 M NaCl, and YPD 1.5 M NaCl.

3.2.3 Rim101 is not activated by high NaCl or iron limitation.

In addition to responding to alkaline pH, *C. neoformans* Rim101 is required for growth in the virulence-relevant conditions of iron limitation and high salt concentrations [81]. These stress responses are linked with increasing pH because alkaline pH both reduces the bioavailability of iron and disrupts the membrane charge gradient necessary for ion channels to properly function [166].To determine whether Rim101 could also be activated by high salt concentrations and/or iron limitation independent of pH, we analyzed Rim101 activation in response to high salt and low iron conditions at pH 4. Neither GFP-Rim101 proteolytic processing nor nuclear localization was induced by the addition of 1 M NaCl (Fig. 11C and D). Similarly, iron deprivation due to the addition of the iron chelator BPS only slightly increased GFP-Rim101 nuclear localization, but it did not induce Rim101 proteolytic processing (Fig. 11C and D). In addition, the *rim101Δ* mutant did not have a growth defect on 1.5 M NaCl at pH 4 (Fig. 11E), whereas it displays a salt sensitive phenotype at more alkaline pH. Therefore, *C. neoformans* Rim101 appears to be activated specifically by neutral/alkaline pH, rather than by other cell stress conditions such as salt stress or limiting iron availability.

3.2.4 Identification and Characterization of *C. neoformans* Rim13 and Rim23 orthologs

The signaling pathway responsible for Rim101 activation is highly conserved throughout fungi in the Ascomycota phylum (Fig. 10). These proteins are typically recognizable by sequence conservation, even among fungi as divergent as the budding yeast *S. cerevisiae* and the hyphal fungus *A. nidulans*. In a previous study, we identified the gene encoding a functional ortholog of the Rim101 scaffolding protein Rim20 in the

basidiomycete fungus *C. neoformans* and confirmed its role in capsule regulation, alkaline pH adaptation, and response to low iron [81]. Using *S. cerevisiae* and *A. nidulans* amino acid sequences for comparisons, we identified single genes encoding other components of the *C. neoformans* Rim101 proteolysis complex, including the Rim13 protease (CNAG_05601) and the Rim23 ESCRT-interacting protein (CNAG_02205) (Fig. 12).

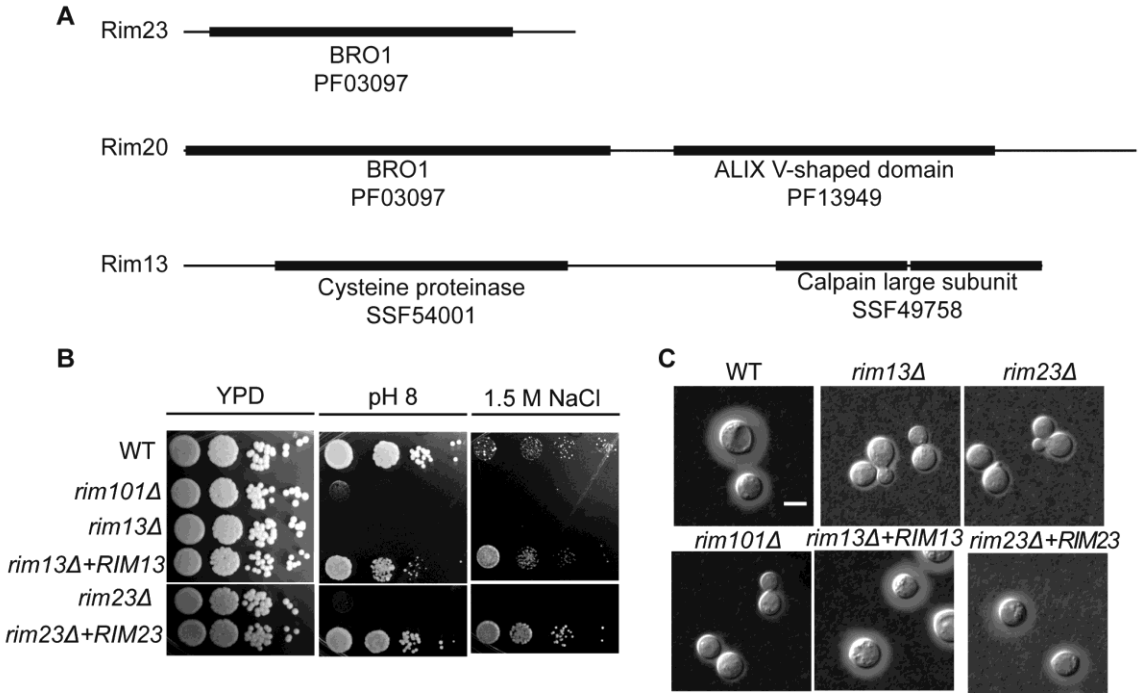

Figure 12: Rim101 proteolysis complex components (A) Model of *C. neoformans* Rim13, Rim20, and Rim23 orthologs. Conserved protein domains were predicted using Pfam and Super Family databases. The E-values for each domain prediction: Rim23 PF03097: 5.50E-9; Rim20 PF03097: 1.90E-97, PF13949: 1.10E-71; Rim13 SSF54001: 1.16E-42, SSF49758 (2 domains): 1.57E-19 and 2.09E-14. **(B)** Expression of *RIM13* and *RIM23* wild type alleles rescues *rim13Δ* and *rim23Δ* pH 8s and 1.5 M NaCl growth defects. **(C)** Expression of the wild type alleles also rescues the *rim13Δ* and *rim23Δ* mutant capsule defects. Cells were cultured for 48 hr in CO_2-independent media 37°C to induce capsule formation. Capsule was visualized by India ink stain.

As expected, none of these genes were essential. Disruption of the *RIM13* and *RIM23* genes resulted in decreased growth on pH 8 and 1.5 M NaCl, similar to the *rim101Δ* mutant (Fig. 13A). Notably, the *rim13Δ* and *rim23Δ* mutants also had a *rim101Δ*-like capsule defect, confirming a role for the pH-responsive signaling pathway in capsule regulation (Fig. 13B). These *rim13Δ* and *rim23Δ* mutant phenotypes were rescued by reintroduction of the respective wild types alleles (Fig. 12).

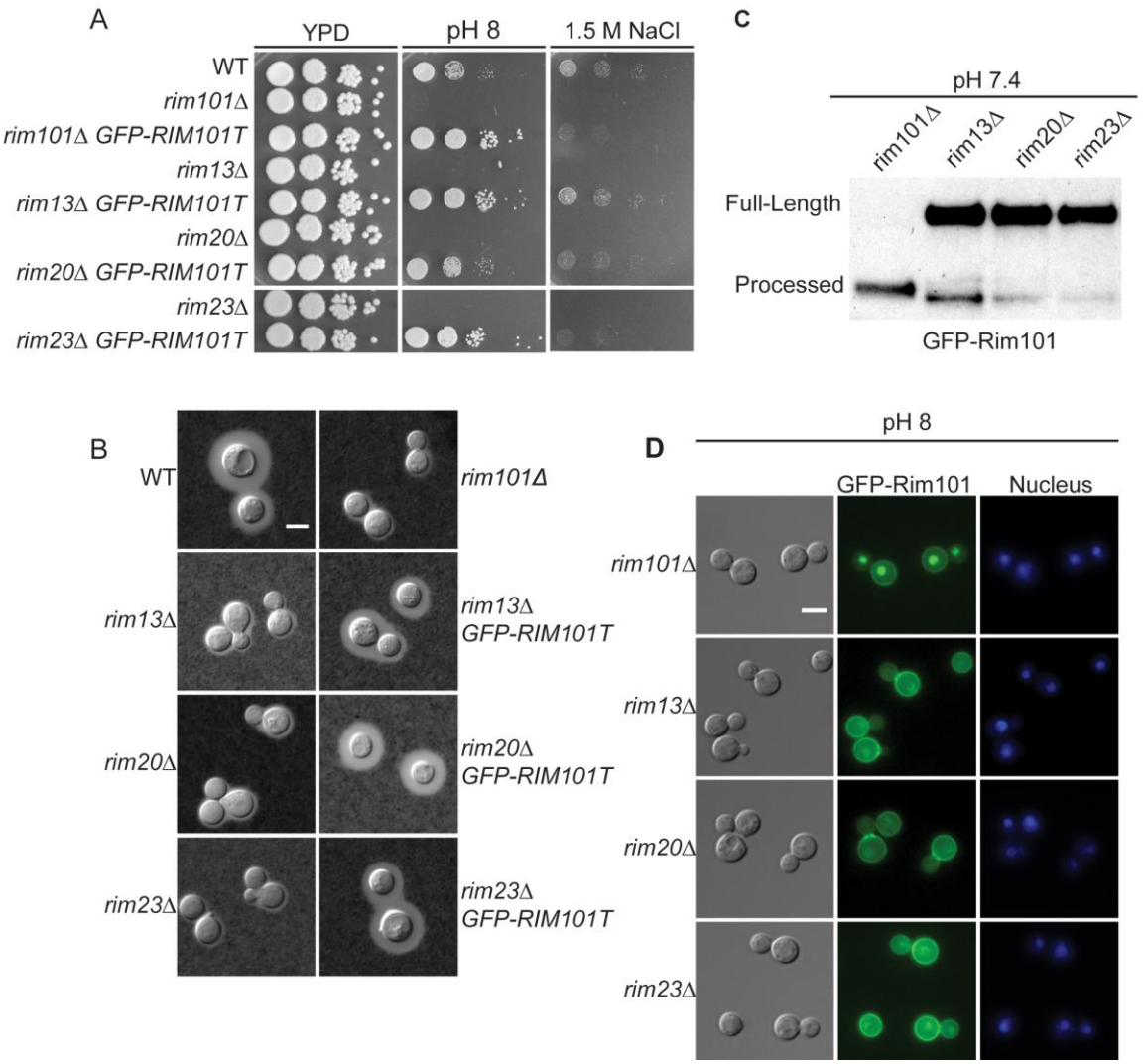

Figure 13: Role of Rim13 and Rim23 orthologs in Rim101-regulated phenotypes. (A) The *C. neoformans RIM13* and *RIM23* orthologs are required for pH 8 and NaCl tolerance. 10-fold serial dilutions of the indicated strains were spotted onto YPD, YPD 150mM HEPES pH 8, YPD 1.5M NaCl and incubated at 30ºC for 48 hr -72 hr **(B)** The *rim13Δ* and *rim23Δ* mutants have a *rim101Δ*-like capsule defect. Cells were incubated in CO_2-independent media for 48hr at 37ºC. Capsule was visualized by counterstaining with India ink. **(C)** Rim101 proteolysis and localization are disrupted in *rim13Δ, rim20Δ,* and *rim23Δ* mutant strains. GFP-Rim101 was immunoprecipitated from each strain after 5 hr incubation in pH 7.4 YPD buffered with 150 mM HEPES. **(D)** GFP-Rim101 localization was assessed in the indicated strains after culturing for 5 hr in SC medium buffered with McIlvaine's buffered to pH 8. Nuclei were stained with Hoechst 33342 live nuclei stain. Scale bar = 5 µm

To directly determine whether Rim13, Rim23, and Rim20 are upstream activators of Rim101, we assessed Rim101 proteolytic activation and nuclear localization in each mutant. All three genes were required for both GFP-Rim101 proteolysis and nuclear localization, demonstrating that Rim101 activation requires each predicted Rim pathway component (Fig.13C and D). In *A. nidulans* and *S. cerevisiae*, expression of an active Rim101/PacC protein, lacking its inhibitory C-terminal domain rescues mutations in upstream Rim pathway components [58,167]. In a similar manner, we expressed of a truncated form of *C. neoformans* Rim101, lacking the C-terminal 603 amino acids, in the *rim13Δ¸rim20Δ,* and *rim23Δ* mutant strains. In these "upstream" mutants, this constitutively active form of Rim101 (GFP-Rim101T) restores capsule formation, as well as growth on pH 8 and in the presence of 1.5 M NaCl (Fig. 13A and B).

3.2.5 ESCRT involvement in *C. neoformans* Rim pathway

In other fungi, the endosomal sorting complex required for transport (ESCRT) serves as a docking platform for Rim23, Rim20, and Rim13 proteins. Deletion of components of the ESCRT-I, -II, or -III complexes disrupts Rim101 activation [45,55,168–171]. In ascomycetes, the Rim pathway-dependent assembly of the ESCRT machinery is initiated by an interaction between the Rim8 arrestin-like protein and the ESCRT-I complex protein, Vps23. This recruits the ESCRT-II and then ESCRT-III complexes, eventually resulting in Rim101 proteolysis and activation [43,49,50].

Based on previous studies, there are several lines of evidence supporting a role for the ESCRT machinery in *C. neoformans* Rim101 activity. First, Hu et al., previously demonstrated that *vps23Δ* mutant phenotypes include sensitivity to pH 8 and 1.5M NaCl,

along with displaying a capsule defect [115]. In addition, Chun and Madhani found that Vps25, a component of ESCRT-II, was required for several Rim101-dependent phenotypes [83]. More recently, Godinho et al demonstrated that the ESCRT-III component, Snf7, was required for capsule formation and full *RIM101* transcription [172]. Rim101 induces its own transcription, which may partially explain the reason that disruption of a Rim pathway component would decrease *RIM101* transcript levels [114]. Finally, both *C. neoformans* Rim23 and Rim20 contain predicted Snf7-interacting BRO1 domains (Fig. 12).

To directly determine whether the ESCRT complex is required for Rim101 activation in *C. neoformans*, we analyzed both the *vps23Δ* and *snf7Δ* mutants for defects in Rim pathway-associated phenotypes and Rim101 activation. Consistent with previously published data, both mutants displayed a marked capsule defect (Fig. 14A). Both mutants were also sensitive to high salt and alkaline pH, similar to the *rim101Δ* mutant (Fig. 14B) We also determined that GFP-Rim101 nuclear localization and proteolysis were disrupted in the *vps23Δ* mutation (Fig. 14C and D). Similar to the *rim13Δ, rim20Δ, and rim23Δ* mutants, expression of the constitutively active, truncated GFP-Rim101T protein fully rescued the *vps23Δ* and *snf7Δ* mutant defects in growth at pH 8 and partially rescued their capsule defects (Fig. 14A and B). Unlike the other Rim pathway mutants, GFP-Rim101T did not rescue the *vps23Δ* and *snf7Δ* growth defects on high salt concentrations. Therefore, both ESCRT-I and ESCRT-III components play conserved roles in *C. neoformans* Rim101 activation and function, although they have pleiotropic roles in regulating salt tolerance and complete capsule formation.

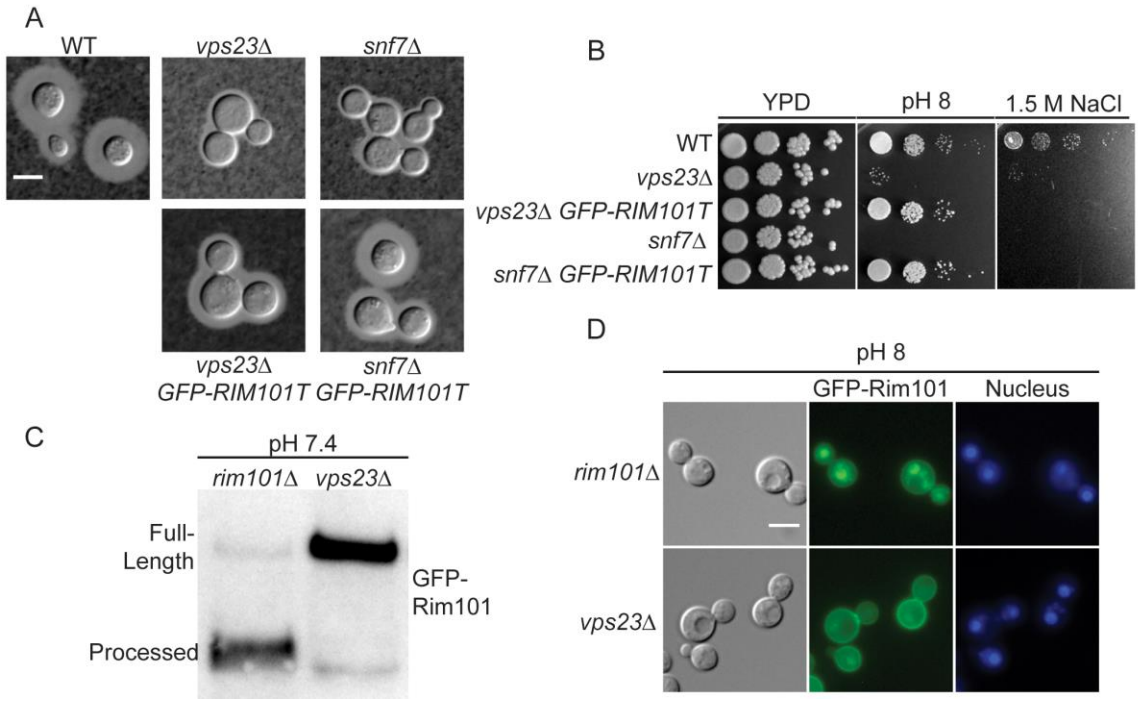

Figure 14: ESCRT complex proteins, Vps23 and Snf7, are required for Rim101 activation. (A) ***snf7Δ*** and ***vps23Δ*** capsule defects are partially rescued by *GFP-RIM101T* expression. Strains cultured for 24 hr in tissue culture media. India ink used to visualize capsule. (B) *GFP-RIM101T* expression rescues the ***vps23Δ*** and ***snf7Δ*** growth defects on pH 8 but not 1.5 M NaCl. (C) GFP-Rim101 was immunoprecipitated from the indicated strains after 5 hr incubation in YPD with 150mM HEPES at pH 7.4. (D) GFP-Rim101 (full-length) nuclear localization is disrupted in the ***vps23Δ*** mutant. Localization was assessed after culturing for 5 hr in SC with McIlvaine's buffer at pH 8. Nuclei were stained with Hoechst 33342 live nuclear stain. Scale bar = 5 μm

3.2.6 Rim pathway membrane sensing complex components are not conserved in *C. neoformans.*

In addition to the ESCRT machinery and the signaling components directly involved in Rim101 proteolytic activation, the classical ascomycete Rim pathway includes the integral membrane pH sensor Rim21/PalH, the integral membrane protein Rim9/PalI, and the arrestin-like Rim8/PalF. *S. cerevisiae* and *C. albicans* have an additional component of the Rim membrane sensing complex, Dfg16, which helps

mediate Rim21/PalH localization and is also required for Rim pathway activation [52]**.** In ascomycetes, these plasma membrane Rim signaling components are identifiable based on highly conserved sequences and protein motifs. However, Rim21/PalH, Rim8/PalF, and Dfg16 orthologs could not be easily identified in *C. neoformans* using this approach. Similar searches did not identify predicted orthologs in any basidiomycete genome [85].

We also searched for predicted proteins with arrestin-like motifs that could be acting as Rim8 orthologs in *C. neoformans*. There were two predicted *C. neoformans* proteins (CNAG_02857, and CNAG_02341) that contained both the N- and C-terminal arrestin domains present in Rim8 proteins from other fungi. These were designated *ALI1* and *ALI2* (Arrestin Like 1 and 2). Disruption of these genes individually or in combination did not affect the Rim101-dependent phenotypes of capsule formation, growth at pH 8, or growth 1.5 M NaCl (Fig. 15) suggesting that these genes are not required for Rim101 activation.

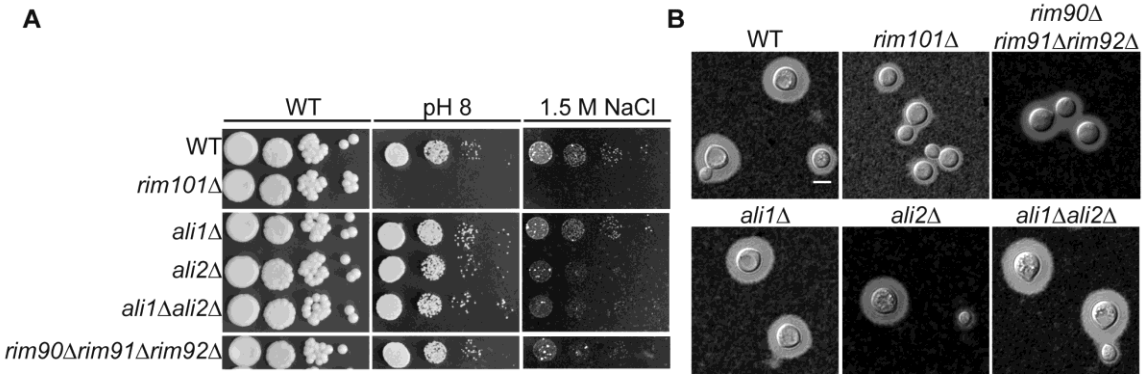

Figure 15: Predicted arrestins and Rim9 orthologs are not required for Rim101-dependent phenotypes. (A) The *ali1Δ, ali2Δ, ali1Δ ali2Δ,* and *rim90Δ rim91Δ rim92Δ* mutants grow like WT on YPD with 150 mM HEPES at pH 8 and YPD + 1.5 M NaCl. 10-fold serial dilutions of each sample were spotted onto the indicated plates. **(B)** The *ali1Δ, ali2Δ, ali1Δ ali2Δ,* and *rim90Δ rim91Δ rim92Δ* mutants do not have a capsule formation defect. Cells were cultured for 48 hr in CO_2-independent media 37^{o}C to induce capsule formation. Capsule was visualized by India ink stain.

We identified one predicted ortholog (CNAG_05654) of the Rim9 component of the sensing complex, which has a 24% sequence similarity to the *S. cerevisiae* Rim9 protein. We also identified 2 other genes (CNAG_02114 and CNAG_04953) predicted to encode proteins with homology to the SUR7/PalI domain, a defining feature of Rim9 proteins. Disruption of any of these potential *RIM9* orthologs, either separately or in combination in a triple mutant strain, did not affect Rim101-dependent phenotypes (Fig. 15).

3.2.7 Identification of novel *C. neoformans* Rim pathway component

As we were unable to identify components of the *C. neoformans* Rim pathway membrane sensing complex using sequence comparisons or searches for conserved protein domains, we designed a forward genetics screen to specifically identify novel Rim101 activators. The defining characteristic of a Rim pathway mutant is that its mutant phenotypes are rescued by expression of the constitutively active form of Rim101. Therefore, we created a strain encoding the truncated *GFP-RIM101T* allele under the control of the galactose-inducible *GAL7* promoter, and we performed *Agrobacterium tumefaciens*-mediated random insertional mutagenesis in this strain. We then selected for mutants with *rim101Δ*-like phenotypes (sensitivity to alkaline pH and 1.5 M NaCl) in the presence of glucose (repressing conditions for GFP-Rim101T expression) and wild-type phenotypes on galactose-containing media (inducing conditions for GFP-Rim101T expression).

Using this random mutagenesis approach, we identified 40 mutants with galactose-suppressible alkaline and/or NaCl sensitivities. After identifying the site of

each mutation, we recognized several disrupted genes among these mutants that were known to be required for Rim101 expression or activation. We identified one insertion in *HAPX*, which encodes a transcription factor required for full induction of *RIM101* expression [173]. In this case, galactose-induced expression of GFP-Rim101T likely rescued the defect in *RIM101* transcription, as opposed to a defect in Rim101 protein activation. We also identified an insertion in the *RIM13* gene encoding the Rim101 activating protease. These data demonstrate that this screening strategy was successful in identifying genes known to be required for Rim101 activity.

Among the additional mutants, we focused on a strain with an insertion in the CNAG_03488 locus due to its striking *rim101Δ*-like phenotypes on both 1.5 M NaCl and pH 8 (Fig. 16A and B). Furthermore, these mutant phenotypes were completely rescued by the expression of GFP-Rim101T on galactose (Fig. 16A). We confirmed these mutant phenotypes by independently disrupting the CNAG_03488 gene in the wild type H99 background (Fig. 16B). In addition to pH 8 and 1.5M NaCl sensitivity, the CNAG_03488 mutant also displayed a *rim101Δ*-like capsule defect (Fig. 16C). We complemented all mutant phenotypes by introduction of the wild type allele (Fig. 16).

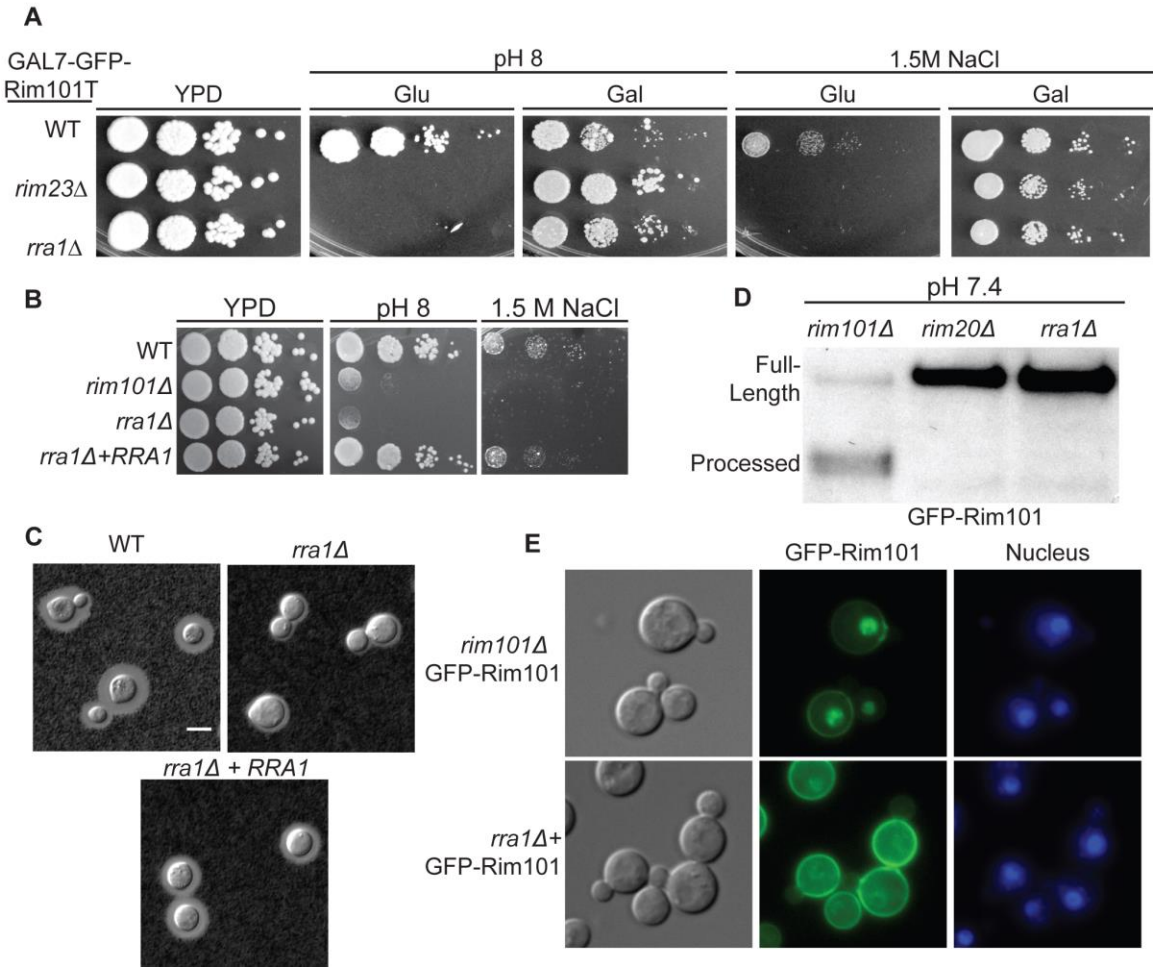

Figure 16: The *rra1Δ* mutant is phenotypically identical to other Rim pathway mutants. **(A)** *rra1Δ* insertional mutant has pH 8 and 1.5 M NaCl growth defects that are rescued by *GFP-RIM101T* expression. 10-fold serial dilutions were spotted onto YPD, YPD with 150 mM HEPES pH 8, and YPD with 1.5 M NaCl. **(B)** Independent *rra1Δ* mutant has a growth defect pH 8 and 1.5 M NaCl. **(C)** The *rra1Δ* strain has a capsule defect. Cells were cultured for 48 hr in CO_2-independent media at 37ºC to induce capsule. Capsule was visualized by India ink staining. Scale bar = 5 µm. **(D)** The *rra1Δ* mutation disrupts GFP-Rim101 proteolysis. GFP-Rim101 was immunoprecipitated from the indicated mutant strains after 5 hr incubation in YPD with 150 mM HEPES at pH 7.4. **(E)** GFP-Rim101 nuclear localization is disrupted in the *rra1Δ* mutant. GFP-Rim101 was assessed after 5 hr incubation in pH 8 SC McIlvaine's buffer.

To determine if the protein encoded by the CNAG_03488 gene was a component of the Rim pathway, we assessed GFP-Rim101 localization and proteolysis in the CNAG_03488 mutant. Like the verified activators of Rim101, CNAG_03488 was required for both Rim101 cleavage and nuclear localization (Fig. 16D and E). Based on these results, we concluded that, like *RIM13, RIM20, RIM23*, and the ESCRT complex, the novel protein encoded by CNAG_03488 is required for Rim101 activation. To reflect its role in the Rim pathway, we named this gene *RRA1* (Required for Rim101 Activation 1).

3.2.8 Rra1 is conserved throughout Basidiomycota.

To determine whether Rra1 is a *C. neoformans*-specific or conserved component of the Rim pathway, we used the predicted Rra1 amino acid sequence to search for possible Rra1 orthologs in other fungal species. We only identified Rra1 homologs in other members of the basidiomycete phylum; however, these predicted proteins demonstrated a high degree of homology to Rra1 (Fig. 17A and Fig. 18), even in distantly related members of this phylum such as *U. maydis* and *P. graminis.* We also demonstrated that Rra1 function in Rim pathway activation is functionally conserved in the divergent sibling species *Cryptococcus gattii.* Disruption of the *C. gattii RRA1* (CNBG_2126) ortholog resulted in alkaline sensitivity and a capsule defect identical to the *C. gattii rim101Δ* mutant (CNBG_4424) (Fig. 17B and C). These results demonstrate that Rra1 orthologs function in Rim101-related processes in different basidiomycete species.

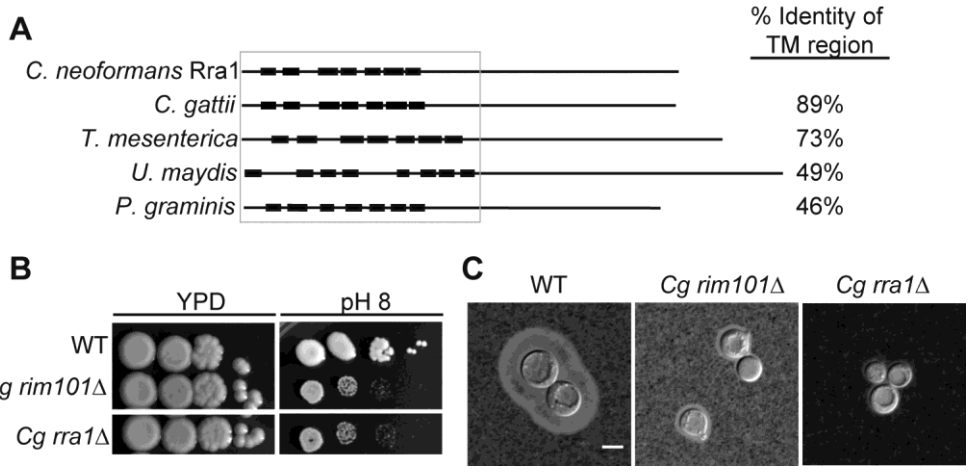

Figure 17: Rra1 is a membrane protein and is conserved through Basidiomycete fungi. (A) *C. neoformans* Rra1 and its predicted basidiomycete orthologs contain 7-8 predicted transmembrane domains (closed boxes). *C. neoformans* CNAG_03488 (Rra1), *C. gattii* CGB_G5320C, *Tremella mesenterica* TREME_69388, *Ustilago maydis* um00299, *Puccinia graminis* PGTG_03106 predicted protein sequences are modeled. The TM domains were predicted using The TMPred TM prediction server [174] The % identity to the transmembrane region of *C. neoformans* Rra1 was determined by comparing 1-290 of the predicted Rra1 amino acid sequence to each of the predicted orthologs. **(B)** *C. gattii rra1Δ* and *rim101Δ* mutants are sensitive to pH 8. **(C)** *Cg rra1Δ* and *rim101Δ* have a capsule defect. Capsules visualized with India Ink after 24 hr incubation in tissue culture media. Scale bar = 5 μm.

C. neoformans Rra1 and its predicted basidiomycete orthologs all contain 7-8 predicted transmembrane domains (Fig. 17A and Fig. 18), suggesting that they may be structurally similar to the Rim21/PalH pH sensors, which also contain 7 transmembrane domains [44] However, Rra1 does not share significant amino acid sequence homology with Rim21/PalH proteins, and direct BLAST comparisons between Rra1 and *S. cerevisiae* Rim21 and *A. nidulans* PalH produced Expected values greater than 1.

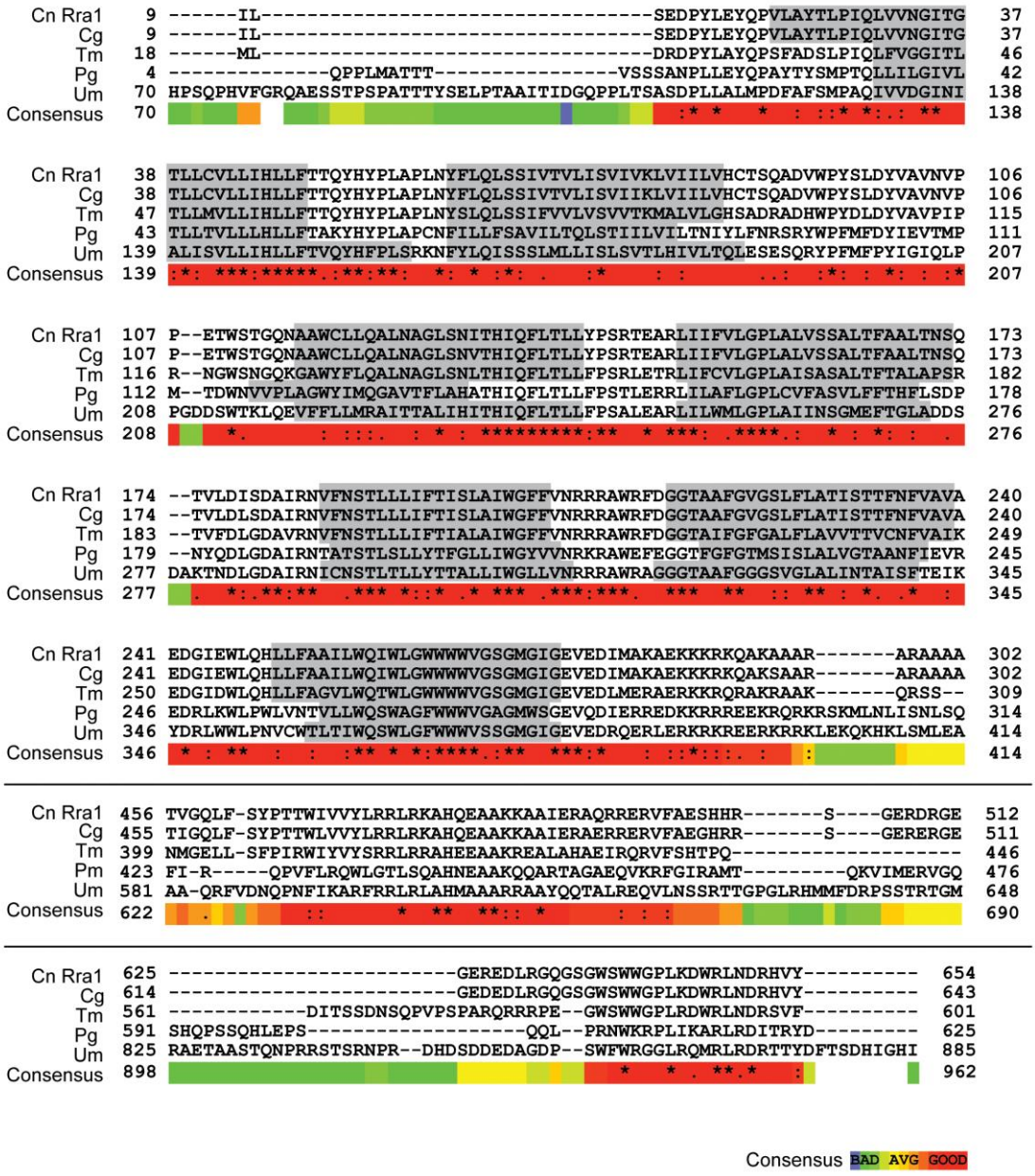

Figure 18: Alignment of the conserved regions of the basidiomycete Rra1 orthologs. The following orthologs are represented: *C. neoformans* CNAG_03488 (Rra1), *C. gattii* CGB_G5320C, *Tremella mesenterica* TREME_69388, *Puccinia graminis* PGTG_03106, *and Ustilago maydis* um00299. The gray shaded regions mark predicted transmembrane helices. The similarity between sequences is represented by color, with red representing the most similar and blue representing the least similar. The numbers indicate amino acid position [175]

3.2.9 The Rim pathway does not require Gα protein activity

With 7 predicted transmembrane domains, Rra1 could also be structurally similar to GPCR proteins (G-protein Coupled Receptors). When activated, GPCRs interact with the Gα subunit of trimetric G proteins, leading to alteration in downstream signaling. *C. neoformans* encodes three characterized Gα proteins, Gpa1, Gpa2, and Gpa3 [176,177]. To begin to explore whether Rra1 is a GPCR and signaling through any of these Gα proteins, we analyzed the *gpa1Δ, gpa2Δ, and gpa3Δ* mutants for *rim101Δ*-like phenotypes. The *gpa1Δ* and *gpa3Δ* mutants grew like wild type on both pH 8 and 1.5 M NaCl, inconsistent with defective Rim pathway signaling. The *gpa2Δ* mutant was slightly sensitive to both pH 8 and 1.5 M NaCl, but these growth defects were not as severe as those displayed by a *rim101Δ* mutant or other Rim pathway mutants (Fig. 19). Moreover, Gpa2 plays a prominent role in *C. neoformans* mating, a cellular process that does not appear to be dependent on Rim signaling in this species [177]. Therefore, Gpa1, Gpa2, and Gpa3, were not required for Rim101 activation in *C. neoformans* and these proteins do not appear to be components of the *C. neoformans* Rim pathway.

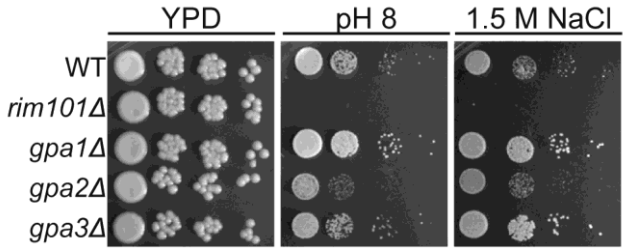

Figure 19: Role of Gpa proteins in pH 8 and 1.5 M NaCl tolerance. The indicated strains were spotted onto YPD, YPD 150mM HEPES pH 8, and YPD 1.5M NaCl and incubated for 2 – 4 days at 30°C.

3.2.10 pH-regulated Rim23-GFP localization requires Rra1 and ESCRT.

When activated, the ascomycete Rim21/PalH sensor recruits downstream Rim pathway components to punctate structures at the plasma membrane [43–45,47]. The order in which these components localize to this complex was used to establish the sequence of Rim/Pal protein activation (Fig. 10). To determine if similar pH-regulated localization changes occur in *C. neoformans*, we expressed a Rim23-GFP fusion protein, regulated by the endogenous *RIM23* promoter, in a *rim23Δ* mutant. This fusion protein was functional, fully rescuing the *rim23Δ* defects in pH 8 growth and capsule formation, and partially rescuing the 1.5 M NaCl growth defect. When incubated at pH 4, Rim23-GFP localized diffusely throughout the cell (Fig. 20A). After shifting the cells to pH 7, Rim23-GFP migrates to distinct, cell surface-associated puncta. The number of puncta/cell increased from 1 to 3.2 between 10 min and 30 min of incubation at neutral pH (Fig. 20B). These puncta appear to be on the plasma membrane or very close to the plasma membrane, co-localizing with non-endocytosed FM4-64 staining of the plasma membranes (Fig. 20C). These punctate structures formed specifically in response to elevated pH, and not to other stress conditions associated with Rim101 function, such as high salt or low iron: the GFP-Rim23-containing puncta were not observed in cells shifted to pH 4+1 M NaCl, or pH 4+150 μM BPS (Fig. 20D). Together, these data indicate that Rim23 cell surface puncta are specifically induced in response to pH signals, consistent with a role for neutral/alkaline pH in inducing Rim101 activation.

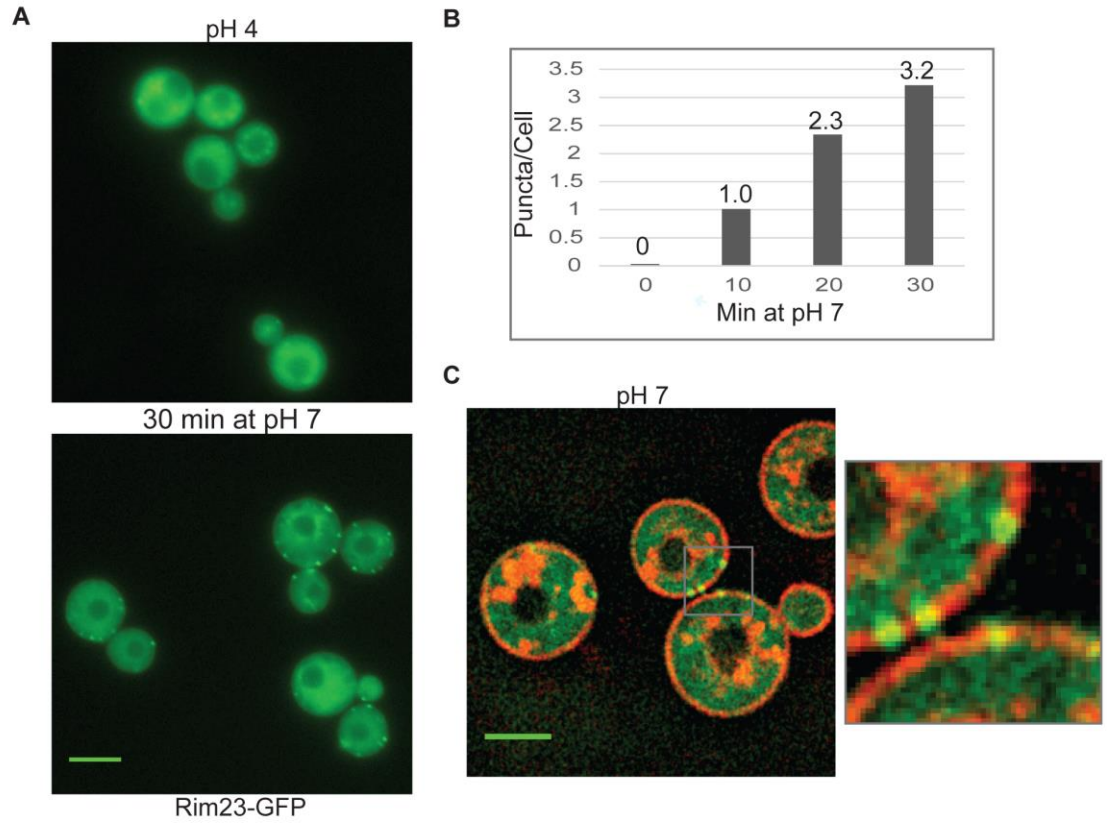
A
pH 4
30 min at pH 7
Rim23-GFP
B
Puncta/Cell
3.5
3
2.5
2
1.5
1
0.5
0
0
1.0
2.3
3.2
0
10
20
30
Min at pH 7
C
pH 7

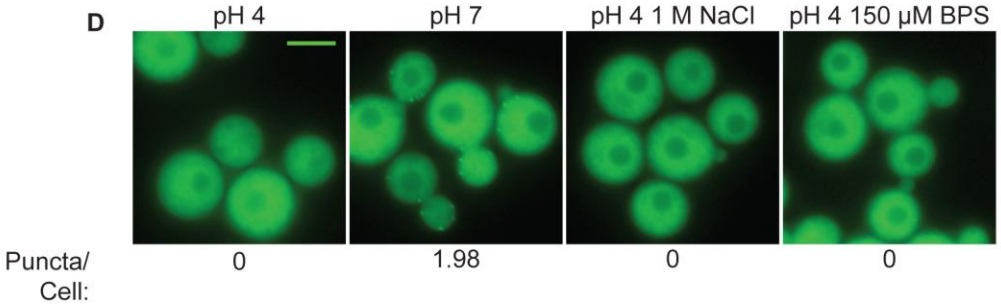
D
pH 4
pH 7
pH 4 1 M NaCl
pH 4 150 µM BPS
Puncta/ Cell:
0
1.98
0
0

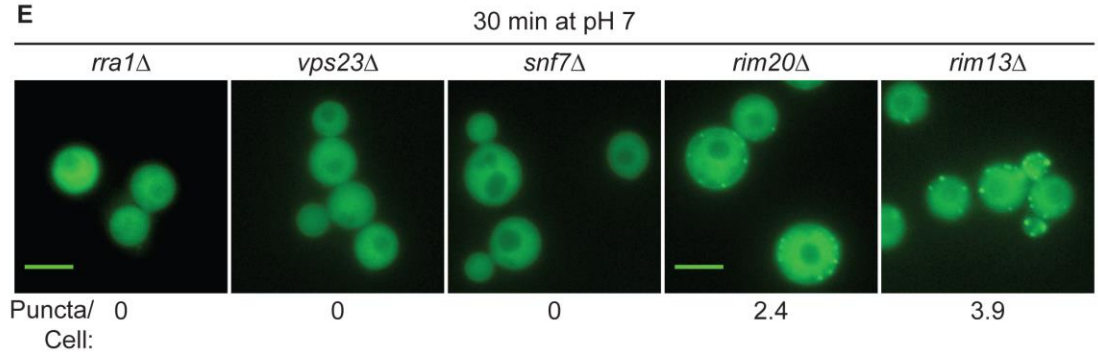
E
30 min at pH 7
rra1Δ
vps23Δ
snf7Δ
rim20Δ
rim13Δ
Puncta/ Cell:
0
0
0
2.4
3.9

Figure 20: Rim23-GFP forms plasma membrane-associated puncta under neutral/alkaline pH conditions. (A) Rim23-GFP was visualized at pH 4 SC McIlvaine's buffer and after 30 min after shift to pH 7 SC McIlvaine's buffer. **(B)** The number of Rim23-GFP puncta increase with time after shifting from pH 4 to pH 7. Quantification Rim23-GFP puncta/cell at pH 4 (0 min) and after 10, 20, 30 min incubation at pH 7. **(C)** Rim23-GFP puncta are closely associated with the plasma membrane. Cells were stained with FM-464 after 1 hr incubation at pH 7. **(D)** 1 M NaCl and 150 µM BPS does not induce Rim23-GFP puncta formation. Cells images after 30 min incubation in indicated culture media. **(E)** Rim23-GFP puncta formation was disrupted by *rra1Δ*, *vps23Δ*, and *snf7Δ* mutants. Cells were imaged after 30 min incubation at pH 7. The number of puncta/cell was quantified for 62-100 cells/strain. All strains in this figure were cultured in SC McIlvaine's buffer media. All scale bars = 5 µm.

We next determined which components of the Rim pathway were required for the observed Rim23-GFP plasma membrane localization. Neither Rim20 nor Rim13, other members of the Rim proteolysis complex, were required for Rim23-GFP cell surface puncta formation. However, pH-driven Rim23 localization to surface punctate structures did not occur in the *rra1Δ, vps23Δ* and *snf7Δ* mutants (Fig. 20E). Therefore, Rim20 and Rim13 are not required for Rim23 localization, while both the ESCRT pathway proteins and Rra1 are functionally upstream of Rim23-puncta formation.

3.2.11 Rra1 localizes to punctate structures near the plasma membrane and endomembranes.

To determine the localization of Rra1, a Rra1-GFP fusion construct was introduced into the *rra1Δ* mutant, under the control of the constitutive *HIS3* promoter. The Rra1-GFP fusion was functional and it rescued all *rra1Δ* mutant phenotypes (data not shown). Cells incubated at pH 4 demonstrated fluorescent protein localization in punctate regions of both plasma and endomembranes (Fig. 21A). 3D projection of Z-stacked images demonstrates numerous, prominent Rra1-GFP punctate structures. Pseudo-coloring, which shows the brightest staining in yellow and dimmest in blue,

demonstrates that the Rra1-GFP puncta are the brightest sites of localization (Fig. 21A). These punctate structures were still prominent after the cells were shifted to pH 7. There was no obvious alteration the Rra1-GFP staining pattern at pH 7.

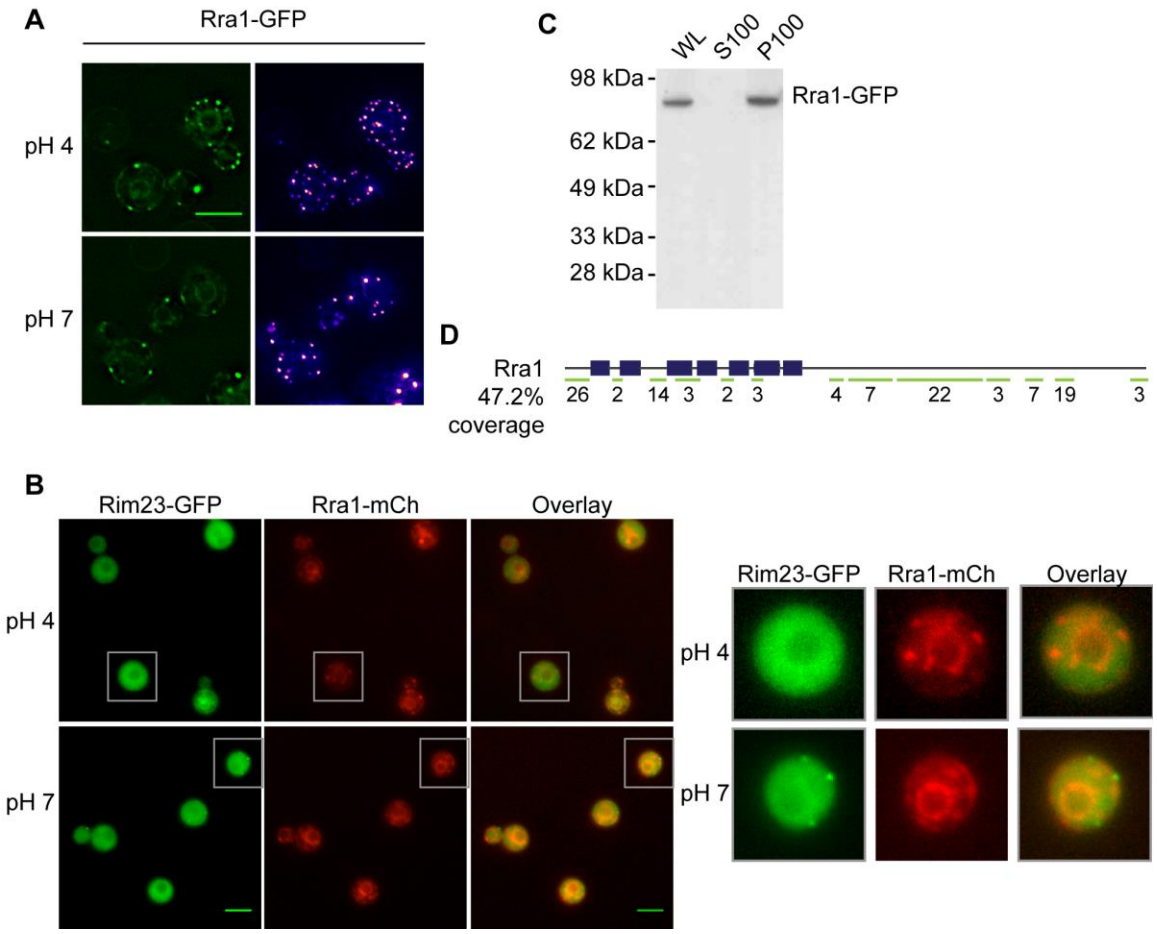

Figure 21: Rra1 localizes to plasma membrane and intracellular punctate structures that do no colocalize with Rim23. A) Localization was assessed after culturing in pH 4 SC and after 1 hr. of incubation in pH 7 SC. 3D projections are pseudo-colored to show the brightest staining in yellow and least bright in blue. **B)** rra1Δ rim23Δ Rra1-mCherry Rim23-GFP cells were incubated in SC pH 4, imaged, and then imaged after shifting the cells to pH 7 SC for 30 min. Scale bars = 5 µm. **C)** Rra1-GFP is present in cellular membranes. Fractionation performed on cells that had been cultured at pH 8 for 1 hr. WL = whole lysate control, S100 = soluble fraction, P100 = insoluble pellet fraction. Rra1-GFP band detected by using an anti-GFP antibody. **D)** MS/MS analysis of Rra1 after Rra1-GFP digestion with chymotrypsin. Green bars show region of peptide coverage with the number of identified peptides found for each region. Rra1-GFP was immunoprecipitated from cells cultured for 1 hr in pH 8 YPD 150mM HEPES. Rra-GFP immunoprecipitated from the membrane fraction.

3.2.12 Rim23 does not co-localized with Rra1 under activating pH conditions.

The Rra1-GFP punctate localization near the plasma membrane appears similar to Rim23-GFP localization at under activating pH. To determine whether Rim23 and Rra1 co-localize to the same punctate structures, we analyze Rim23-GFP and Rra1-mCherry localization at both pH 4 and pH 7 (Fig. 21B). At both pH 4 and pH 7 Rra1-mCh localized to punctate structures and to endomembranes. Like previously observed, Rim23-GFP moved to plasma membrane-associated punctate structures when shifted to pH 7. At pH 7, we did not observe Rim23-GFP and Rra1-mCherry co-localization in any cells imaged. This result suggests that Rra1 is not present in the Rim101 processing complex, marked by Rim23-GFP that forms in response to neutral to alkaline pH.

3.2.13 Full-length Rra1-GFP is present in the membrane fraction

Constitutive expression of membrane proteins can lead to mislocalization and degradation [46], making it difficult to determine the true localization. This phenomenon complicated the original localization studies on PalH in *A. nidulans,* where PalH was originally shown to localize to intracellular punctate structures [46]. This localization was later shown to be an artifact of overexpression, and PalH, with the help of PalI, localizes to the plasma membrane. There are several lines of evidence suggesting that Rra-GFP localization is not an artifact. As mentioned before, Rra1-GFP is fully functional, indicating that enough of the protein localizes to the appropriate location. Mis-localized or surplus Rra1-GFP would likely be degraded. To analyze Rra1-GFP stability, we analyzed Rra1-GFP by western blot from cells cultured for 1 hr at pH 8. Using an anti-GFP antibody, Rra1-GFP was detected primarily in one band at 90 kDa with no

prominent smaller MW bands that would indicate protein degradation. We also fractionated the lysate into a soluble fraction and the insoluble membrane fraction. The Rra1-GFP band was present exclusively in the insoluble membrane fraction (P100 Fig. 21C), demonstrating that Rra1-GFP localizes to cellular membranes. To determine whether this prominent Rra1-GFP band represents the full-length protein, we immunoprecipitated Rra1-GFP from the membrane fraction and analyzed the protein sequence using mass spectrometry. We identified peptides for all expected protein fragments that spanned 47.2% of the protein sequence (Fig. 21D). Identified peptides covered both the N and C-terminus, demonstrating that the entire protein is present in the 90 kDa band. These data demonstrate that despite over-expression, Rra1-GFP is stable and is localized to cellular membranes.

3.2.14 Membrane localization of the Rra1 C-terminus is regulated by pH.

Recent work on Rim21 in S. cerevisiae demonstrated that this pH sensor may detect alterations in charge of the cytoplasmic leaflet of the plasma membrane. Disrupting the inner leaflet charge by mutating flippases or floppases genes that regulate lipid charge asymmetry induces Rim101 activation independent of pH [43,47,178,179]. While the mechanism is still being elucidated, a recent study found that the Rim21 C-terminus interacts with the plasma membrane under acidic culture conditions but not under alkaline conditions [178]. To determine whether the Rra1 C terminus behaves similarly, we expressed the C-terminal 273-655 amino acids, which was N-terminally tagged with GFP, under the regulation of the constitutively expressing *HIS3* promoter (Fig. 22A). We then analyzed the localization of GFP-CtRra1 at both pH 4 and after

shifting to pH 8 for 30 min (Fig. 22B). At pH 4, we observed prominent plasma membrane staining with some endomembrane staining. The fluorescence intensity plot for one cell demonstrates that the brightest GFP-CtRra1 staining was at the cell edges, consistent with PM staining. After shifting the cells to pH 8, we observed a marked decrease in plasma membrane staining. In these cells, GFP-CtRra1 localized faintly to the plasma membrane but also with increased cytoplasmic, endomembrane, and intracellular punctate localization. A fluorescence intensity plot of one cell demonstrates that most of the GFP-CtRra1 fluorescence was concentrated in the cytoplasm. These results demonstrate that, like Rim21, the Rra1 C-terminus interacts with the plasma membrane in a pH dependent manner.

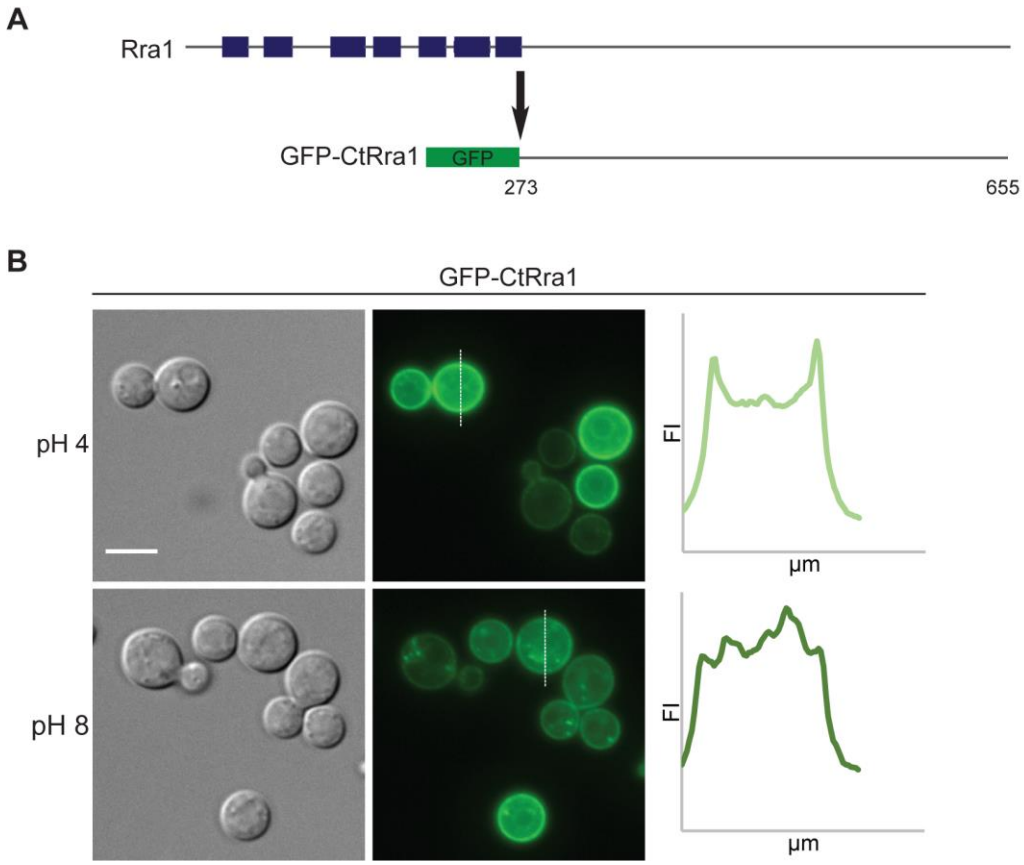

Figure 22: The Rra1 C-terminus displays pH dependent plasma membrane localization. A) GFP-CtRra1 diagram. **B)** WT cells expressing GFP-CtRra1 were cultured overnight in pH 4 SC, transferred to either fresh pH 4 SC or pH 8 SC for 30 min. The fluorescence intensity (FI) values were plotted along the dotted white line for each image. FI values were measured using FIJI. Scale bars = 5 µm

3.2.15 The majority of the Rra1 C-terminus is dispensable for alkaline pH tolerance.

To determine the function of the Rra1 C-terminus, we expressed Rra1 lacking the C-terminal 359 (296T) or 382 (273T) amino acids. The 273T form lacks all amino acids that follow the last transmembrane domain while the 296T form contains 23 amino acids following this TM domain (Fig. 23A). These 23 amino acids are highly conserved throughout Rra1 orthologs in other basidiomycete fungi and consist primarily of positively

and negatively charged amino acids. We C-terminally tagged each form with GFP, expressed them in the *rra1*Δ mutant under the control of the *HIS3* promoter, and analyzed their ability to rescue *rra1*Δ mutant growth on pH 8 and 1.5 M NaCl. Unexpectedly, we found that 296T-GFP fully rescued growth at pH 8, but did not rescue growth on 1.5 M NaCl (Fig. 23B). The 273T-GFP form rescued neither pH 8 nor 1.5 M NaCl growth. Rescue by 296T-GFP did not require overexpression, as endogenous expression of 296T, tagged with 4FLAG, also rescued pH 8 growth. In this strain, Rim101 localized to the nucleus at pH 7, indicating that Rim101 is likely proteolytically activated in the 296T-4FLAG strain (Fig. 23C).To determine whether Rra1 truncation altered the cellular localization of these proteins, we compared 273T-GFP and 296T-GFP localization to the full-length Rra1-GFP localization at pH 4 and pH 7. Like the full-length protein, each truncation localized to endomembrane structures that resemble nuclear and cortical ER (Fig. 23D). However, both truncations displayed fewer punctate structures that prominent in cells expressing full-length Rra1-GFP. This may indicate that the C-terminus is required for cellular localization or oligomerization. Together, these results demonstrate that the C-terminus is largely dispensable for Rra1 function and that the conserved region of charged residues following the 7th TM domain serves an essential role in Rra1 function.

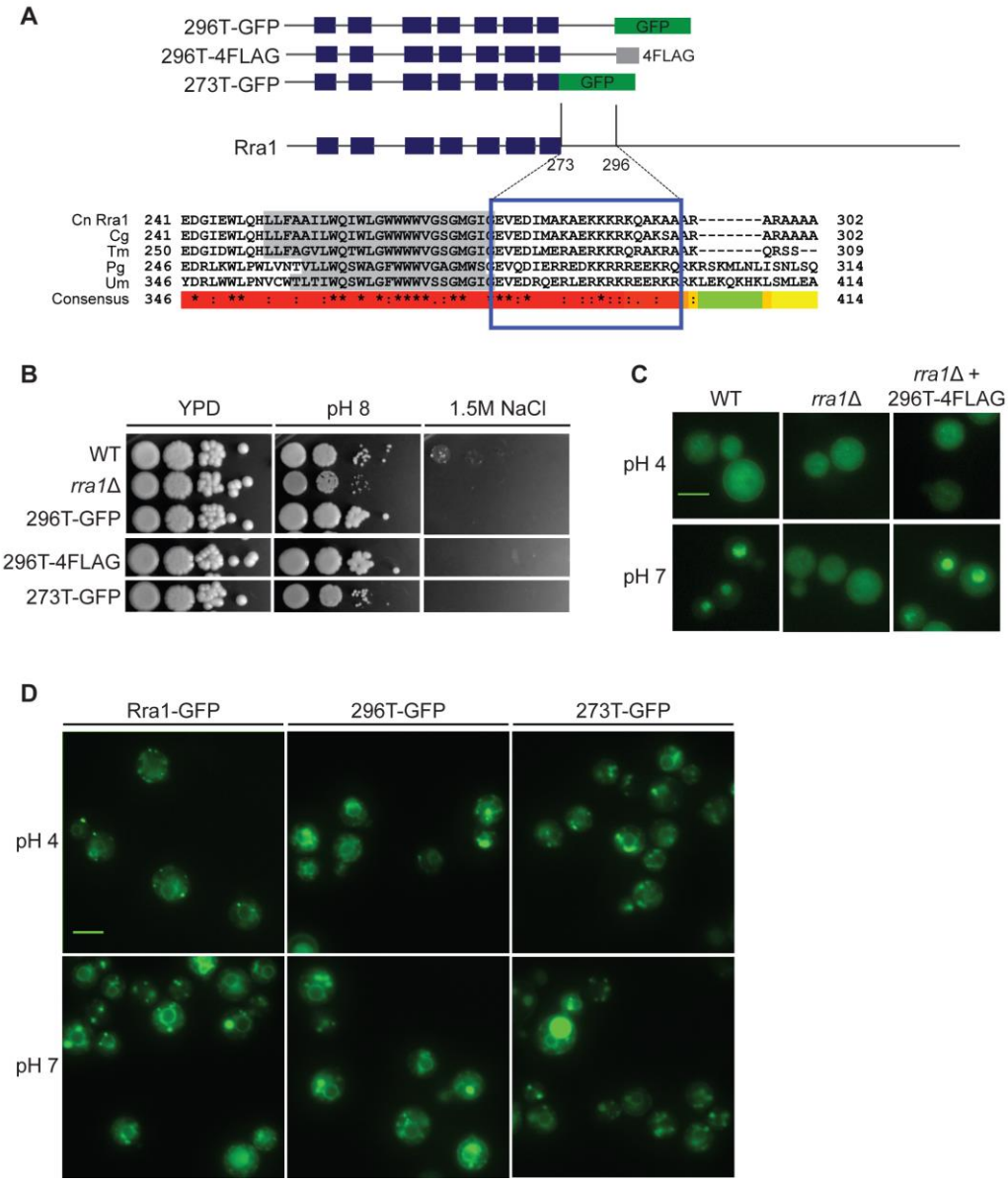

Figure 23: Rra1 C-terminus is dispensable for alkaline pH tolerance but not for concentrated NaCl tolerance. A) Diagram of the 296T-GFP, 296T-4FLAG, and 273T-GFP truncations. **B)** Spot dilution plate of WT, *rra1*Δ, *rra1*Δ + 296T-GFP, *rra1*Δ + 296T-4FLAG, *rra1*Δ + 273T-GFP. 10-fold serial dilutions were spotted onto indicated media and incubated at 30°C for 2-5 days. **C)** GFP-Rim101 localization in rra1Δ + Rra1-296T-4FLAG was assessed after a 1 hr incubation in pH 4 or pH SC media. **D)** Localization of Rra1-GFP, 296T-GFP, and 273T-GFP were compared to Rra1-GFP after 30min incubation in pH 4 or pH 7 SC. Scale bars = 5 µm.

3.2.16 Rim pathway mutants induce an increased inflammatory response during infection.

During infection, *C. neoformans* Rim101 regulates the expression of several genes involved in cell wall synthesis and maintenance by directly binding to elements in their promoters [114,117]. In the absence of Rim101-directed cell wall maintenance, the *rim101Δ* strain induces a hyper-inflammatory response in the lungs of infected mice. In this way, infection with this attenuated strain results in the paradoxical death of the host. We previously demonstrated that Rim101 activity is also regulated by the PKA/cAMP pathway, and *pka1Δ* mutant displays cell wall changes similar to the *rim101Δ* mutant [114,117]. As Rim101 activation is regulated by both the cAMP/PKA pathway and the Rim pathway, we examined whether mutations in other components of the Rim pathway were sufficient to alter virulence in a murine inhalation model of cryptococcosis. For each strain, 8-10 A/J mice were intranasally inoculated with $5x10^4$ *C. neoformans* cells. Mice were monitored daily and sacrificed when they displayed symptoms of disease consistent with imminent death. In each experiment, all mice infected with the wild type died between 18-20 days. In contrast to the mice infected with the wild type and reconstituted strains, all mice infected with the *rim13Δ*, *rim23Δ*, or *rra1Δ* mutant cells succumbed to the infection by day 12 (Fig. 24A). This statistically significant decrease in survival ($p>0.001$) was consistent with the mortality of mice infected with a *rim101Δ* mutant [81,117]. Both the *rim13Δ+RIM13* and *rra1Δ+RRA1* reconstituted strains resulted in animal mortality at a rate very similar to WT. The *rim23Δ+RIM23* reconstituted strain displayed a mild delay in virulence, which we subsequently found was likely due to a temperature sensitive phenotype specific only to this isolate. An independent

rim23Δ+RIM23 isolate without a temperature-sensitive phenotype was used for the rest of these experiments.

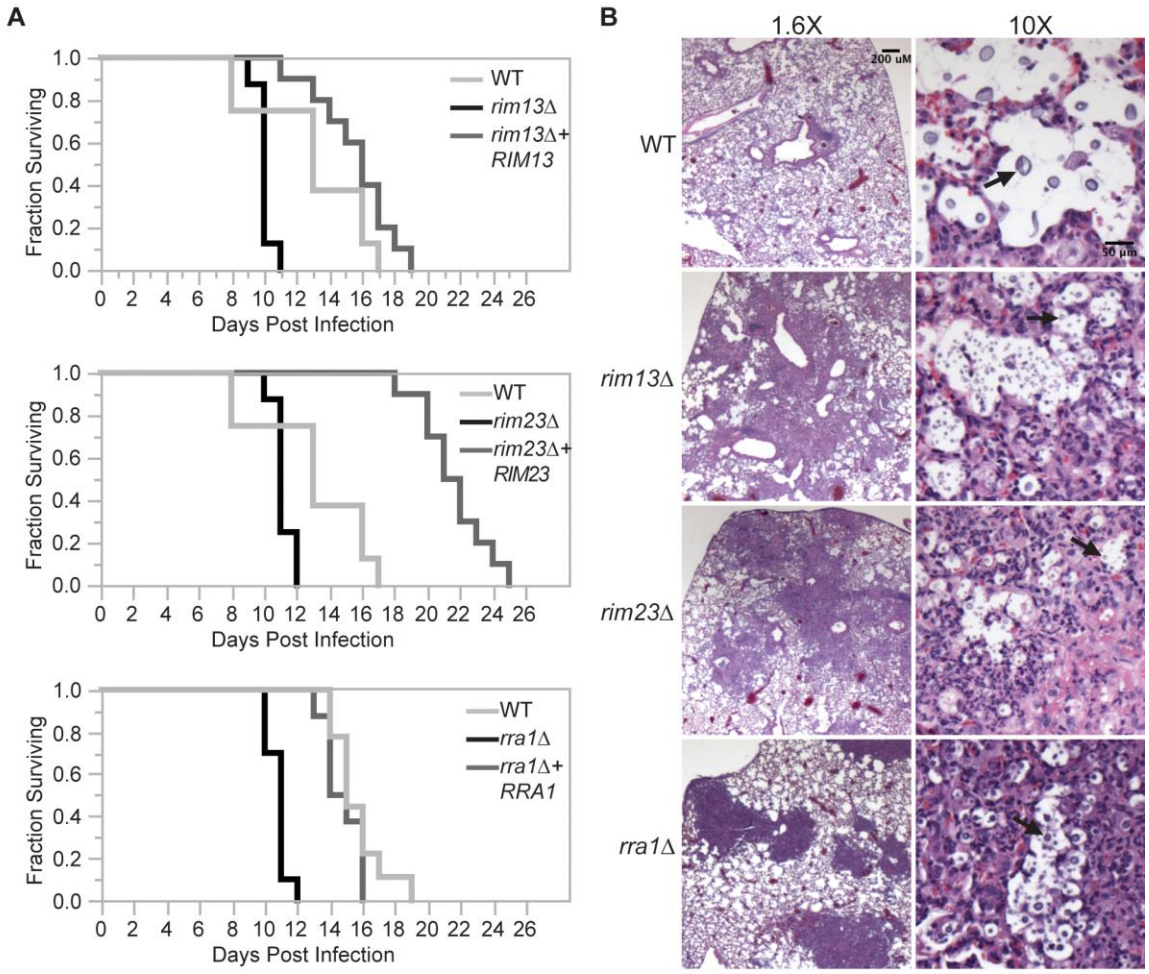

Figure 24: Effects of Rim pathway mutants on virulence. (A) *rim13Δ, rim23Δ,* and *rra1Δ* mutants are hypervirulent in a murine model of cryptococcosis. 8-10 A/Jcr female mice were intranasally inoculated with $1X10^5$ cryptococcal cells and monitored daily for survival. **(B)** Histopathological analysis revealed increased inflammatory cell infiltration in Rim-pathway mutants. Infected A/Jcr mouse lungs were harvested on day 7 post inoculation and H & E stain. Black arrows mark *C. neoformans* cells.

Like the *rim101Δ* mutant, the *rim13Δ, rim23Δ,* and *rra1Δ* mutants induced an increased infiltration of inflammatory cells in the lungs of infected mice. Histologic examination of infected mouse lungs 7 days after infection revealed that, unlike the lungs infected with wild type, those infected with Rim pathway mutants were characterized by diffuse regions of intense inflammatory cell infiltration (Fig. 24B). This type of inflammation is consistently observed in mice infected with the *rim101Δ* mutant strain [117]. These results suggest that the immune system recognizes other Rim pathway mutants in a similar manner to a *rim101Δ* mutant.

The histopathological images also allowed us to analyze size and morphology of the *C. neoformans* cells. In the wild type infected lungs, there were numerous titan-sized cells [28,29]. In contrast, the *rim13Δ*, *rim23Δ*, and *rra1Δ* mutant cells were noticeably smaller in size (Fig. 24B). Therefore, like *rim101Δ*, these mutants also have a defect in titan cell formation in vivo [82]. Together, these results are consistent with a model in which Rim13, Rim23, and Rra1 act as mediators of Rim101 activation in the context of infection.

3.3 Discussion

In this study, we identified both conserved and novel components of the *C. neoformans* Rim pathway. Based on our results as well as investigation of this pathway in other fungi, we propose the model in Fig. 25 for Rim101 activation in *C. neoformans.* In response to neutral/alkaline pH, both the newly discovered Rra1 membrane protein and the ESCRT –I, -II, -III complex proteins control Rim23 relocation to punctate structures on the plasma membrane. In addition to Rim23, the other components of the

Rim101 proteolysis complex are also functionally conserved in *C. neoformans.* Proteolysis enhances Rim101 nuclear localization, where it acts as both a transcriptional activator and repressor of a large group of genes, some of which are necessary for adaption to neutral/alkaline pH [114,117].

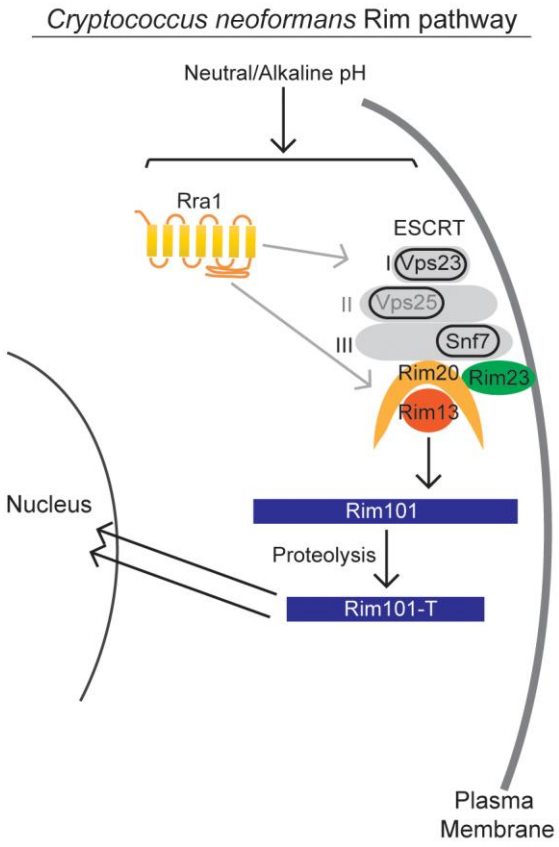

Figure 25: Model of *C. neoformans* Rim pathway. Our data supports a model in which the Rim pathway is activated by neutral/alkaline pH. In this pathway, the newly discovered Rra1 membrane protein and the ESCRT complex, including Vps23 (ESCRT-I) likely Vps25 (ESCRT-II) and Snf7 (ESCRT-III), induce Rim23 puncta formation and activate the Rim101-proteolysis complex. The Rim13 protease cleaves the Rim101 transcription factor, inducing its nuclear localization. Active Rim101 then transcriptional changes necessary for adapting to alkaline pH.

While the *C. neoformans* Rim pathway is required for responding to several stressful conditions, our results suggest that it is specifically activated by increased pH. We found that neither iron limitation nor high NaCl concentrations could alone induce Rim101 processing. In contrast, increasing pH resulted in a dose-dependent increase in Rim101 proteolytic processing and nuclear localization. The marginally increased intensity of GFP-Rim101 nuclear staining under iron limitation was likely due to increased levels of full-length Rim101; which may possess some intrinsic signaling activity. Rim101 transcription is activated by iron-responsive transcription factors, such as HapX, which themselves are activated by this low-iron growth condition [173] The exact mechanism of Rim pathway pH sensing is still largely unknown in any system, although recent research in *S. cerevisiae* Rim signaling suggests that altered membrane polarity serves as at least one of the pathway activating signals [47,179].

The ascomycete Rim101/PalC proteolysis complex consists of Rim23/PalC, Rim20/PalA, and Rim13/PalB. Upon pathway activation, these proteins are recruited by the ESCRT complex to plasma membrane puncta [43,45,47]. We demonstrate here demonstrate that the Rim101 proteolysis complex is functionally conserved in *C. neoformans* and is likely assembled and localized similarly to the ascomycete Rim101/PacC proteolysis complex. In addition to the required role of Rim23, Rim20 and Rim13 in Rim101 activation, we demonstrated that Rim23 is recruited to plasma membrane puncta when the pathway is activated. Rim23 is likely recruited to these punctate structures through an interaction with the assembled ESCRT machinery. The majority of the Rim23 protein sequence consists of the conserved Snf7-interacting domain, which likely facilitates an ESCRT-III/Rim23 interaction. Further supporting this

model, both Vps23 (ESCRT-I) and Snf7 (ESCRT-III) were required for Rim23 puncta formation. The same Snf7-interacting domain is also present in the Rim20 amino acid sequence, indicating that, like in ascomycetes, both Rim23 and Rim20 interact with the assembled ESCRT-III complex in *C. neoformans.* [43–45]. Taken together, our results suggest that the *C. neoformans* Rim101 proteolysis complex is recruited to the plasma membrane after Rim pathway activation and organized in a similar manner to the ascomycete Rim101 proteolysis complex.

The role of the *C. neoformans* ESCRT complex in Rim101 activation has been suggested by several studies on ESCRT components [115,172,180]. We demonstrated that at least two documented ESCRT-mutant phenotypes, alkaline pH sensitivity and a capsule formation defect, result from failed Rim101-activation. This suggests that other ESCRT-dependent processes, such as heme acquisition [115], may also be dependent on the Rim pathway. However, we also observed that the ESCRT complex regulates multiple processes independent of Rim101 activation. First, the *vps23Δ* and *snf7Δ* mutants displayed NaCl sensitivity that was more severe than other Rim pathway mutants, and this was not rescued by expression of the constitutively active Rim101T. Furthermore, constitutively active Rim101T expression only partially rescued the *vps23Δ* and *snf7Δ* capsule defects. Perhaps the most striking difference between the ESCRT mutants and other Rim pathway mutants is their differing roles in pathogenesis. Unlike the Rim pathway mutants, which are hypervirulent in a murine inhalation infection model, both *snf7Δ* and *vps23Δ* mutants are avirulent [115,172]. These more severe ESCRT mutant phenotypes reflect the multiple roles the ESCRT machinery serves in *C. neoformans* biology and pathogenesis.

Prior to this study, the only identified basidiomycete Rim pathway components were identified based on sequence similarity to components of the ascomycete Rim/Pal pathway [84,85]. This strategy failed to identify the most upstream Rim pathway components in both *U. maydis* and *C. neoformans* or other members of this phylum. In this study, we performed a forward genetics screen and identified a novel component of the *C. neoformans* Rim pathway. This novel protein, Rra1, is functionally conserved in at least one related basidiomycete, *C. gattii,* and is conserved at a sequence level in more distantly related basidiomycetes. Rra1 is required for all Rim101-dependent phenotypes and is functionally upstream of the pH-regulated subcellular localization of the Rim101 proteolysis complex protein, Rim23. Unlike the ESCRT complex components, disruption of *RRA1* did not lead to additional, non-Rim101 dependent phenotypes, suggesting that Rra1 functions specifically in Rim pathway activation.

While the exact function of Rra1 is unknown, it has several characteristics that suggest that it may function as a Rim pathway pH sensor. Like the ascomycete Rim21/PalH pH sensor, Rra1 was required for Rim23 puncta formation [45]. In addition, Rra1 contains 7 predicted TM domains and its C-terminus associates with the plasma membrane in a pH dependent manner. It was shown that at least two Rim21 C-terminal motifs containing positively and negatively charged amino acids facilitate membrane localization and alkaline-induced dissociation in *S. cerevisiae* [178]. While Rra1 does not share significant amino acid sequence homology with Rim21/PalH protein, its C-terminus contains a stretch of highly conserved charged amino acids immediately following the 7th predicted TM domain. This domain is required for Rra1 function, though it is still unknown whether this region is involved in membrane interaction.

Despite its similarities to Rim21/PalH, Rra1 also had a number features that suggest it is functionally distinct. First, Rra1 does not co-localize with Rim23 punctate structures under activating conditions, suggesting the Rim101 proteolysis complex does not physically interact with Rra1. While it is possible that some of the Rra1-GFP localization is an artifact of overexpression, it is both stable and functional in cells cultured in alkaline conditions, making this possibility unlikely. In addition to having distinct cellular localization, much of the Rra1 C-terminus is not required for responding to alkaline pH. Rim21/PalH requires its C-terminus to interact with Rim8/PalF and other downstream Rim pathway components, making it an essential part of the protein. In contrast, the Rra1 C-terminal 359 amino acids were dispensable for Rim101 activation in response to alkaline pH. However, this domain was required for growth on concentrated NaCl. It is possible that the Rim pathway response to pH and ion are regulated by different regions of Rra1 and the C-terminus may be an interaction site for an unknown Rim component that functions only during cation and alkaline pH stress. This region may also serve to regulate Rra1-Rra1 interactions as the Rra1-GFP truncations displayed fewer punctate structures evident in the cells expressing full-length Rra1-GFP.

The data presented here demonstrates that the true function of Rra1 has yet to be determined. It is possible that Rra1 serves as an intracellular pH sensor on the vacuolar, ER, or Golgi membrane, which are all known sites of pH-sensing and pH homeostasis [181,182]. Rra1 could also sense alterations in lipid charge and asymmetry and more work is needed to determine if disruption of flip and/or floppases, such as Dnf1 or Dnf2**,** activate Rim101 activation in *C. neoformans* [178]**.** It is also possible that Rra1 serves a different purpose in Rim pathway activation. Like Dfg16 in *S. cerevisiae,* Rra1

may serve a supportive role in the proper localization of the Rim pathway pH sensor [43,47,52]. Further studies on this novel protein will significantly advance our understanding of how *C. neoformans,* and other basidiomycetes sense pH.

Other components of the *C. neoformans* Rim membrane sensing complex remain elusive. None of the three potential Rim9/PalI orthologs nor the two candidate Rim8/PalF arrestin-like proteins were required for Rim pathway activation. Given the Rra1 structural similarity to GPCRs, we also examined whether the Rim pathway could signal through a canonical Gα protein, but none of the three known Gα proteins were required for Rim pathway activation. More extensive genetic screens will likely identify additional components for the *C. neoformans* Rim pathway, including cell surface chaperones and linking proteins.

The role of the Rim pathway in *C. neoformans* pathogenesis is complex. First, this pathway is required for *C. neoformans* survival in the host and *rim101Δ* mutants are rapidly and efficiently cleared in animal models of infection. Mechanistically, we have demonstrated that Rim101 is required for survival in the face of specific conditions found in micro-niches of the host; alkaline pH, iron deprivation, salt stress. Paradoxically, while these attenuated strains are poorly viable, they simultaneously induce an overly exuberant immune response. This is likely due to failed organization of the cell wall-masking phenotype and exposure of highly immunogenic epitopes. Interestingly, in human cases of cryptococcal meningitis, transcriptional studies of the pathogens at the site of infection demonstrate that *RIM101* transcripts are among the most highly induced during infection [183]**.** These previous studies suggested that Rim101-regulated cell wall changes in *C. neoformans* may be induced by the cAMP/Pka1 pathway. Here, we show

that other elements of the Rim pathway are also required for Rim101-mediated interactions with the host.

In this study, we have provided the most thorough investigation of the Rim pathway in any basidiomycete fungus. Together, these data demonstrate the importance of microbial adaptation to environmental and host-specific signals for pathogen survival. Additionally, they further enrich our understandings of pathogen adaptation and host immune recovery to minimize host damage during infections.

3.4 Materials and Methods

3.4.1 Strains, media, and growth conditions

Gene loci analyzed in this study are shown in Table 3.The strains used in this study are shown in Table 4. The *C. neoformans* H99 Matα genetic background was used to create each mutant and fluorescent strain [184]. Unless otherwise stated, cells were grown in YPD (1 % yeast extract, 2 % peptone, 2 % dextrose) [134]. To create the *eGFP-RIM101* strains (KS88-2, KS87-2, and KS118) each mutant strain was crossed with KN99 Mat**a** on MS mating media [135]. Spores were isolated by microdissection and recombinant spores were identified by PCR and nourseothricin (*NAT*) or neomycin (*NEO*) resistance. The resulting Mat**a** mutant strains were crossed with *rim101Δ* + *GFP-RIM101* (TOC105) and recombinant spores were isolated by microdissection. The *rim90*△ *rim91*△ *rim92*△ (KS136) strain was created by first creating *rim91Δ rim92Δ* MAT**a** KS117 and crossing it with the KS63 strain. The *GAL7-RIM101 70T* strains were created by crossing *rim23Δ* + *GAL7-RIM101 70T* (KS159) with KN99 Mat**a** and isolating recombinant progeny. The KS161 strain was identified by PCR and phenotype.

Table 3: Chapter 3 Gene Loci

Genes	CNAG number	GeneBank
RIM13	CNAG_05601	AFR99029.2
RIM20	CNAG_03582	AFR96803.1
RIM23	CNAG_02205	AFR95615.1
RRA1	CNAG_03488	AFR96713.2
RIM90	CNAG_05654	AFR99085.1
RIM91	CNAG_02114	AFR94219.1
RIM92	CNAG_04953	AFR94219.1
ALI1	CNAG_02857	AFR93834.1
ALI2	CNAG_02341	AFR95488.1
CgRIM101	CNGB_4424	
CgRRA1	CNGB_2126	

Table 4: Chapter 3 Strains

Strains	Genotype	Source
H99	*MAT*α	[185]
KN99	*MAT***a**	[186]
KS33	*rim13*Δ*::NEO MAT*α	this study
KS110	*rim13*Δ*::NEO MAT***a**	this study
TOC66	*rim13*Δ*::NEO + RIM13 + pCH233 (NAT) MAT*α	this study
KS88-2	*rim13*Δ*::NEO + eGFP-RIM101 pCH233 (NAT) MAT*α	this study
KS140	*rim13*Δ*::NEO +GFP-RIM101T* + pCH233 (*NAT*) MATα	this study
KS94	*rim23*Δ*::NEO MAT*α	this study
KS82-2	*rim23*Δ*::NEO MAT***a**	this study
KS81-2	*rim23*Δ*::NEO + RIM23 + pCH233 (NAT) MAT*α	this study

KS87-2	*rim23Δ::NEO* + *eGFP-RIM101* + pCH233 *(NAT) MATα*	this study
KS141	*rim23Δ::NEO +GFP-RIM101T* + pCH233 (*NAT*) *MATα*	this study
KS159	*rim23Δ::NEO* + pTO22 (*GAL7-GFP-RIM101T NAT) MATα*	this study
TOC17	*rim20Δ::NAT MATα*	[8]
KS118-2	*rim20Δ::NAT* + *eGFP-RIM101* pJAF (*NEO*) MATα	this study
KS77-2	*rim20Δ::NAT +GFP-RIM101T* + pJAF (*NEO*) *MATα*	this study
TOC2	*rim101Δ::NAT MATα*	[8]
TOC105	*rim101Δ::NAT* + *eGFP-RIM101* MATα	[2]
KS208	*rim101Δ::NAT* + *eGFP-RIM101 MAT**a***	this study
TOC65	*rim101Δ::NAT* + *GFP-RIM101T* + pJAF (*NEO*) *MATα*	this study
vps23-9	*vps23Δ::NEO MATα*	[20]
KS211	*vps23Δ::NEO* + *eGFP-RIM101* + pCH233 *(NAT) MATα*	this study
KS75-2	*vps23Δ::NEO +GFP-RIM101T* + pCH233 (*NAT*) MATα	this study
snf7Δ	*snf7Δ::NEO*	[172]
KS151	*snf7Δ::NEO +GFP-RIM101T* + pCH233 (*NAT*) MATα	this study
KS63	*rim90Δ::NEO MATα*	this study
KS57	*rim91Δ::NEO MATα*	this study
KS53	*rim92Δ::NEO MATα*	this study
KS117	*rim91Δ::NEO rim92Δ::NEO MAT**a***	this study
KS136	*rim90Δ::NEO rim91Δ::NEO rim92Δ::NEO MATα*	this study
KS118	*ali1Δ::NEO MATα*	this study

KS94-2	*ali2Δ::NAT MATα*	this study
KS97-2	*ali1Δ::NEO ali2Δ::NAT MATα*	this study
KS161	*H99* + pTO22 (*GAL7-GFP-RIM101T NAT) MATα*	this study
KS216	*AGRO MUTANT rra1Δ::NEO* + (GAL7-GFP-RIM101T NAT)MATα	this study
KS183	*rra1Δ::NEO MATα*	this study
KS202	*rra1Δ::NEO* + pKS38 (*RRA1 NAT*) *MATα*	this study
KS185	*rra1Δ::NEO + eGFP-RIM101 MATα*	this study
KS214	*rra1Δ::NEO* + pKS34 (p*HIS3-GFP-RRA1 NAT*) *MATα*	this study
KS289	*rim23Δ::NEO* + *GFP-RIM23* + *NAT MATα*	this study
KS290	*rim23Δ::NEO* + *GFP-RIM23* + *NAT MAT**a***	this study
KS292	*snf7Δ::NEO rim23Δ::NEO* + *GFP-RIM23* + pCH233 (*NAT)*	this study
KS296	*vps23Δ::NEO rim23Δ::NEO* + *GFP-RIM23* + pCH233 (*NAT)*	this study
KS298	*rim13Δ::NEO rim23Δ::NEO* + *GFP-RIM23* + pCH233 (*NAT)*	this study
KS299	*rim20Δ::NEO rim23Δ::NEO* + *GFP-RIM23* + pCH233 (*NAT)*	this study
KS301	*rra1Δ::NEO rim23Δ::NEO* + *GFP-RIM23* + pCH233 (*NAT)*	this study
YSB25	*gpa2Δ::NEO*	[177]
YPH105	*gps3Δ::NEO*	[177]
YSB83	*gpa1Δ::NAT*	[187]
R265	*C. gattii*	[188]
KS260	*C. gattii rra1Δ::NEO*	this study

KS261	*C. gattii rim101::NEO*	this study
KS310	*rra1*Δ + *RRA1-GFP*	this study
KS234	*GFP-ctrra1*	this study
KS338	*rra1*Δ + *pHIS3-RRA1 296T-GFP*	this study
KS340	*rra1*Δ + *pHIS3-RRA1 273T-GFP*	this study
KS342	*rra1*Δ + *RRA1 296T-4FLAG + GFP-RIM101*	this study

YP-Gal media contained 1% yeast extract, 2% peptone, and 3% galactose. The pH 4 and pH 8 media was made by adding 150 mM HEPES buffer to YPD or YP-Gal liquid media, adjusting the pH with concentrated HCl (for pH 4) or NaOH (for pH 8), prior to autoclaving. The NaCl plates were made by adding NaCl to YPD to a concentration of 1.5 M. To induce capsule, strains were incubated for 48 hr in CO_2-independent medium (Gibco) with 150 rpm shaking at 37^{o}C.

To analyze GFP-Rim101 localization, strains were grown overnight (~18 hr) at 30^{o}C with 150 rpm shaking. Cells were then pelleted and resuspended in either pH 4 or pH 8 Synthetic Complete media buffered with McIlvaine's buffer. Strains were shaken at 150 rpm, 30^{o}C for 5 hr

3.4.2 Molecular Biology

The primers used to create each mutant and fluorescent strain are listed in Table 5. The *rim13Δ* (KS33)*, rim23Δ* (KS94)*, ali1*Δ (KS118)*, ali2*Δ (KS94-2)*, rim90* (KS63)*, rim91* (KS57)*, rim92Δ* (KS53) strains were created by replacing the entire open reading frame with the dominant selectable *NAT* or *NEO* resistance genes. Overlap PCR was

used to create each KO cassette as previously described [137], which was introduced into the recipient strain by biolistic transformation [138]. The following primer combinations were used to create each KO construct: *RIM13* 5' fragment: AA1796 and AA1792, *RIM13* 3' fragment: AA1793 and AA1795, *NEO* resistance marker: AA1797 and AA1794. AA1796 and AA1795 were used to amplify the final deletion construct. *RIM23* 5' fragment: AA3361 and AA3362, *RIM23* 3' fragment: AA3365 and AA3366, *NEO* resistance marker: AA3363 and AA3364, AA3361 and AA3366 were used to amplify the final deletion construct. *ALI1* 5' fragment: AA3254 and AA3255, *ALI1* 3' fragment: AA3258 and AA3259, *NEO* resistance marker: AA3256 and AA3257. AA3254 and AA3259 were used to amplify the final deletion construct. *ALI2* 5' fragment: AA3505 and AA3506 *ARR2* 3' fragment: AA3509 and AA3510, *NEO* resistance marker: AA3507 and AA3508. AA3505 and AA3510 were used to amplify the final deletion construct. *RIM90* 5' fragment: AA3267 and AA3268, *RIM90* 3' fragment: AA3271 and AA3272, *NEO* resistance marker: AA3269 and AA3270. AA3267 and AA3272 were used to amplify the final deletion construct. *RIM91* 5' fragment: AA3226 and AA3227, *RIM91* 3' fragment: AA3230 and AA3231, *NEO* resistance marker: AA3228 and AA3229. AA3226 and AA3231 were used to amplify the final deletion construct. *RIM92* 5' fragment: AA3260 and AA3261, *RIM92* 3' fragment: AA3264 and AA3265, *NEO* resistance marker: AA3262 and AA3263. AA3260 and AA3265 were used to amplify the final deletion construct. The *ali1*Δ *ali2*Δ (KS97-2) strain was created by disrupting the *ALI2* gene in the KS118 strain. The *rra1Δ* (KS183) and *rra1*Δ + *eGFP-RIM101* (KS185) strain was created by using primers AA3970 and AA3971 to PCR amplify the *NEO* resistance marker from KS216 and introduce it into wild type H99. Each mutant strain was confirmed by Southern blot.

The primers used to create each Southern probe were: *RIM13:* AA1812 and AA1813, *RIM23:* AA3401 and AA3402, *RIM90*: AA3292 and AA3267, *RIM91*: AA3241 and AA3242. *RIM92* AA3293 and AA3294, *ALI1*: AA3295 and AA3296. *ALI2*: AA3672 and AA3673, *RRA1*: AA4011 and AA4012.

Table 5: Chapter 3 Primers

Primer name	5'-3' Primer sequences
AA1792	GTCATAGCTGTTTCCTGGGGCGGATGATGCAGAGTTA
AA1793	ACTGGCCGTCGTTTTACTAACAAAGGTAACCGTCGGT
AA1794	ACCGACGGTTACCTTTGTTAGTAAAACGACGGCCAGT
AA1795	AAGTCAGCGGTCTTGAGGAA
AA1796	TAAGGGCTAAAGTCGGAGCA
AA1797	TAACTCTGCATCATCCGCCCCAGGAAACAGCTATGAC
AA1812	ATCTTGCCATTGATGATAG
AA1813	GTCGGAAGATTAAAAAGTG
AA3226	GGATTGGTCTAGGGCCTCTT
AA3227	GTCATAGCTGTTTCCTGTATGTATAATGATTATATCTG
AA3228	CAGATATAATCATTATACATACAGGAAACAGCTATGAC
AA3229	CGTATATCATATTCAACTTTCTCGTTTTCCCAGTCACGAC
AA3230	GTCGTGACTGGGAAAACGAGAAAGTTGAATATGATATACG
AA3231	ATTTAGCCCCGTCGTCTTCT
AA3241	CCGATGTAGTGGCCAAGTCT
AA3242	TGGACATACCAGACGATCCA
AA3254	GAGGACTACTTGGGCGTCAA
AA3255	GTCATAGCTGTTTCCTGCTGTCGGACCGTGTTTATCG
AA3256	CGATAAACACGGTCCGACAGCAGGAAACAGCTATGAC
AA3257	ATATTATAAGTTAGAGGTTAGGTTTTCCCAGTCACGAC
AA3258	GTCGTGACTGGGAAAACCTAACCTCTAACTTATAATAT
AA3259	GGACGGGAGTGTAATGAGGA
AA3260	TGTGCATTCTGCATGGTTTT
AA3261	GTCATAGCTGTTTCCTGGTTTTATAGTTCCGAAGTTGAC
AA3262	GTCAACTTCGGAACTATAAAACCAGGAAACAGCTATGAC
AA3263	GGATGGAATTATAGAATGGCGTTTTCCCAGTCACGAC
AA3264	GTCGTGACTGGGAAAACGCCATTCTATAATTCCATCC
AA3265	CTTCGCCCTTTGATCTTGAG
AA3267	AAGATGTGATCGCGTGAATG
AA3268	GTCATAGCTGTTTCCTGGATGGCAGTTTAGTTGTGAG
AA3269	CTCACAACTAAACTGCCATCCAGGAAACAGCTATGAC
AA3270	GATGAAGATGGCAAAATATATTGTTTTCCCAGTCACGAC

AA3271	GTCGTGACTGGGAAAACAATATATTTTGCCATCTTCATC
AA3272	TGAAGAAAGGGGAGGTGATG
AA3292	GCTTTTGATGACCCTGTCGT
AA3293	CCAAAGACGTGTGATTGTGG
AA3294	TGGTGATCCATGCTTGTTGT
AA3295	AATTTATCCGGGAGGAATCG
AA3296	ATTTCTTACGGCCGGAACTT
AA3361	GACTGGGCCTATGTTGAGGA
AA3362	GTCATAGCTGTTTCCTGCGTGAGGTGTAGGGAAGGAGCAG
AA3363	CTGCTCCTTCCCTACACCTCACGCAGGAAACAGCTATGAC
AA3364	GCAAAATAAAAAGAATGTATCAAGTTTTCCCAGTCACGAC
AA3365	GTCGTGACTGGGAAAACTTGATACATTCTTTTTATTTTGC
AA3366	ACGAATAATAGGGGGCATCC
AA3401	ACGAATAATAGGGGGCATCC
AA3402	ACATCGCATCTCGAGGTTTC
AA3505	CTGAGCGGTGTCCTTTTCTC
AA3506	GTCATAGCTGTTTCCTGGGTGTGGGTGTGGTTGTCGTGGT
AA3507	ACCACGACAACCACACCCACACCCAGGAAACAGCTATGAC
AA3508	GTATATCTAGATTGAACAACTAAGTTTTCCCAGTCACGAC
AA3509	GTCGTGACTGGGAAAACTTAGTTGTTCAATCTAGATATAC
AA3510	TTTCAGTTCCGAGGTGCTCT
AA3672	GATTCGCACCATTGGTCTTT
AA3673	TAACGCGGAGCTCTGATCTT
AA4011	CTCCCTCCACCAGATACCAA
AA4012	CTGCCACAAAGTTGAACGTC
AA3970	ACCACCACCATCCTAACCAG
AA3971	ACGAGGAAGAAGGGTAAGGC
AA4031	GGATCCATGGATGCAGGGACT
AA4032	GGATCCAAGGCCAAGAAGGGAAA
AA4033	GGATCCAAGGGATTGCAAGTGGTCAG
AA1551	AGCTGTGCGTATCCAATAAT
AA3358	CTCCTCGCCCTTGCTCACCATCTTGGCCTTGCTGTTAAC
AA3357	GTTAACAGCAAGGCCAAGATGGTGAGCAAGGGCGAGGAG
AA1879	GCAAGAATTGGCTGCCCTCTAGGCATACCTGCCAAACCTAA
AA1880	TTAGGTTTGGCAGGTATGCCTAGAGGGCAGCCAATTCTTGC
AA1752	ACTGATAGATCTGAGGAAAGCGTCAAGGATATG
AA1463	AGTTCCGCATCAGTCTTGCT
AA1657	GAGGAAAGCGTCAAGGATATG
AA1489	CCTGAGGACGCTTGAAAGTC
AA3305	GGAGTTCGTGACCGCCGC
AA1753	AGTTAAGATCTATGGCTTACCCAATTCTCCC
AA3078	CAAGAATTGGCTGCCCTCTAAGTCGAGTTGGAAGAGAGTG
AA3079	AAGAGGGTCCACGCCTCCCTAGAGGGCAGCCAATTCTTGC
AA3491	CCTCGCCCTTGCTCACCATGAAGTAGTTGCCCTTGCCGGC

AA3492	GCCGGCAAGGGCAACTACTTCATGGTGAGCAAGGGCGAGG
AA3493	CAAAATAAAAAGAATGTATCAATCAGTACAGCTCGTCCATG
AA3494	CATGGACGAGCTGTACTGATTGATACATTCTTTTTATTTG
AA4206	GCAGTACAGGTGGAGATTGC
AA4207	GTCATAGCTGTTTCCTGGTTGGCCTTGTTGCTTCA
AA4208	ACTGGCCGTCGTTTTACGGAGATAACCAACTCTTG
AA4209	CCCTCACTCTCAGATCGGTC
AA4210	GCCTCATCCAACGTCCTTTC
AA4211	GTCATAGCTGTTTCCTGGACTGTAATGGCCTTATG
AA4212	ACTGGCCGTCGTTTTACGGATCATGATGAAGGAGA
AA4213	TAAAGAGCTGGGTGTCTGGG
AA3934	TCGATGCGATGTTTCGCT
AA3935	CCTGAATGAACTGCAGGA
M13R	CAGGAAACAGCTATGAC
M13F -20	GTAAAACGACGGCCAGT

The *C. gattii rim101Δ* and *rra1Δ* mutants were created in the R265 background using the split marker method previously described [189]. For the *Cgrim101Δ* mutant the following primers were used with R265 gDNA as the template. *CgRIM101* 5' fragment: AA4206 and AA4207, *CgRIM101* 3' fragment: AA4208 and AA4209. The 5' region of the *NEO* cassette was amplified from pJAF using the M13R primer and AA3935 and the 3' region with M13F -20 and AA3934. The *Cgrim101Δ* 5' KO cassette was created by combining the 5' *CgRIM101* and *NEO* PCR PCR products by overlap PCR using AA4206 and AA3935. The 3' KO cassette was similarly made using AA3932 and AA4209. These overlap PCR products were combined and transformed into R265. The *Cgrra1Δ* mutant was created in the same way, using the following primer pairs. *CgRRA1* 5' fragment : AA4210 and AA4211 and *CgRRA1* 3' fragment: AA4212 and AA4213. Southern blot analysis was used to confirm a insertion at the correct locus.

The *GFP-RIM101T* strains were created by first creating TOC65 (*rim101Δ + GFP-RIM101T*). The following PCR primer combinations were used to amplify the *RIM101* promoter and terminator (from H99 gDNA) and a truncated *GFP-RIM101* fusion (from pTO2): *RIM101* promoter: AA1551 and AA3358, GFP-RIM101 truncation:AA3357 and AA1879, *RIM101* terminator: AA1880 and AA1752. Overlap PCR was then performed and was transformed, along with pJAF (*NEO*), into TOC2. Replacement of the *rim101*Δ NAT disruption construct was confirmed by PCR, and the expression and functionality of *GFP-RIM101T* was verified by reconstitution of the *rim101*Δ mutant phenotypes. Primers AA1463 and AA1657 were then used to amplify the promoter, ORF, and terminator of the GFP-70T from the TOC65 gDNA. The *GFP-RIM101T* was then co-transformed with either pJAF (*NEO*) or pCH233 (*NAT*) into the following mutant strains: *vps23*Δ (*vps23-9*), *rim13*Δ (KS33), *rim20*Δ (TOC17), *rim23*Δ (SK94). Transformants were screened using PCR (AA1489 and AA3305) and epifluorescence microscopy to detect the presence and expression of the *GFP-RIM101* fusion respectively.

KS289 (*rim23Δ::NEO + GFP-RIM23 + NAT MATα)* was created by creating a *RIM23-GFP* fusion using the following PCR reactions. AA3361 and AA3491 were used to amplify *RIM23* and its promoter from H99 gDNA. AA3492 and AA3493 were used to amplify GFP from a GFP-containing vector. AA3494 and AA3166 were used to amplify that *RIM23* terminator region. These PCR products were mixed and overlap PCR was performed using AA3361 and AA3366. The overlap piece was mixed with pCH233 (NAT) and transformed into KS94 (*rim23*Δ*).* Transformants that had rescued growth on pH 8 all displayed GFP fluorescence. The isolate chosen for this study was rescued for

1.5 M NaCl growth and capsule formation. The other *RIM23-GFP* strains were created by crossing KS289 or KS290 (Mat**a**) to the each mutant strain. Progeny were selected based on pH 8 and 1.5M NaCl sensitivity and the genotypes were confirmed using PCR. *GFP-RIM23* was the only *RIM23* allele in each of these strains.

To reconstitute the *rim13*Δ mutant, primers AA1796 and AA1795 were used to amplify the *RIM13* promoter, gene, and terminator sequence and then co-transformed with pCH233 (*NAT*) into the KS33 strain. PCR and rescued phenotype were used to verify restored expression of *RIM13*. The *rim23*Δ mutant was similarly reconstituted using primers AA3361 and AA3366. The *rra1*Δ mutant was reconstituted by amplifying the *RRA1* promoter, ORF, and terminator using primers AA4033 and AA4032 and then TA cloning into pCR2.1. The insert was digested from the TA vector with BamHI cloned into the single BamHI site in pJAF to create pKS38. The KS183 strain (*rra1Δ*) was then transformed with pKS38 and transformants were screened for rescued mutant phenotypes.

The pKS34 vector was created by using AA4031 and AA4032 to amplify the *RRA1* gene from H99 genomic DNA and then TA cloned into pCR2.1. *RRA1* was then cloned into the single BamHI site in pCN19 [154].To create *rra1*Δ + *GFP-RRA1* (KS214), KS183 was transformed with pKS34.

The pTO22 construct was created by amplifying and truncating the *RIM101* gene using the following primer pairs: 5' flank: AA1753 and AA1879, 3' flank: AA1880 and AA1752. The entire piece was amplified using AA1753 and AA1752, TA cloned into pCR2.1, and then cloned into the single BamHI site in pCN70 (*pGAL7-GFP-NEO*).

3.4.3 Insertional Mutagenesis and assessment of mutants

Agrobacterium tumefaciens-mediated random mutagenesis was carried out as previously described [190]. Briefly, *A. tumefaciens* expressing the pPZP-NEOcc plasmid was incubated with shaking at room temperature for 48 hr in Luria-Bertani (LB) medium containing kanamycin. Cells were washed and resuspended to an OD_{600} of 0.15 in liquid induction media (IM) containing 200 µM acetosyringone (AS) and incubated for 6 hr An overnight YPD culture of KS161 was harvested, washed with IM and resuspended in IM at a concentration of 10^7 cells/mL. 200 µL of the *A. tumefaciens* and KS161 suspensions were mixed and aliquoted on IM agar containing acetosyringone. Cells were incubated for 3 days and then scraped onto selection media (YPD + Neo + 100 µg/mL cefotaxime). Colonies passaged 1X on the selection plates and then inoculated into liquid selection media in 96-well plates. Duplicates of each isolate were inoculated. Mutants were then inoculated onto YP Dextrose or YP Galactose media containing 1.5M NaCl or 150mM HEPES adjusted to pH 8. A total of 3500 mutants were screened in duplicate. Mutants with growth defects on either condition were selected and rescreened. The genetic location of each insertion was identified by deep sequencing using MiSeq deep sequencing.

3.4.4 Protein extraction, immunoprecipitation, and western blot

Protein extracts were prepared as previously described [112]. To initially assess GFP-Rim101 proteolytic processing at multiple pH's, the *rim101Δ* + *GFP-RIM101* (TOC105) strain was grown overnight (~18 hr) in 50ml YPD, 30^{o}C, 150 rpm shaking. Cells were pelleted and resuspended in SC McIlvaine's buffer at pH 4, pH 6, or pH 8 to

an OD_{600nm} of 1. Samples were further incubated at 30°C 150 rpm for 3 or 5 hr Cells were harvested, flash frozen on dry ice, and lysed in 0.4 mL lysis buffer containing 2x protease inhibitors (Complete, Mini, EDTA-free; Roche) and 1x phosphatase inhibitors (PhosStop; Roche) and 1 mM phenylmethanesulfonylfluoride (PMSF). Lysis was performed by bead beating (0.5 mL of 3 µM glass beads in a Mini-BeadBeater-16 (BioSpec), 10 cycles for 30 s each). Supernatants were transferred to new tubes and glass beads washed 2 times with 0.4 mL lysis buffer. Lysates were cleared by centrifugation at 15,000 rpm, 4°C, for 10min. 5 µLGFP-TRAP resin (Chemotek), which was equilibrated in lysis buffer, was added to the cleared lysate and inverted at 4°C for 4 hr GFP-TRAP resin was washed 3 times with 1 mL lysis buffer and protein was eluted in 30 µL NuPage sample buffer with 1X NuPage Reducing Agent by boiling for 5 min. Western blots were performed as described previously using 4-8 % NuPage BisTris gels to separate the samples. To detect GFP-Rim101, blots were incubated in anti-GFP primary antibody (Roche) (using a 1/10,000 dilution) and then in secondary anti-mouse peroxidase-conjugated secondary antibody (using a 1/25,000 dilution, Jackson Labs).

Assessment of GFP-Rim101 proteolysis in the upstream Rim pathway mutants was performed as described above but with several alterations. First, YPD 150 mM HEPES adjusted to a pH 7.4 was used instead of SC McIlvaine's buffer. Second, GFP-Rim101 was immunoprecipitated with anti-GFP antibody (Roche) for 1 hr and then incubated 2 hr with 80 µL Protein G Sepharose (Thermo Scientific). Finally, a 3-8 % NuPage Tris-Acetate gel was used to separate samples.

Subcellular fractionation was performed to analyze the localization of Rra1-GFP. Cells were lysed by bead beating in 1 mM EDTA with 1X protease inhibitor coctail

(Complete, Mini, EDTA-free; Roche). Unlysed cells and glass beads were cleared by centrifugation at 1000 xg for 5 min. Cleared lysates were normalized to the same protein concentration. Lysates were then spun at 100,000 xg for 1 hr. at 4^{o}C. Supernatant was saved as the S100 fraction. Pellet was resuspended in an equal volume of 1 mM EDTA 1mM 2-mercaptoethanol 33% v/v glycerol and homogenized using a dounce homogenizer. Each fraction was analyzed by western blot using an anti-GFP primary anitbody and an anti-mouse peroxidase-conjugated secondary antibody. For immunoprecipitation of Rra1-GFP for MS/MS analysis, subcellular fractionation was performed, and the membrane fraction was solubilized in 50 mM Tris HCl pH 7.5, 1 mM EDTA, 1 mM 2-mercaptoethanol, 1X PIC, 1 mM PMSF. Fos-14-choline was slowly added to a final concentration of 1 %. Rra1-GFP was then immunoprecipitated with 50 µl GFP-TRAP and analyzed by coomassie gel. Rra1-GFP band was sent to Duke Proteomic core facility for chymotrypsin digest and MS/MS analysis.

3.4.5 Microscopy

The high-resolution fluorescent images of Rim23-GFP were captured using a Delta Vision Elite deconvolution microscope equipped with a Coolsnap HQ2 high resolution charge-coupled-device (CCD) camera. All other differential interference (DIC) and fluorescent images were captured using a Zeiss Axio Imager A1 fluorescence microscope equipped with an AxioCam MRM digital camera.

3.4.6 Virulence studies

Virulence studies were carried out according to [142]. 8-10 female A/Jcr mice were anesthetized with 100-140 µL of 12 mg/ml ketamine HCl and 1 mg/ml Xylazine in

PBS. Each mouse was intranasally inoculated with $1X10^5$ cells in a volume of 25 µL. Mice were monitored and weighed daily and sacrificed based on predetermined symptoms that predict imminent death. Kaplan-Meyer curves were analyzed by log-rank test (JMP software; SAS Institute, Cary, NC). All studies were performed in compliance with Duke University institutional guidelines for animal experimentation.

All animal work was performed according to the Duke University Institutional guidelines for animal experimentation. All mice were anesthetized using an intraperitoneal injection of Ketamine/Xylazine mixture and were sacrificed by CO2. Approved secondary methods of ensuring animal death were also used. These techniques are consistent with IACUC-approved animal handling protocol - A217-11-08.

4. Increased chitin exposure on the Cryptococcus neoformans cell wall is associated with increased immune recognition and inflammation

This chapter was modified from a manuscript in preparation. The authors are Kyla S. Ost, Shannon K. Esher, Maria Kohlbrenner, Chrissy Leopold-Wagner, Louise Walker, Carol Munro, Floyd Wormley, J. Andrew Alspaugh

4.1 Introduction

Over the last several decades, increased use of immunosuppresive drugs and the HIV/AIDS pandemic has greatly expanded the population of people that are susceptible to disseminated fungal infections. The opportunistic fungal pathogen, *Cryptococcus neoformans* has emerged as a particularly deadly pathogen, causing over 300,000 deaths each year, primarily among those suffering from HIV/AIDS [1,2]. *C. neoformans* initially colonizes the lungs, where it can disseminate to the CNS to cause life-threatening fungal meningitis that is universally fatal without treatment [1]. Initial interactions between *C. neoformans* and the innate immune cells in the lung direct either a robust, protective immune response or a weak, non-protective response. This initial interaction can also lead to an over-exuberant response that causes host damage that can be fatal. Understanding this initial interaction is vital in understanding what constitutes a beneficial immune response to this pathogen.

C. neoformans has a highly dynamic cell surface that changes in composition and architecture during infection. Some of the changes include alterations in the cell wall carbohydrate composition and the attachment of the characteristic polysaccharide capsule [25,117,191]. These changes dramatically alter the interaction of *C. neoformans*

with immune cells. The capsule, which is primarily composed of the polysaccharide glucuronoxylomannan (GXM), shields potentially immune-stimulatory molecules in the cell wall from detection. GXM also actively inhibits pro-inflammatory receptors and signaling in innate immune cells [17–21]. While no detailed analysis has been performed on the *C. neoformans* cell wall during infection, increased levels of chitin and α -1,3-glucan have been noted in *C. neoformans* cells recovered from infected mice, or from cells cultured in host-mimicking tissue culture media [117,192]. The *C. neoformans* cell wall has also been shown to thicken during infection [193]. *C. neoformans* also produce titan cells during infection, which are giant, super-resilient cells that have a very thick cell wall and dense capsule [28,29]. The surface propertied of titan cells have recently been shown to guide the immune response toward a more favorable environment for *C. neoformans* survival [103]. Compared to other prevalent fungal pathogens, relatively little is known about what components of the *C. neoformans* cell surface, and especially the cell wall, are recognized by the innate immune system.

Previously, our lab identified the Rim101 transcription factor as an important regulator of these adaptive cell surface changes during infection. The *rim101*Δ mutant has a significant defect in capsule attachment as well as aberrant cell wall morphology [81,117]. Despite these cell surface defects, this mutant was unexpectedly hypervirulent in a mouse inhalation model of infection. Further investigation demonstrated that *rim101*Δ induces a dramatic inflammatory response in the lungs of infected mice, leading to host damage through a detrimental immune response [81,117].

The particular cell surface changes on the *rim101*Δ mutant that drive an increased inflammatory response are still unknown. During infection, and when cultured

in host-mimicking tissue culture media, this mutant has increased staining for the fungal cell wall carbohydrate, chitin [103,117]. Chitin is a polymer composed of repeating subunits of β -1,3- N-acetyl glucosamine, which serves as an important structural component of most fungal cell walls [94]. Chitin makes up a particularly high proportion of the *C. neoformans* cell wall and significantly more than other important fungal pathogens, such as *C. albicans* [95,157]. Compared to these organisms, *C. neoformans* cells walls also contain significantly more of the chitin-related carbohydrate, chitosan [95,102]. Chitosan a polymer of β -1,3-N glucosamine and is synthesized by the deacetylation of chitin. As such, *C. neoformans* provides an excellent model to better understand the immune response toward fungal cell wall chitin and chitosan. Previous work has shown that immune recognition of chitin molecules is complex and can result in both increased or decreased inflammatory responses depending on the source and size of the chitin molecule [101–103].

In this study, we explore the cell wall changes associated with the *rim101*Δ mutation, finding that it has a dramatic increase in chitin exposure, while having just a modest increase in total cell wall chitin. We also identify a novel *Cryptococcus*-specific gene, *MAR1,* that when disrupted, results in several *rim101*Δ mutant-like cell surface defects. These defects are more pronounced in the *mar1*Δ mutant and include increased chitin exposure and a capsule attachment defect. Rim101 and Mar1 operate in separate cellular pathways to regulate similar cell wall modifications. These results are therefore especially informative about the interaction of the cell wall features and host immune cells. Using both mutant strains, we demonstrate that these cell wall defects increase recognition by macrophages and dendritic cells *in vitro*, and that this response likely

involves members of the C-type lectin receptor and Toll-Like receptor families. Consistent with our previous study, we find that the *rim101*Δ mutant induces a dramatic inflammatory response in infected mice. Unlike *rim101*Δ, the *mar1*Δ mutant is rapidly cleared from the lungs of infected mice and does not induce the same inflammatory response. Our results demonstrate that increased chitin exposure may induce an increase in *C. neoformans* recognition by the immune system, and that the resulting immune response may delay pathogenesis in one case while increasing host damage in another, likely depending of the ability of each strain to persist and replicate in the host.

4.2 Results

4.2.1 Analysis of chitin content and organization in the *rim101*Δ mutant cell wall

We previously demonstrated that host-mimicking conditions induced the *rim101*Δ mutant to produce a thick, disordered cell wall [117]. The *rim101*Δ mutant cell wall demonstrated a dramatic increase in cell surface staining with wheat germ agglutinin (WGA), a lectin that binds chitin and chito-oligomers [117]. This result suggested a very different cell wall structure in this strain. To better define the actual composition of the cell wall of the *rim101*Δ mutant compared to WT, we biochemically quantified the level of three major cell wall carbohydrates that comprise a typical fungal cell wall: glucosamine, glucan, and mannose. After culturing the strains in host-like tissue culture media, the cell walls were extracted and hydrolyzed into their individual sugar components. This technique deacetylates the chitin to chitosan and therefore measures chitin and chitosan together as glucosamine. The level of glucosamine, glucan, and mannose in these cell wall fractions were quantified using HPLC (Fig. 26A)**.** We found that the level of

mannose, which is found on cell wall mannoproteins, was not significantly different between the WT, *rim101*Δ, and *rim101*Δ + *RIM101* strain. We did observe a significant increase in *rim101*Δ glucan levels compared to WT, although the *rim101*Δ + *RIM101* reconstituted strain had glucan levels similar to *rim101*Δ. Compared to glucan and mannan, we found that glucosamine made up a relatively small portion of the cell wall. Despite the relatively low level of glucosamine, we observed a modest increase in the level of glucosamine in the *rim101*Δ mutant compare to both the WT and *rim101*Δ + *RIM101* reconstituted strain, suggesting that the chitin and/or chitosan levels are increased in the *rim101*Δ mutant cell wall. Overall, however, by this method the relative levels of glucosamine, glucan, and mannose were not dramatically different in the *rim101*Δ mutant cell wall.

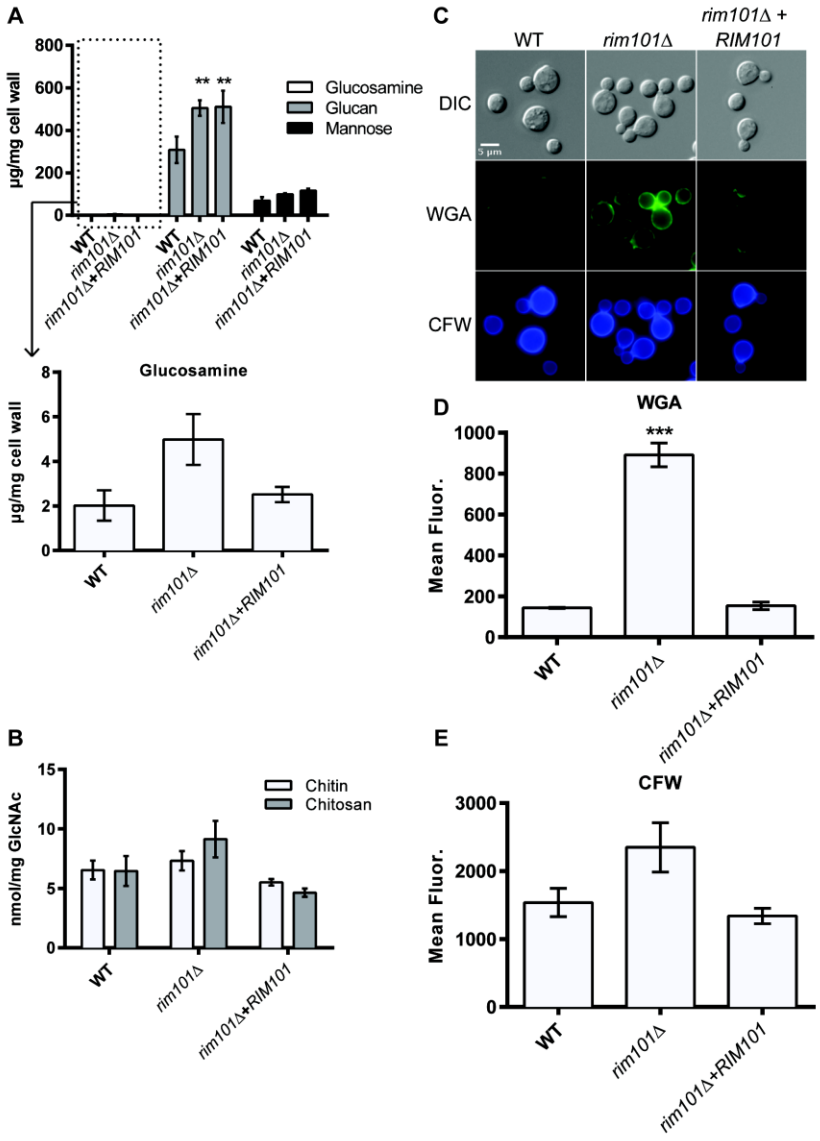

Figure 26: *rim101*Δ strain has increase chitin exposure. A) *C. neoformans* strains were cultured overnight in tissue culture media. Glucosamine, glucan, and mannan content were quantified in the cell wall fractions using high-performance anion exchange chromatography with pulse amperometric detection (HPAEC-PAD). Glucosamine, it is shown in a separate graph **B)** Chitin and chitosan levels were quantified for each strain after **C)** *C. neoformans* strains stained with WGA-FITC and CFW. Fluorescence levels were quantified using Fiji. One-way ANOVA and Tukey's multiple comparison test used to compare means to the WT values. ***p<0.001, **p<0.01, *p<0.05. Error bars represent standard error of the mean.

To differentiate between alterations in chitin and chitosan levels separately in the *rim101*Δ mutant, we utilized an enzymatic method to quantify these components separately [157] (Fig. 26B). The *rim101*Δ mutant had a modest increase in chitosan levels compared to both WT and the *rim101*Δ + *RIM101* reconstitute. The *rim101*Δ mutant also had a modest increase in chitin levels compared to *rim101*Δ + *RIM101* but not compared to WT. Our previous observation of a 10-15 fold increase in staining of the *rim101*Δ mutant cell wall with the chitin-binding lectin WGA suggested that the *rim101*Δ mutant cell wall contained significantly higher levels of chitin [117,194]. However, this result is not consistent with the relatively small and statistically insignificant increases in relative chitin/chitosan levels observed in the HPLC analysis and biochemical chitin/chitosan quantification. To explore the discrepancy between the WGA staining and HPLC analysis, we analyzed *rim101*Δ mutant cell wall chitin levels using a different fluorescent stain, calcofluor white (CFW). CFW is a small (917 Da) fluorescent molecule that specifically binds chitin. We compared the mean CFW fluorescent levels between WT, *rim101*Δ, and *rim101*Δ + *RIM101* reconstituted strains that were cultured in tissue culture media, the condition in which we observed increased WGA binding (Figure 26 C and D). We also stained the cells with WGA. Similar to our previous study, we found that WGA cell wall fluorescence was 6 fold higher for the *rim101*Δ mutant, compared to the WT and *rim101Δ* + *RIM101* reconstituted strains. For the same cells, the CFW fluorescence was only 1.5 fold higher in the *rim101*Δ mutant cells, compared to the WT and *rim101*Δ + *RIM101* strains. CFW also displayed a different staining pattern than WGA, with CFW staining the entire cell wall while WGA brightly stained only the bud necks and bud scars on the WT and *rim101*Δ + *RIM101* strains as well as in punctate

staining throughout the *rim101*Δ cell surface. Chitin makes up the base, structural layer of the fungal cell wall, and it is in higher levels and is more exposed at bud necks and bud scars [94]. This suggests that WGA, which is a 38 kDa protein dimer [194], stains exposed chitin, while the much smaller molecule, CFW, has access to total cell wall chitin [105,195]. Together, these data suggest that the *rim101*Δ cell wall has a modest increase in total chitin content, but it displays an altered pattern of organization with a more dramatic increase in the chitin exposure.

4.2.2 Identification of a Rim pathway-independent regulator of cell wall chitin during infection

We previously performed an *Agrobacterium tumifaciens*-mediated random mutagenesis screen, to discover mutants with *rim101*Δ-like cell wall changes [196]. From this screen, we identified a mutant with an insertion in a previously uncharacterized gene, which we have named *MAR1*, for Macrophage Activating Regulator of cell wall. We found that this insertional mutant displayed several cell surface defects similar to *rim101*Δ. The *mar1*Δ mutant had a significant defect in capsule attachment; this mutant displayed a smaller capsule despite secreting WT-levels of the major capsule component, GXM (Fig. 27 A and B) [117]. In addition, *mar1*Δ bound significantly more CFW and WGA than the WT and *mar1*Δ + *MAR1* reconstituted strain, similar to the *rim101*Δ mutant suggesting that the *mar1*Δ mutant also has a pronounced and increased chitin exposure (Fig. 27 C). Also similar to *rim101*Δ, *mar1*Δ displayed increased CFW staining that was not as dramatic as the increase in WGA staining. Finally, the *mar1*Δ cell wall phenotypes were specifically induced by host-mimicking tissue culture media, with the CFW and WGA staining were indistinguishable from WT

when cultured in rich YPD media. These *mar1*Δ phenotypes are not due to alterations in Rim pathway function: the Rim101 protein is proteolytically activated in a normal manner in the *mar1*Δ mutant, and *MAR1* is not transcriptionally regulated by Rim101 (Figure. 28). Therefore, *MAR1* regulates these cell surface processes independent of the Rim pathway.

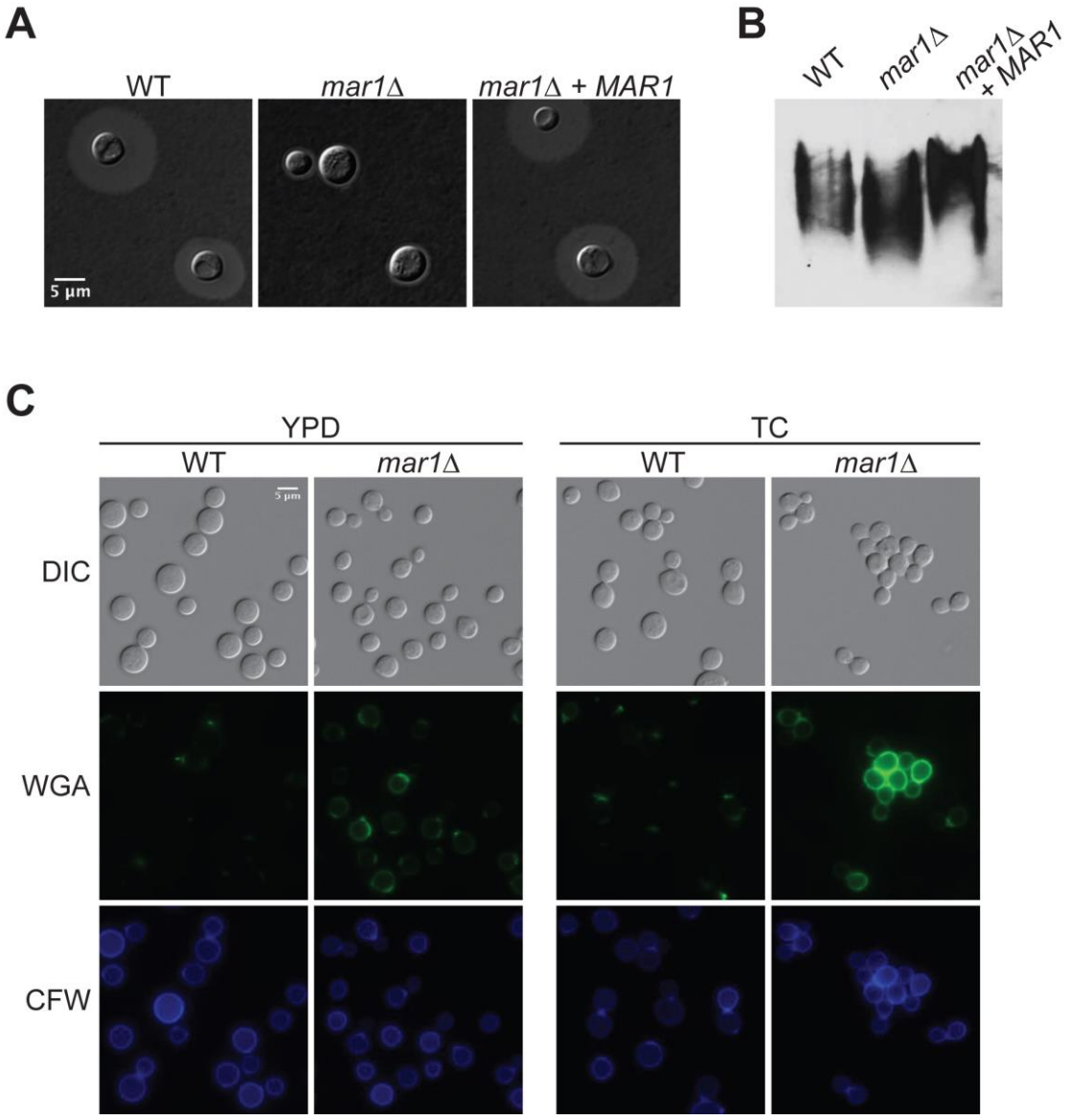

Figure 27: *MAR1* is required for capsule attachment and maintaining chitin levels/exposure in host-mimicking conditions. A) Capsule was visualized by india ink after 48 hr. incubation in tissue culture media. **B)** GXM in culture supernatant was detected using the 18B7 anti-GXM antibody. Cells were cultured in tissue culture media for 5 days. **C)** Cells were stained with WGA-FITC and CFW after overnight culture in the indicated media.

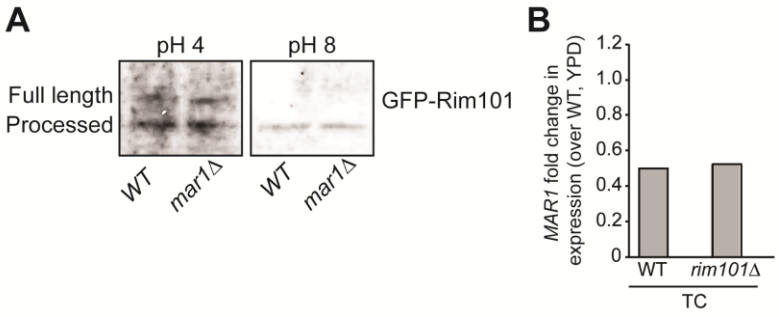

Figure 28: Mar1 function is independent of Rim101. A). Rim101 is processed normally in the *mar1*Δ mutant strain**. B)** *MAR1* expression does not require Rim101 in tissue culture media.

4.2.3 The *rim101Δ* and *mar1Δ* cell surface defects are associated with increased recognition by macrophages and dendritic cells

We previously found that the *rim101Δ* mutant induces a dramatic inflammatory response in the lungs of infected mice [117]. During a *C. neoformans* infection, both macrophages and dendritic cells serve as the primary cells responsible for the initial identification and response to *C. neoformans.* To determine whether macrophages and dendritic cells would respond differently to the *mar1Δ* and *rim101Δ* mutants, we quantified the TNF-α secreted by bone marrow derived macrophages and dendritic cells that were co-cultured both mutant strains, along with the WT and reconstituted strains (Fig. 29A, B, C). *rim101*Δ was previously shown to induce significantly more TNF-α in the lungs of infected mice [117], and TNF-α production is one marker of macrophage and dendritic cell activation *in vitro*. In this assay, both *mar1Δ* and *rim101Δ* mutants induced significantly more TNF-α secretion by both bone marrow-derived macrophages (BMMs) and bone marrow-derived dendritic cells (BMDCs). These mutant strains induced a similar increase in TNF-α secretion when the *C. neoformans* cells were heat-killed prior to co-incubation with BMMs (Fig. 29B).

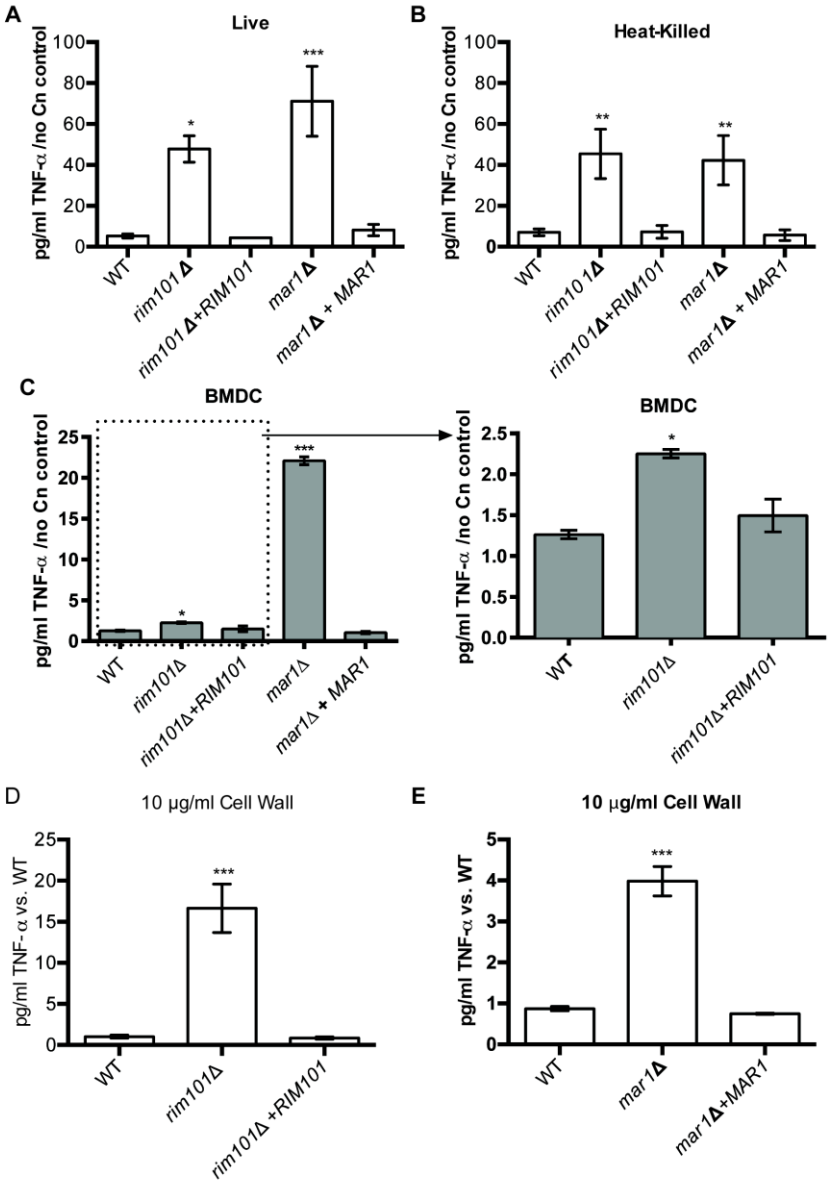

Figure 29: *rim101*Δ and *mar1*Δ cells and cell walls increase TNF-α secretion from macrophages and dentritic cells. BMMs were coincubated with the indicated live **(A)** or heat-killed **(B)** strains at an MOI of 10 *C. neoformans* to 1 BMM. Secreted TNF-α levels were quantified after 6 hr of co-incubation. **(C)** Normalized TNF-α levels secreted by BMDCs after co-incubation with indicated strains. TNF-α levels secreted by BMM after treatment with 10 µg/ml cell wall material from indicated strains. TNF-α levels normalized to WT cell wall material for each experiment. One-way ANOVA and Tukey's multiple comparison test used to compare means. ***p<0.001, **p<0.01, *p<0.05. Error bars represent standard error of the mean**.**

To determine whether the *mar1*Δ and *rim101*Δ cell walls could independently induce increased BMM activation, we purified the cell wall material from *C. neoformans* strains after growth in TC media and treated BMMs with10 μg/ml of cell wall material. Similar to whole cells, cell wall material from the *rim101*Δ and *mar1*Δ mutants induced significantly more TNF-α from BMMs than the cell walls isolated from either the WT or the reconstituted strains (Fig. 29D and E). When examined microscopically, the isolated cell wall material was composed of empty cell-shaped particles (data not shown); indicating that architecture of the cell wall may be largely maintained in the cell wall fractions. Therefore, the arrangement of the cell wall, and the increased exposure of chitin may still be an important factor in the interaction with the immune cells. These data demonstrate that macrophages and dendritic cells recognize both *mar1*Δ and *rim101*Δ more readily than WT *C. neoformans,* which is likely due to changes in the composition or architecture of the *rim101*Δ and *mar1*Δ cell walls.

*4.2.4 mar1*Δ and *rim101*Δ mutations increase recognition of acapsular *cap59*Δ mutant

C. neoformans polysaccharide capsule components actively suppress innate immune cell activation, and also serve to shield the cell wall from recognition [17][197]. As such, we considered that the *rim101*Δ and *mar1*Δ capsule defects could potentially explain the increased immune recognition of these mutant strains. To determine the role of the capsule in the recognition of *rim101*Δ and *mar1*Δ, we compared the BMM and BMDC response to the acapsular mutant, *cap59*Δ, and *rim101*Δ *cap59*Δ and *mar1*Δ *cap59*Δ double mutants. Due to cell aggregation, we normalized the cell concentrations based on weight instead of cell number. Overall, we observed an increased TNF-α

response to all three acapsular strains compared to the WT strain (data not shown), though direct comparisons could not be performed due to the need for differing cell normalization methods. We noted that the double *cap59*Δ *rim101*Δ and *cap59*Δ *mar1*Δ mutants induced significantly more TNF-α production than the single *cap59*Δ mutant alone (Fig. 30). These data indicate that the *rim101*Δ and *mar1*Δ cell wall defects increase immune recognition by a mechanism independent of the effect of loss of surface capsule.

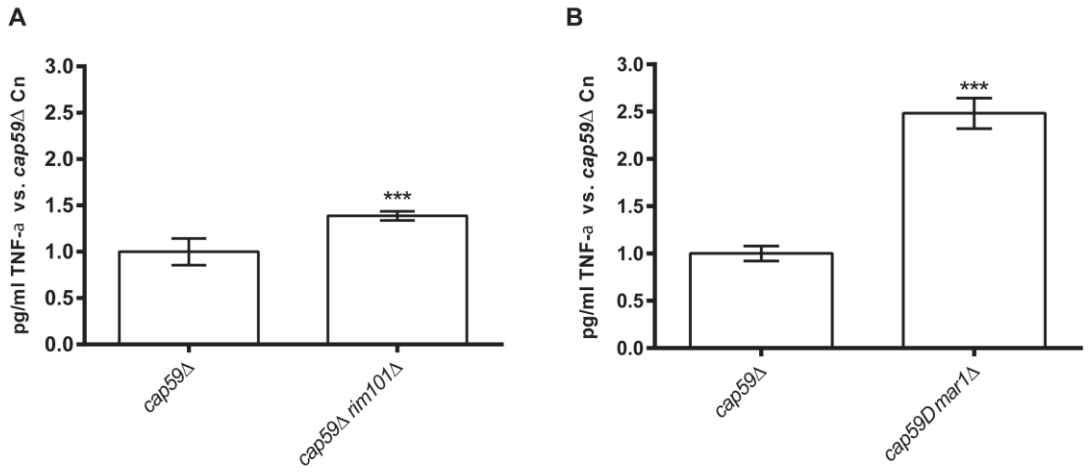

Figure 30: *rim101*Δ and *mar1*Δ mutations increase BMM TNF-α secretion independent of capsule. BMMs co-incubated with 2 mg/ml of *cap*59Δ, *cap*59Δ *rim101*Δ (**A),** and *cap59*Δ *mar1*Δ **(B)**. Secreted TNF-α levels measured after 6 hr, pg/ml TNF-α normalized to *cap59*Δ for each experiment. One-way ANOVA and Tukey's multiple comparison test used to compare means. ***p<0.001, **p<0.01, *p<0.05. Error bars represent standard error of the mean.

4.2.5 Alteration in chitin synthesis and exposure increases recognition by BMMs.

To further explore the role of cell wall chitin levels and exposure in the increased recognition of *rim101*Δ by immune cells, we disrupted two chitin synthase genes, *CHS3* and *CHS5,* in the *rim101*Δ mutant background. Previous studies demonstrated that of

the eight chitin synthases that have been characterized in *C. neoformans,* disruption of either *CHS3* or *CHS5* alone was sufficient to decrease cell wall chitosan and/or chitin; the *chs3*Δ mutant lacks most detectable cell wall chitosan and the *chs5*Δ mutant had significantly decreased chitin levels [157].

We first compared CFW and WGA staining of the *rim101*Δ *chs3*Δ and *rim101*Δ *chs5*Δ cell walls to the single *rim101*Δ mutant and the WT strain (Figure 31A). Similar to our previous results, we observed a significant increase in *rim101*Δ CFW and WGA staining compared to WT. When incubated in tissue culture media, we found that both the *chs3*Δ and *chs5*Δ single mutants had significantly higher CFW and WGA fluorescence levels compared to WT, suggesting that both strains have increased chitin levels (CFW) and exposure (WGA) in these growth conditions. This result contrasts with previous studies demonstrating that these mutants displayed reduced chitin/chitosan content when the strains were incubated in a rich culture medium. Despite these unexpected results, we found that disrupting the *CHS5* chitin synthase gene in the *rim101*Δ mutant background significantly decreased its CFW staining, but it had no effect on WGA staining. Conversely, disruption of *CHS3* in the *rim101*Δ strain significantly increased CFW staining, but had no effect on the level of WGA staining compared to the *rim101*Δ single mutant (Fig. 31). Interestingly, *chs3*Δ *rim101*Δ displayed significantly less WGA compared to *chs3*Δ, indicating that the *rim101*Δ mutation decreases the chitin exposure in the *chs3*Δ background. Together, these chitin staining data demonstrate that *chs3*Δ and *chs5*Δ mutations have differing effects on cell wall chitin levels (CFW staining) and chitin exposure (WGA staining) depending on the background of the mutant strain and the growth conditions.

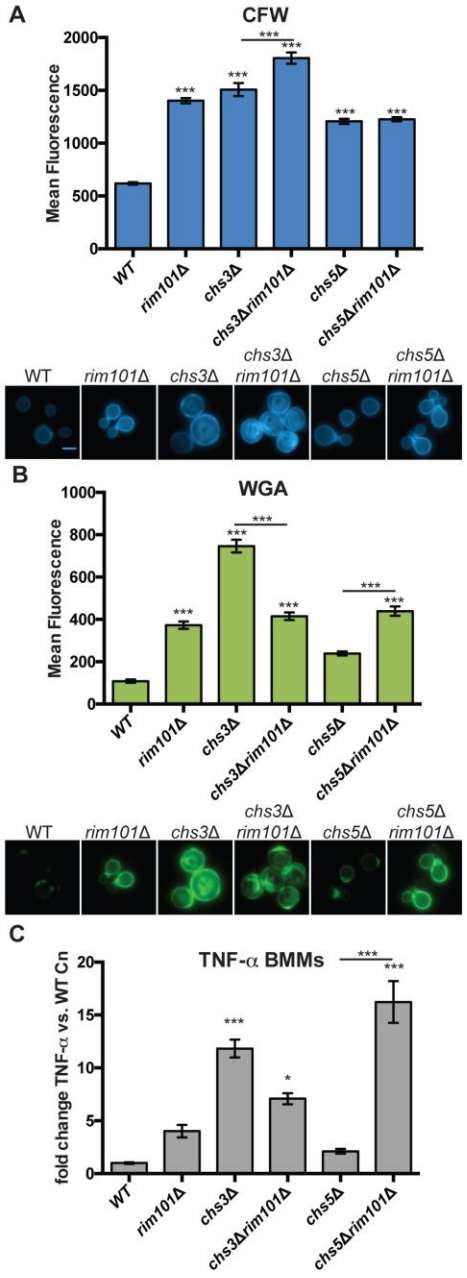

Figure 31: Cell wall mutants with increased WGA induce more TNF-α secretion from BMMs. *C. neoformans* strains were stained with WGA **(A)** and CFW **(B)** after culturing overnight in tissue culture media. **(C)** *C. neoformans* strains co-incubated with BMMs at a 10:1 MOI. TNF-α levels normalized to levels induced by WT *C. neoformans.* One-way ANOVA and Tukey's multiple comparison test used to compare means. ***p<0.001, **p<0.01, *p<0.05. Error bars represent SEM.

By disrupting *CHS3* and *CHS5* in the *rim101*Δ mutant, we inadvertently created strains that had varying levels of CFW and WGA staining. We decided to use these strains as tools to further probe the association between CFW and WGA staining levels with detection by macrophages. Consistent with our previous experiments, we observed that *rim101*Δ induced more TNF-α secretion from BMMs compared to the WT strain. We also noted that the *chs3*Δ, *chs3*Δ *rim101*Δ, and *chs5*Δ *rim101*Δ mutants induced even more TNF-α secretion than the *rim101*Δ strain, while the *chs5*Δ mutation alone had no significant effect of the TNF-α levels (Figure 31C). Interestingly, the relative level of WGA staining of each strain correlated with the level of BMM TNF-α secretion; each strain with increased WGA staining also induced more TNF-α secretion. In contrast, increased CFW staining was not associated with increased BMM TNF-α secretion in each case (Fig. 31A and B). The *chs5*Δ *rim101*Δ was somewhat of an exception to this pattern, as it displayed significantly lower WGA staining than *chs*3Δ, but induced significantly more TNF-α secretion. Together, these data suggest that increased chitin exposure, but not necessarily total cell wall chitin levels, is associated with increased detection by macrophages.

4.2.6 In vitro response to *rim101Δ* and *mar1Δ* requires MyD88 and CARD9

Dendritic cells and macrophages recognize and respond to fungi through the activation of multiple pattern recognition receptors, or PRRs. Of these receptors, members of the Toll-Like receptor (TLR) and the C-type lectin (CTL) receptor families have been shown to be responsible for recognizing fungal cell wall carbohydrates and mannoproteins. [99]. To determine whether members of the TLR or CTL receptor

families are responsible for the increased recognition of the r*im101*Δ and *mar1*Δ mutant strains, we utilized BMMs from mice lacking key downstream signaling adaptor proteins required for TLR and CTL activity. Most TLRs require the adaptor protein, MyD88, to activate cytokine production, while the CTL receptors require CARD9 to propagate their downstream stimulatory signals [99].

We co-incubated *C. neoformans* strains with BMMS derived from MyD88 -/- or CARD9 -/- deficient mice, and compared their TNF-α response to WT BMMs. To better visualize subtle alterations in the TNF-α response toward the *rim101*Δ, we utilized the acapsular *cap59*Δ background to amplify the TNF-α response (Fig. 32A and C). Although the response to WT *C. neoformans* cells were not altered in the MyD88$^{-/-}$ and CARD9$^{-/-}$ BMMs, these mutant macrophages failed to induce TNF-α production in response to the *rim101*Δ *cap59*Δ strain.

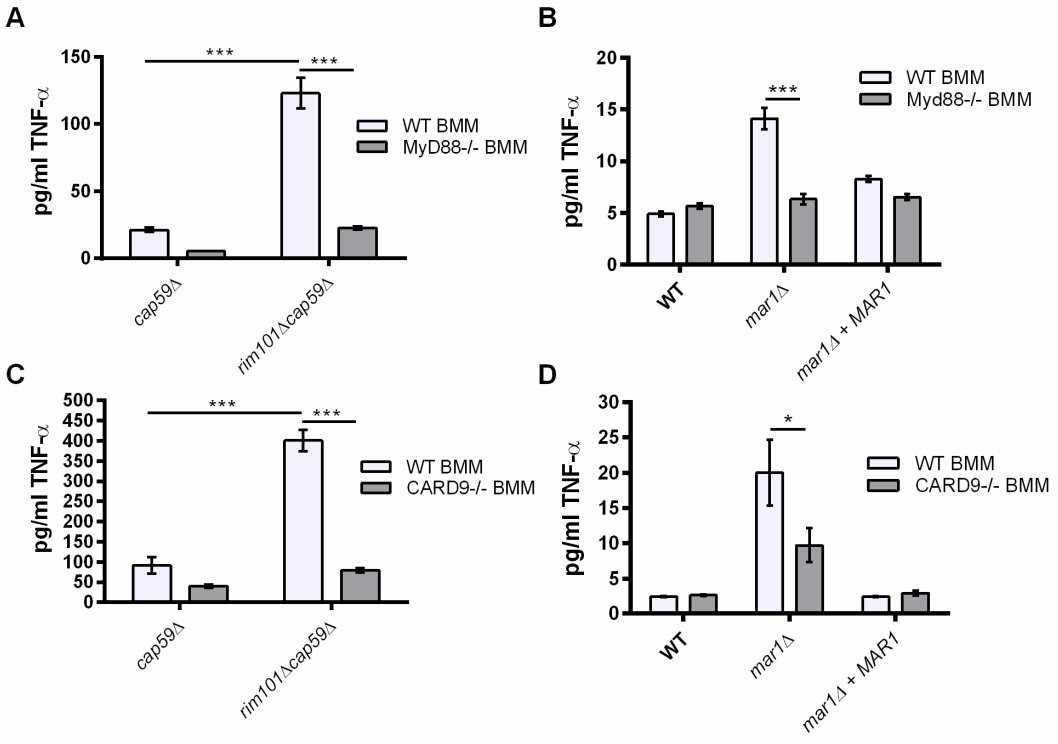

Figure 32: MyD88 and CARD9 contribute to the TNF-α response to *rim101*Δ and *mar1*Δ. A) and **C)**. BMMs were incubated with 2 mg/ml *cap59*Δ and *rim101*Δ *cap59*Δ. TNF-α quantified after 6 hr. co-incubation.**B)** and **D).** BMMs were incubated at an MOI of 10 fungal cells to 1 BMM. TNF-α was quantified after 6 hr. of co-incubation. 2-way ANOVA and Tukey's multiple comparison test used to compare means. ***p<0.001, **p<0.01, *p<0.05. Error bars represent standard error of the mean.

We also analyzed the role of MyD88 and CARD9 in responding to *mar1*Δ (Fig. 32 B and D). The *mar1*Δ strain induces more TNF-α than *rim101*Δ, and we were therefore able to use the single mutant for these experiments. Similar to *cap59*Δ *rim101*Δ, we found that MyD88$^{-/-}$ and CARD9$^{-/-}$ BMMs secreted significantly less TNF-α in response to *mar1*Δ compared to WT BMMs. We also determined that the CARD9 $^{-/-}$ BMMS secreted significantly less TNF-α than WT BMMs in response to the *cap59*Δ mar11Δ double mutant strain. These results demonstrate that the increased recognition of the *mar1*Δ *cap59*Δ and *rim101*Δ *cap*59Δ strains by macrophages requires both MyD88 and

CARD9, suggesting that one or more members of the TLR and CTL receptor families are involved in the increased TNF-α response toward *rim101*Δ and *mar1*Δ.

4.2.7 In vitro response to the *rim101Δ* mutant does not require Dectin-1

Dectin-1 is a CTL receptor that recognizes β-1, 3-glucan, a key component of most fungal cell walls. Dectin-1 is the best characterized fungal-sensing PRR, and is required for the immune response toward many important fungal pathogens, such as *Candida albicans* and *Aspergillus nidulans* [99]. While we did not observe a significant alteration in the level of β-1, 3-glucan in the cell wall of *rim101*Δ cell wall by staining [117], it is possible that the altered cell wall has increased exposure of this Dectin-1-stimuating carbohydrate.

We assessed the amount of TNF-α secreted by Dectin-$1^{-/-}$ and WT BMMs after co-incubation with WT, *rim101Δ,* and *rim101Δ+RIM101* (Fig. 33). In contrast to the MyD88$^{-/-}$ and CARD9$^{-/-}$ macrophages, the Dectin-$1^{-/-}$ deficient macrophages had no defect in activation in response to the *rim101*Δ strain. This assay demonstrates that, *in vitro*, Dectin-1 is not required for the increased recognition of macrophages to the *rim101*Δ strain.

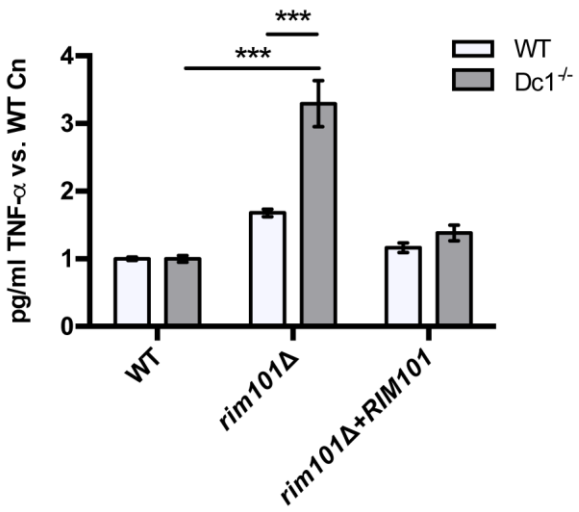

Figure 33: Dectin 1 is not required for the increased TNF-α response to *rim101*Δ. BMMs were co-incubated with the indicated strains at an MOI of 10 fungal cells to 1 BMM. TNF-α was quantified after 6 hr. 2-way ANOVA and Tukey's multiple comparison test used to compare means. Dc1$^{-/-}$ + *rim101*Δ was significantly different than all other means with a ***p<0.001. Error bars represent standard error of the mean.

*4.2.8 rim101*Δ induces a global increase in immune cell infiltration and inflammatory cytokine production in the lungs of infected mice.

To compare the immune response toward the *rim101*Δ and *mar1*Δ mutants in vivo, we intranasally inoculated BALB/c mice with 10^4 cells of each strain and analyzed the total number and percentage of leukocytes in whole lung homogenates at day 7 and day 14 post infection (Fig. 34 and Table 6). We also analyzed the number of viable *C. neoformans* at each time point in the lungs of each mouse and in the brain at day 14 (Fig. 35). At both time points, the *mar1*Δ-infected lungs had an overall decrease lung leukocytes compared to both the WT and *mar1*Δ + *MAR1* strains. The quantitative cultures demonstrated that the *mar1*Δ mutant is largely cleared from the lungs at day 7, perhaps explaining the marked decrease in immune cell infiltration. In contrast, the

*rim101*Δ mutant induced an increase in leukocyte infiltration, which was most evident at day 14. Compared to WT infections, each subpopulation of leukocytes that was tested was increased in the *rim101*Δ infection, and the percentage of neutrophils, dendritic cells, and pDCs were particularly increased (Fig. 34C, E, F and Table 6). The marked increase in the percentage of neutrophil infiltration at these time points is consistent with our previous study [117]. The enhanced leukocyte infiltration cannot be explained by an increased proliferation of *rim101*Δ; there were slightly but significantly more *rim101*Δ than WT cells in the lungs at day 7 post infection, but there were slightly fewer *rim101*Δ lung CFUs at day 14 compared to both WT and *rim101*Δ + *RIM101* (Fig. 35A and B). Therefore, the *rim101*Δ mutant induces significantly more leukocyte infiltration, primarily consisting of neutrophils, in the lungs of infected mice despite proliferating similarly to WT and *rim101*Δ + *RIM101* reconstituted strains.

Table 6: Percent Leukocytes

Percent (%) Leukocytes						
		WT	***rim101Δ***	***rim101Δ + RIM101***	***mar1Δ***	***mar1Δ + MAR1***
Macrophages	**Day 7**	27.9	26.9	32.4	14.3	23.5
	Day 14	24	28	22.2	15.1	19.6
Neutrophils	**Day 7**	11.2	12.9	12.4	4.2	11.3
	Day 14	8.3	24.6	10.4	5.1	12.7
Eosinophils	**Day 7**	1.7	2.7	2.4	0.6	2
	Day 14	5.1	6.7	6.9	0.08	0
DCs	**Day 7**	11.5	15.4	13	3.6	9.2
	Day 14	8.6	14.7	8.9	2.1	7.7
pDCs	**Day 7**	1.3	1.1	2.1	1	1.6
	Day 14	0.5	1.2	0.4	0.8	0.5
CD4+ T cells	**Day 7**	16.3	15	15.4	16.3	15.5
	Day 14	4.8	8.2	6.2	9.3	6.4
CD8+ T cells	**Day 7**	6.3	5.4	6.3	6.7	6
	Day 14	2.6	2.9	2.5	3.4	2.3
B cells	**Day 7**	13	12.4	13.9	17	16
	Day 14	11.2	12.3	11.8	10.9	17.1
γδ T cells	**Day 7**	4.2	7.9	4.5	3.4	3.5
	Day 14	2	4.9	0.4	4.4	4.2
NK cells	**Day 7**	4.4	4.3	4.6	3.1	4.1
	Day 14	1.7	1.4	1.7	2.5	1.5

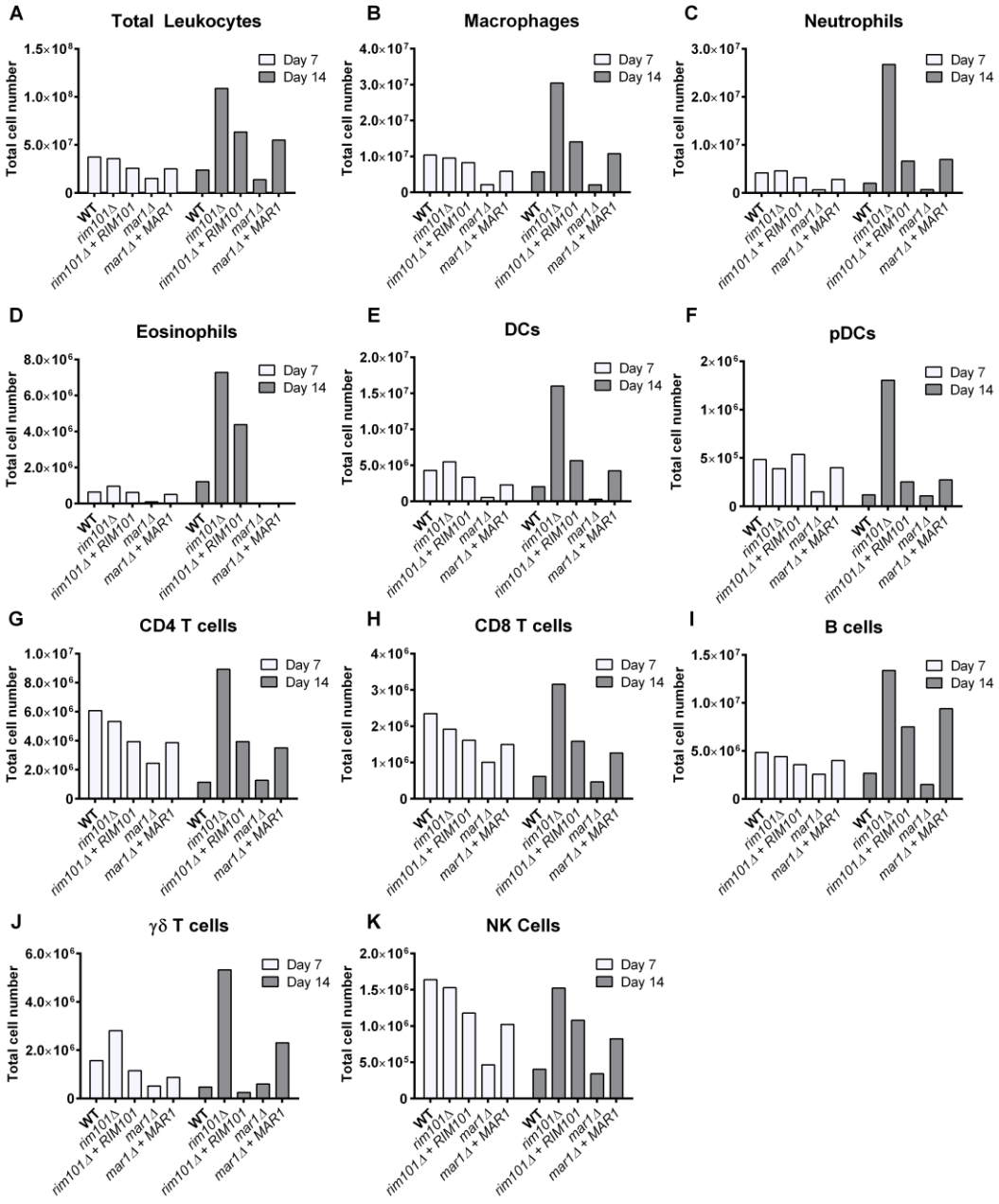

Figure 34: *rim101*Δ induces increased leukocyte recruitment to infected lungs. At day 7 and day 14 post infection, Indicated leukocytes were quantified from whole lung digests from BALB/c mice infected with 10^4 fungal cells.

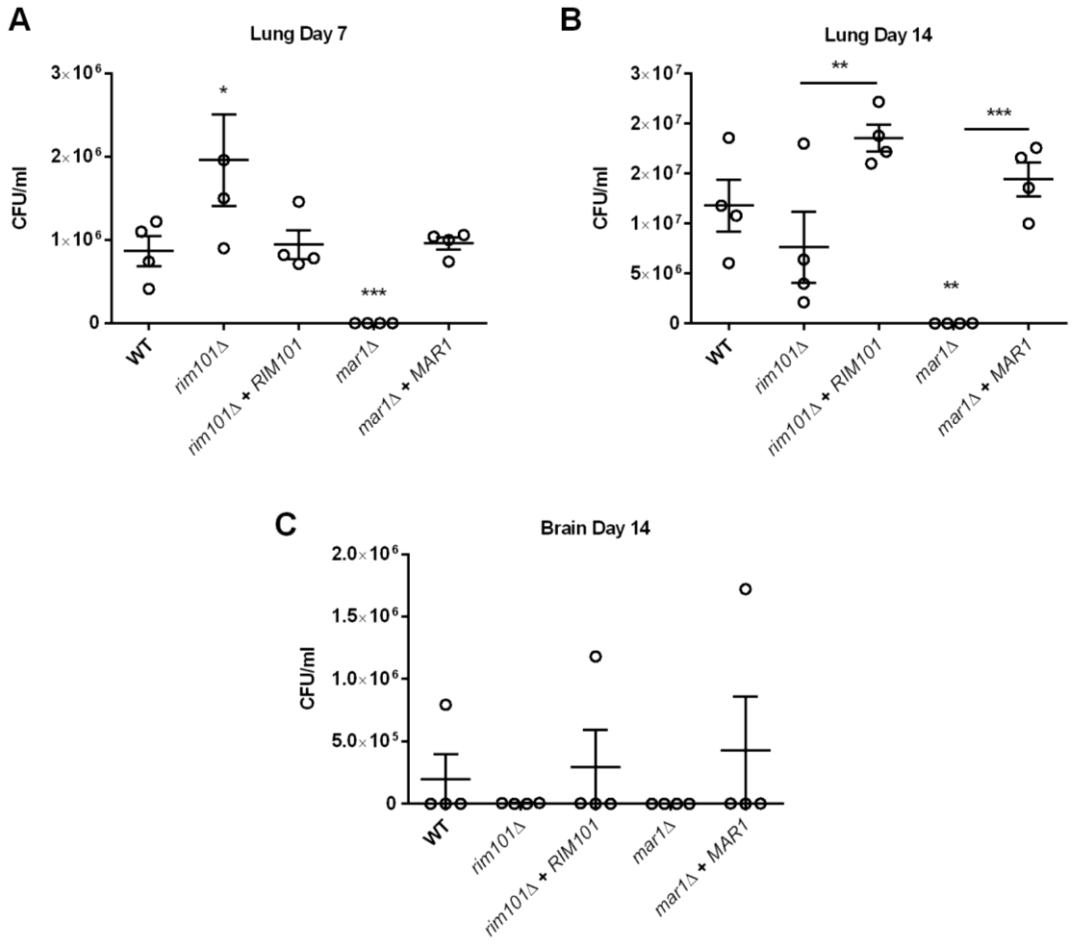

Figure 35: *mar1*Δ has a significant growth defect in vivo. Fungal CFUs were quantified from whole lung (A and B) or whole brain (C) homogenates. 4 BALB/c mice were intranasally infected with 10^4 cells for each strain. One-way ANOVA and Tukey's multiple comparison test used to compare means. ***p<0.001, **p<0.01, *p<0.05. Error bars represent standard error of the mean.

To better characterize the immune response to both *rim101*Δ and *mar1*Δ mutants, we analyzed the levels of 18 cytokines in infected lungs at day 7 and day 14 post infection (Fig 36). We found that lungs infected with *mar1*Δ had significantly lower levels of most cytokines at both time points, consistent with this strain being cleared from the lungs prior to these time points. In the *rim101*Δ mutant infected lungs, there was a global

increase in almost all cytokines measured at day 7 and day 14 compared to the WT and *rim101*Δ + *RIM101* infections. Several of the most highly up-regulated cytokines are known to induce inflammatory cell infiltration, including the neutrophil chemoattractant CXCL1 (Fig. 36D), and the inflammatory cytokines IL-1α, IL-1β, TNF-α, and IL-6 (Fig. 36A, B, C, H). Several Th1, Th2, and Th17 (inflammatory) driving cytokines were upregulated by the *rim101*Δ mutant, making it difficult to determine the specific type of adaptive immune response induced by this strain. Notably however, the only cytokine that was significantly reduced in the *rim101*Δ-infected lungs at day 14 was the Th2 driving cytokine, IL-4 (Fig. 36O). In contrast, key Th1 and Th17 (inflammatory) polarizing cytokines, INF-γ and IL-17 remained significantly higher at day 14 (Fig. 36G and K). Overall, the *rim101*Δ mutant induces a dramatic immune response in the lungs of infected mice, characterized by a global increase in cytokine secretion and neutrophil influx.

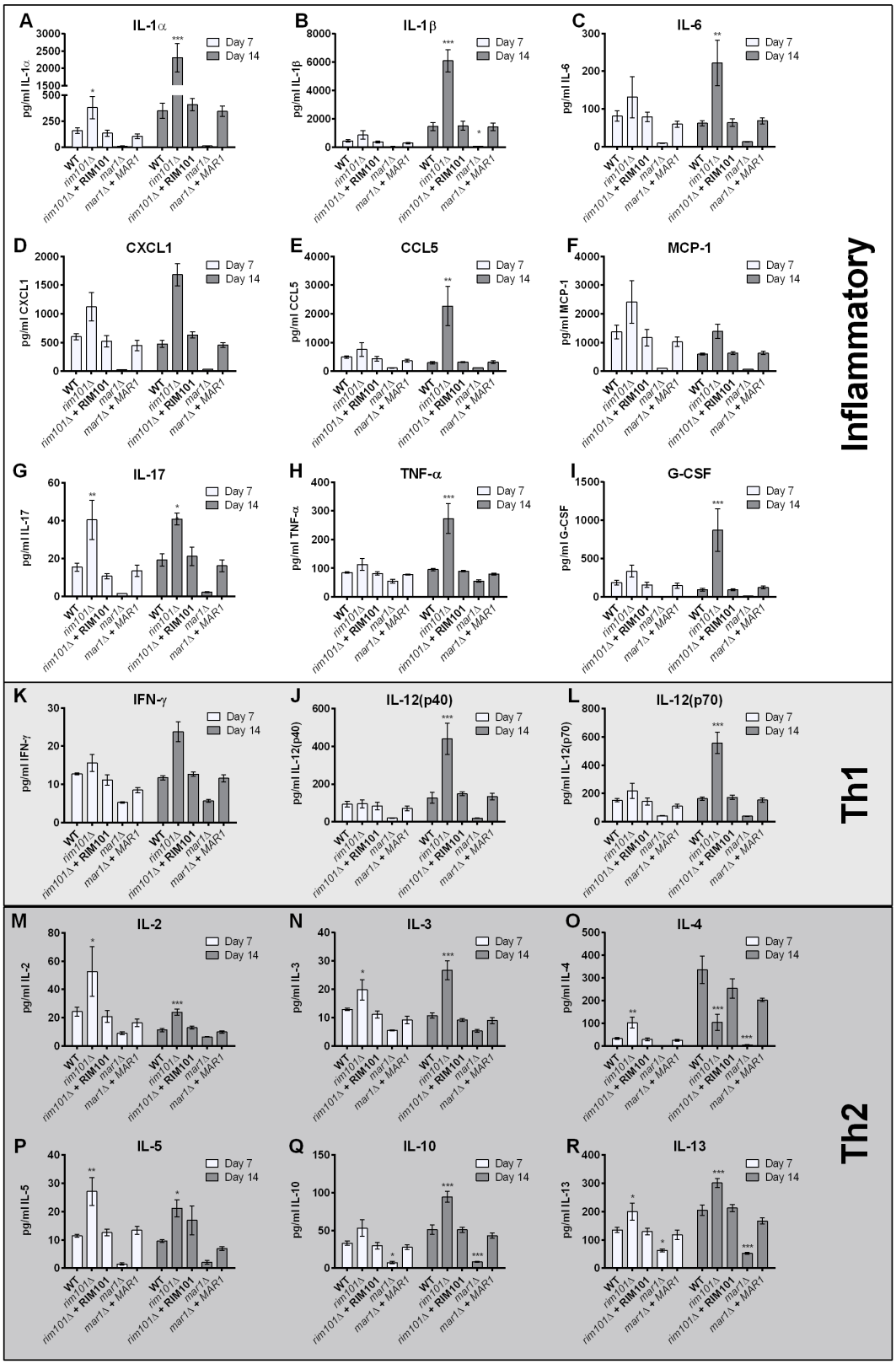
A
IL-1α
pg/ml IL-1α
B
IL-1β
pg/ml IL-1β
C
IL-6
pg/ml IL-6
D
CXCL1
pg/ml CXCL1
E
CCL5
pg/ml CCL5
F
MCP-1
pg/ml MCP-1
G
IL-17
pg/ml IL-17
H
TNF-α
pg/ml TNF-α
I
G-CSF
pg/ml G-CSF
K
IFN-γ
pg/ml IFN-γ
J
IL-12(p40)
pg/ml IL-12(p40)
L
IL-12(p70)
pg/ml IL-12(p70)
M
IL-2
pg/ml IL-2
N
IL-3
pg/ml IL-3
O
IL-4
pg/ml IL-4
P
IL-5
pg/ml IL-5
Q
IL-10
pg/ml IL-10
R
IL-13
pg/ml IL-13
Day 7
Day 14
WT
rim101Δ
rim101Δ + RIM101
mar1Δ
mar1Δ + MAR1
Inflammatory
Th1
Th2

Figure 36: *rim101*Δ elicits an inflammatory and Th1 cytokine response in infected lungs . At day 7 and day 14 post infection, indicated cytokines were quantified from whole lung digests from BALB/c mice infected with 10^4 fungal cells. 4 mice were infected for each strain. One-way ANOVA and Tukey's multiple comparison test used to compare means back to the WT infection for each day. ***p<0.001, **p<0.01, *p<0.05. Error bars represent standard error of the mean.

4.3 Discussion

The composition and architecture of the *C. neoformans* cell wall directs the immune response to this fungal pathogen. *C. neoformans* has a highly dynamic cell surface that it actively modifies during infection, dramatically altering the way the immune system interacts with these fungal cells. Resulting immune responses can range from non-protective and weak, in the case of *Cryptococcal* meningitis, to over-exuberant and damaging. Damaging immune responses toward *C. neoformans* infection have become significant issues for people recovering from immune suppression, such as those just beginning antiretroviral treatment for HIV infections. This condition is known as Immune Reconstitution Inflammatory Syndrome, or IRIS, and has mortality rates similar to *C. neoformans* meningitis [14]. Typical infections models of cryptococcosis explore infection in a highly susceptible host with non-protective weak immune responses, with few models exploring the damaging immune responses that can also occur during these infections in humans. Therefore, little is known about the *C. neoformans* attributes that drive highly active inflammatory responses. The *rim101*Δ mutant was previously shown to induce a detrimental inflammatory response and an increased death rate in two separate mouse strains [81,117]. Alterations in the cell wall structure and composition, and the associated capsule defect, were hypothesized to increase immune recognition and drive the inflammatory response. In this study, we

demonstrate that the *rim101*Δ mutant has increased chitin exposure on its cell surface in response to host-like conditions, without a major change in total cell wall content. This cell wall alteration, in addition to its decreased capsule, leads to increased recognition by macrophages and dendritic cells in vitro, and increase inflammation in vivo. We show that very similar cell surface defects present in a different mutant strain, *mar1*Δ, also increased recognition by macrophages and dendritic cells *in vitro*. Unlike *rim101*Δ however, *mar1*Δ is rapidly cleared from the lungs of infected mice and therefore does not appear to induce a hyperinflammatory response in this *in vivo* setting. Therefore, the same immune stimulatory cell surface attribute can contribute to a damaging immune response in the case of *rim101*Δ, and also to increased microbial recognition and killing in the case of *mar1*Δ.

4.3.1 Role of chitin exposure in the immune detection of *C. neoformans*.

Rim101 and Mar1 independently limit *C. neoformans* chitin exposure under host-mimicking conditions and similarly suppress recognition by innate immune cells. While other *rim101*Δ and *mar1*Δ cell surface attributes undoubtedly contribute to immune recognition, our data strongly associates chitin exposure with immune stimulation by *C. neoformans*. Chitin exposure also appeared to be more important than total chitin levels, which suggests that chitin is physically detected by immune cells primarily at the exposed cell surface.

The role of chitin in the immune response toward fungi is complex. Unlike β-1, 3-glucan, which is usually pro-inflammatory, chitin has been shown to both stimulate and inhibit immune responses, depending on the source and size of the chitin molecule. The

reported type of immune response to chitin can range from an allergic Th2 response [102,198], to a proinflammatory Th1 response [104,199,200], to anti-inflammatory [102,201]. Several recent studies have just begun to reveal the mechanisms behind the opposing responses to chitin observed. Wagener et. al. found that initial interactions between purified chitin from several fungal pathogens, including *C. neoformans*, and BMMs induce pro-inflammatory cytokine secretion. Once the BMMs are activated, chitin is digested by secreted mammalian chitinases, phagocytosed, and then stimulate the secretion of an anti-inflammatory cytokine, IL-10, that acts to inhibit the pro-inflammatory response [102]. Our in vitro experiments explored the initial interaction between macrophages and dendritic cells and the strains with elevated chitin exposure. The resulting increase in secretion of the pro-inflammatory cytokine TNF-α is therefore consistent with these described responses to chitin in vitro.

The innate immune receptors responding to increased *C. neoformans* chitin exposure are still unknown, however we demonstrated here that multiple receptors are likely involved. The adaptor proteins required for most TLR and CTL receptor signaling, MyD88 and CARD9 respectively, were both required for the full response toward *rim101*Δ and *mar1*Δ in vitro. Members of the TLR and CTL families have been previously implicated in chitin sensing; MyD88 and TLR2 were shown to be required for the in vitro, pro-inflammatory, response to chitin [104]. TLR9 was more recently shown to detect chitin that had been phagocytosed, though this interaction induced an anti-inflammatory response [102]. Mannose Receptor and Dectin-1 have also been implicated in chitin detection [102,105], athough Dectin-1 was not required for the response toward *rim101*Δ. Host chitinases also play an important role in the detection

and killing of invading fungal pathogens. Chitotriosidase, Chit1 has been associated with the induction of the non-protective Th2 immune response during *C. neoformans* infections [13], and the acidic mammalian chitinase (AMCase) suppresses the Th2 response toward fungi and other chitin-containing organisms [198,202]. *rim101*Δ, *mar1*Δ and other strains with increased chitin exposure are likely more prone to attack by Chit1 and AMCase, athough it is still unclear how this interaction would affect the immune response toward these mutant strains.

4.3.2 Other cell surface alteration that may contribute to *rim101*Δ and *mar1*Δ immune recognition.

It is likely that increased chitin exposure is not the only *rim101*Δ and *mar1*Δ cell surface alteration that stimulates macrophages and dendritic cells. Each also has a significant capsule defect, which would further expose cell surface PAMPs to the immune system. There is an extensive body of research demonstrating the anti-immune recognition properties of the polysaccharide capsule, showing that it acts as both a barrier against direct detection of cell wall PAMPs in addition to actively suppressing immune signaling pathways [17–21]**.** While direct comparisons were difficult in our in vitro assays, we consistently observed an increase in TNF-α secretion by macrophages and dendritic cells when stimulated with *cap59*Δ single and double mutants compared to WT or single *rim101*Δ and *mar1*Δ mutant strains. This finding also suggests that the GXM secreted by *rim101*Δ and *mar1*Δ is still able to suppress immune responses.

Alteration in cell wall chitosan levels may also play a role in the detection *rim101*Δ and *mar1*Δ. Our biochemical analysis showed that the *rim101*Δ mutant had a slight, though statistically insignificant, increase in cell wall chitosan. *C. neoformans* is

one of the few prominent fungal pathogens that has significant levels of chitosan in its cell wall [95,102]. Chitosan alone has been shown to activate the the inflammasome in macrophages, inducing the secretion of inflammatory cytokines such as IL-18 and IL-1β. Notably, IL-1β was one of the most upregulated cytokines in the mouse lungs infected with *rim101*Δ [203,204]. However, we also found that the *chs3*Δ mutation did not reduce the in vitro TNF-α response to *rim101*Δ. The *chs3*Δ mutation disrupts almost all chitosan production [157] and would significantly reduce chitosan levels in the *chs3*Δ *rim101*Δ strain. However, as we have observed with chitin, perhaps chitosan exposure is more important for immune recognition that total levels. Further experimentation is needed to more precisely determine the role of chitosan in the immune response to *rim101*Δ and *mar1*Δ.

4.3.3 Characterization of the immune response to *rim101*Δ and *mar1*Δ in vivo.

The immune response to the *rim101*Δ mutant in a murine lung infection model was characterized by an increase in many pro-inflammatory cytokines. Certain cytokines, including several favoring Th1 and Th17 upregulated responses, were particularly high during this infection. This response is consistent with previous studies demonstrating a strong Th1 and Th17 response toward chitin, or high chitin-producing fungal mutants [104,199,200]. While several Th2 cytokines were elevated during the entire *rim101*Δ infection, IL-4 was the only cytokine that was significantly decreased in the *rim101*Δ infection at day 14 post infection. IL-4 secretion is an important driver of the Th2 response, as it induces the production of other Th2 cytokines while suppressing Th1 and Th17 responses [205]. This observation, along with the dramatic neutrophil

infiltration during the *rim101*Δ mutant infection, demonstrates that alteration of the *rim101*Δ cell wall primarily induced a proinflammatory Th1/Th17 immune response in this infection model. The immune response observed here is largely consistent with our previous analysis of the *rim101Δ* infection [117]. Here however, we analyzed the response at later time points, and in a different mouse background (BALB/C vs. C57B/6), demonstrating a consistent pro-inflammatory response to *rim101*Δ throughout the infection and independent of mouse genotype.

Many studies have demonstrated that a strong Th1 immune response is essential for clearing *C. neoformans* infections, and a Th2 response is associated with a worse disease outcome [3]. However, the inflammatory condition, IRIS, results primarily from an over-exuberant Th1 immune response [14]. Our findings suggest that increase chitin exposure may drive, or worsen, the inflammatory response in Cryptococcus-associated IRIS. *C. neoformans* cells have a wide range of morphologies, sizes, and cell surface properties during infection. This includes the production of titan cells, which have recently been shown to increase chitin levels compared to regular cells [13]. In addition, dead or dying fungal cells often have aberrant cell wall composition and arrangement [105] .The chitin synthase mutants analyzed in this study demonstrate that mutations disrupting cell wall composition can increase chitin exposure, even when these mutations are expected to decrease total chitin levels [157]. These *C. neoformans* cells with altered cell wall architecture may be present in patients with recurrent or latent *C. neoformans* infections, who are particularly susceptible to developing IRIS. In contrast to *rim101*Δ, the increased immune response to the *mar1*Δ mutant in vitro was associated with clearance of the mutant from the lungs of infected mice. The same response to

chitin exposure on this mutant also induces a protective response in some cases. We previously found that the *cap59*Δ *rim101*Δ double mutant was also avirulent and cleared from infected mice, despite being immune stimulatory in vitro [117]. In addition, the *chs3*Δ mutant, shown here to have increased chitin exposure, is more readily recognized by BMMs and is avirulent in mice. These examples demonstrate that the particular response to increased chitin exposure can be both beneficial and detrimental to the host. These mutants also have additional phenotypes, such as temperature sensitivity, that would affect their fitness during infection. Therefore, the duration of fungal cell persistence is likely an equally important contributor as cell wall organization to the ultimate outcome of the infection.

4.3.4 Conclusion and future directions

We have demonstrated that the combination of increased chitin exposure along with decreased capsule attachment in *C. neoformans* is strongly associated with immune stimulation in vitro and in vivo. Future experiments are needed to determine whether immune cells directly detect chitin exposure, or if it serves as a binding site for unknown immune stimulatory molecules. Furthermore, while *rim101*Δ and *mar1*Δ mutants would rarely be encountered in the environment, understanding *C. neoformans* cell surface patterns that stimulate immune recognition are vitally important for vaccine development and prevention of damaging inflammation. These studies also increase our understanding of how *C. neoformans* utilizes Rim101 and Mar1 to actively avoid immune recognition. While the function of Rim101 has been extensively studied by our lab and others, Mar1 is a newly identified *Cryptococcus*-specific protein that is required for

growth in vivo. Future work will reveal how this novel protein contributes to *C. neoformans* adaptation to the host environment.

4.4 Materials and Methods

4.4.1 Strains, media, and growth conditions

C. neoformans strains used in this study are listed tin Table 7. All strains were generated in the *C. neoformans* var *grubii* strain H99 and were maintained on YPD medium (yeast extract 2%, peptone 1%, dextrose 2%). Unless otherwise stated, *C. neoformans* strains were cultured in CO_2-independent media (Gibco) at 37^{o}C for cell wall analysis, cell wall staining, and prior to immune cell co-culture experiments.

Table 7: Chapter 4 Strains

Strain	Genotype	Source
TOC35	*rim101*Δ :: *NAT*	[81]
KS182	*rim101*Δ :: *NAT + RIM101*	this study
MAK1	*mar1Δ::NEO*	this study
MAK11	*mar1*Δ::*NEO + MAR1*	this study
KMP18	*chs3*Δ::*NEO*	this study
KS239	*chs3*Δ::*NEO rim101*Δ::*NAT*	this study
*chs5*Δ	*chs5*Δ::*NEO*	[157]
KS241	*chs5*Δ::*NEO rim101::*NAT	this study
*cap59*Δ	*cap59*Δ::*NEO*	[117]
TOC39	*cap59*Δ::*NEO rim10*Δ::*NAT*	[117]
SKE60	*cap59*Δ::*NEO mar1*Δ:*NAT*	this study
MAK8	*mar1Δ::NEO + GFP-RIM101*	this study

4.4.2 Molecular biology

Gene disruptions were made as previously described previously [137,138] using nourseothricin (NAT) or neomycin (NEO) as dominant drug resistance genes. Disruption

cassettes were transformed using biolistic transformation [138]. All disruptions were confirmed by Southern blot.

4.4.3 Cell wall isolation and HPLC

C. neoformans strains were inoculated from an overnight YPD culture into 25 ml CO_2-independent media and incubated for 18-20 hr at 37ºC. Cell wall isolation and high-performance anion-exchange chromatography with pulsed amperometric detection (HPAEC-PAD)analysis performed as previously described in [206]. The enzymatic analysis of chitin and chitosan was performed as described in [157].

4.4.4 Cell wall staining and Microscopy

Cells from overnight culture in either CO_2-independent media or YPD were harvested, washed with phosphate buffered saline pH 7.4. Cells were stained with 100 µg/ml WGA, Alexa Fluor 488 (Molecular Probes) for 45 min in the dark. The same cells were also stained with 25 µg/ml CFW for 10 min. Cells were washed 2 times with PBS and imaged on a Zeiss Axio Imager A1 fluorescence microscope equipped with an AxioCam MRM digital camera. The same exposure time was used to image each strain.

4.4.5 In vitro macrophage and dendritic cell experiments

Bone marrow derived macrophages and dendritic cells were prepared as previously described [207,208]Both macrophage and dentritic cells were plated in 96-well plates at a concentration of 5 X 10^4 cells/well for each experiment. 5 X 10^5 *C. neoformans* cells (10:1 Cn:Macrophage or DC) were added to each well with the exception of the *cap59*Δ mutant strains. All strains with the *cap59*Δ mutation stuck together in large clumps that made accurate quantification by hemocytometer or optical

density impossible. Instead, these were normalized to 2 mg wet cell pellet per ml of media. 2 mg/ml was approximately the mg/ml concentration of the *rim101*Δ mutant inocula. *rim101*Δ was used because it has a significant capsule defect and therefore has a mass/cell ratio to the acapsular *cap59*Δ strains. Secreted TNF-α was quantified by ELISA (Biolegend).

4.4.6 Animal experiments.

To assess organ fungal burden, 4 BALB/c mice were intranasally infected with 10^4 cells for each strain. Lungs and brains were dissected and homogenized in 2 ml PBS. Viable cells were quantified by quantitative culture. Pulmonary leukocyte isolation, staining, and flow cytometry was assessed as described in [209]. Lung cytokine levels were quantified from lung homogenate as described in [209].

5. Thesis conclusion

My goal for this thesis was to explore *C. neoformans* signaling pathways required for adaptation to the host environment. I found that highly conserved eukaryotic or fungal signaling pathways have been adapted in *C. neoformans* to increase resistance to stresses often encountered during infection. Unique aspects of these signaling pathways offer important insights into how this fungus causes disease, providing a foundation for future treatment strategies.

My first projects explored the role of post-translational modifications on target proteins involved in cryptococcal morphogenesis and pathogenesis. I determined that the *C. neoformans* GGTase I prenyltransferase enzyme was an important regulator of thermotolerance, mating, and virulence. I also established that the GTPase, Cdc42, is a major GGTase I substrate, requiring geranylgeranylation to appropriately associate with membranes. Despite its important role in virulence, I found that the GGTase I substrates were limited in *C. neoformans,* and several conserved GGTase-I substrates did not require this enzyme for membrane localization. This work suggests that the other prenyltransferase, farnesyltransferase, has an expanded substrate repertoire in *C. neoformans*. It also demonstrates that the features specifying GGTase vs. FTase substrates may not be as straightforward in *C. neoformans* as has been suggested in other systems. These experiments build an important foundation for ongoing translational studies for using prenyltransferase inhibitors as novel antifungal agents.

I also characterized both conserved and novel components of the *C. neoformans* alkaline response Rim pathway. Prior to this work, our lab found that the central

component of this pathway, the Rim101 transcription factor, regulated key stress response genes necessary for adapting to the host environment. Genes regulating low iron tolerance, high cation response, and cell wall synthesis and maintenance were primary targets of Rim101 regulation. Despite having a detailed understanding of the downstream targets of Rim101, we knew very little about the signaling elements responsible for Rim pathway activation. I found that only a portion of the canonical Rim pathway characterized in ascomycete fungi (*S. cerevisiae, C. albicans, A. nidulans, A. fumigatus*) was conserved in *C. neoformans.* These components include the ESCRT complex, Rim23, Rim20, and the Rim13 protease, which assemble together, bind and activate Rim101 by proteolytic cleavage. However, homologs for the ascomycete pH sensing complex were not present in the genomes of *C. neoformans* or other members of the basidiomycete phylum. Using an unbiased genetic screen, I identified Rra1, a novel Rim pathway component functioning upstream of the Rim101 proteolysis complex. While Rra1 has a predicted structure that is similar to the ascomycete pH sensor, Rim21, its subcellular localization suggests that it may have a distinct function. If Rra1 and its basidiomycete orthologs are pH sensors, their pH sensing mechanism are likely distinct from the ascomycete pH sensors. I propose that Rra1 is the first identified member of a novel, basidiomycete-specific, pH-responsive Rim pathway activation complex.

Finally, I explored the Rim101-regulated cell surface changes necessary for preventing immune detection during infection. From previous work, we found that the *rim101*Δ mutant induced an over-exuberant inflammatory response in the lungs of infected mice. Closer examination demonstrated that this mutant had a significantly

altered cell wall and a capsule attachment defect. In the current study, we found that the *rim101*Δ mutant has a significant increase in chitin exposure on its cell wall. Chitin exposure and decreased capsule attachment was associated with increased recognition by macrophages and dendritic cells in vitro and a dramatic lung immune response in mice. We demonstrate that a novel gene, *MAR1,* regulates chitin exposure and capsule attachment in a remarkably Rim101-like manner, though is functionally independent of the Rim pathway. We find that the *mar1*Δ cell wall alterations induce macrophage and dendritic cell responses in very similar manner to the *rim101*Δ. Finally, we demonstrate that the immune detection of both *rim101*Δ and *mar1*Δ require members of the TLR and C-type lectin receptor families. These studies are the first to demonstrate that increases in cell wall chitin exposure increases the immune detection of *C. neoformans*, with important implications for understanding both protective and detrimental immune responses to *C. neoformans* infection.

5.1 Future Directions

5.1.1 Defining the mechanism of Rim pathway activation

The ability for *C. neoformans* to quickly adapt to a wide variety of pH ranges is important for its ability to cause disease. During the course of infection, this fungal pathogen endures several dramatic shifts in pH that include entry into the lungs (pH 6.8-7.4), entry into the acidic macrophage phagolysosome (pH ~5), and finally transfer to the cerebral spinal fluid (pH. 7.4). Alterations of pH on this scale have profound effects on many cellular processes that include changes in membrane potential, ion channel function, iron acquisition, and protein folding. Alterations of any of these processes can

serve as surrogate markers of acidic or alkaline pH stress. For this reason, many pH sensing proteins serve other cellular functions that are altered in some way by pH changes. Ion channels are an excellent example and often serve as both intracellular and extracellular pH sensor [210]. There are also designated pH sensors with the primary function of detecting proton levels [211].

Despite almost 30 years of research on the fungal Rim/Pal pathway in many organisms, the mechanism of Rim21/PalH pH sensing is still largely unknown. Several studies have recently suggested that in *S. cerevisiae,* Rim21 responds to changes in membrane charge that results from alkaline pH stress [43,178,179]. In my work on the *C. neoformans* Rim pathway, I found that typical alkaline pH-associated stresses, such as low iron or concentrated cation levels, were not sufficient to activate the Rim pathway. However, I present evidence suggesting that membrane charge may serve as an important activating signal. The proposed *C. neoformans* Rim pathway pH sensor, Rra1, has a C-terminal tail that binds to cellular membranes in a pH-dependent manner. To further explore the role of membrane charge in Rim pathway activation, I would genetically alter the membrane charge by disrupting genes encoding flippase or floppase enzymes. I would then analyze these strains for pH-independent activation of Rim101.

Rra1 is the first basidiomycete Rim pathway component shown to activate the Rim101 proteolysis complex. While I have established its position in the Rim pathway, it role in activating this pathway is still undefined. The first step to determine Rra1 function would be to define its localization in detail. I would use microscopy to co-localize Rra1 with strains or molecular probes targeting specific organelles or cellular structures. Identifying proteins that interact with Rra1 would also provide useful information about its

function in the Rim pathway. I have already developed Rra1 purification protocol to perform protein pull-downs under different pH conditions. These initial experiments will begin to define this novel Rim pathway component and potentially identify other novel members of the *C. neoformans* Rim pathway.

5.1.2 Expanding *C. neoformans* Rim pathway

Our detailed examination of the Rim pathway has left us uniquely poised to identify and characterize the entire Rim pathway in *C. neoformans.* We have a powerful, unbiased screening method to specifically identify Rim101 activators. We also have tools to identify the functional location of novel Rim pathway components. Our initial screen that identified Rra1 was highly successful, but it did not reach genome saturation, with just one other known Rim pathway component, Rim13, identified in the initial screen. A saturating mutagenesis screen, in which all known Rim components were identified, would likely reveal other novel pathway activators, further expanding the understanding of the Rim pathway in *C. neoformans* and other basidiomycetes.

Our genetic screening strategy, and others performed in ascomycete species, have largely focused on the Rim pathway activators and very few Rim pathway inhibitors have been identified. Recently, a negative pathway regulator was identified in *A. nidulans,* after a reexamination of mutants from the very first mutagenesis screen performed on this pathway [212]. Pathway inhibitors likely provide tight regulation of Rim101 activity, rapidly inhibiting the pathway when environmental pH decreases. Negative regulators likely play an important role in *C. neoformans* survival during an infection, where this organism experiences rapid alterations in pH as it moves in and out

of macrophage phagolysosomes. To identify negative regulators, we could use our detailed knowledge of Rim101-regulated promoters to create Rim101 reporter constructs that are induced by Rim101 activation. For example, we could place a drug resistance gene under the control Rim101-activated *ENA1* or *CDA1* promoters. Using this reporter, we could then carry out a screen for drug resistant mutants in acidic pH, where Rim101 is typically inactive. To increase the specificity of this screen, we could utilize multiple reporter constructs with different Rim101-regulated promoters. We also have the truncated, constitutively active Rim101 construct, which would serve as an excellent positive control. Since this is a positive selection strategy, thousands of mutants could be rapidly analyzed.

We now have the foundational knowledge to design and perform the most detailed analysis of the Rim pathway in any basidiomycete fungus. The results of this analysis would significantly increase our understanding of the ability of *C. neoformans* to adapt to the host environment in addition to serving as a model for other basidiomycete fungi.

5.1.3 Define role of Rim101 in titan cell formation and capsule attachment

The signals and signaling pathways that induce titan cell formation are just now being defined. In recent reports, Rim101 activity was required for the formation of titan cells in the lungs of infected mice [82]. Our unpublished observations confirm the lack of titan cells at any stage of a murine lung infection with the *rim101*Δ mutant strain. To date, the Rim pathway is the strongest identified activator of titan cell formation, and

mutation of any component practically abolishes titan cell formation during infection. How Rim101 regulates titan cells is still unknown.

Titan cells are characterized by a number of attributes, but their defining feature is their size: 15-100 μm in diameter [28,29]. These specialized cells are usually identified solely by size, and are typically described as any cell with a diameter greater than 15 μm [82]. Titan cells also contain a thick cell wall and an extremely dense capsule.

It is possible that the *rim101*Δ cells cannot reach titan cell size, but that they may have other attributes of titan cells. For example, we could determine whether a proportion of *rim101*Δ mutant cells were polyploid and/or particularly resistant to nitrosative or oxidative stress during infection. If the *rim101*Δ mutants retained other titan cell-like phenotypes, it would suggest that titan cell size can be functionally separated from their other features.

I hypothesize that Rim101 regulation of the cell wall and capsule attachment is required for normal titan cell formation. If this is the case, then other proteins that regulate the cell surface similar to Rim101 would also be required for titan cell formation. Mar1 regulates chitin exposure and capsule attachment in a Rim101-like manner, despite functioning independent of the Rim pathway. If *mar1*Δ mutant also has a defect in titan cell formation, it would suggest that the cell wall processes regulated by Rim101 and Mar1 are important for titan formation.

Another unexplored *rim101*Δ phenotype is its capsule attachment defect. Only one cell wall component, α-1,3-glucan, has been definitively shown to bind capsule [213]. However, our recent studies have demonstrated that the *rim101*Δ mutant actually contains more α-1,3-glucan than WT cells, suggesting that decreased α-1,3-glucan is

not the mechanism of failed capsule attachment in the *rim101*Δ strain [117]. Recent work has suggested that capsule can also interact with chitin and that this interaction may regulate capsule assembly [214,215]. One possibility is that altered cell wall architecture in the *rim101*Δ mutant interferes with capsule attachment sites or that too many chitin/capsule interactions inhibit proper capsule formation.

In summary, the *C. neoformans* Rim101 transcription factor controls many cellular features associated with pathogenesis, including cell wall structure, capsule binding, and titan cell formation. In spite of this, the *rim101*Δ mutant strain retains virulence, even inducing a more intense inflammatory response than the wild type strain. Therefore, the Rim pathway is also required for the complex and composite phenotype of immune evasion.

5.1.4 Identify innate immune receptors that recognize *rim101*Δ

The detrimental inflammatory response induced by the *rim101*Δ mutant is similar to the damaging inflammation induced during *Cryptococcus*-associated IRIS. Understanding *C. neoformans* and host factors that induce an over-exuberant response may lead to new treatment strategies aimed to prevent IRIS development. While we have begun to define the *rim101*Δ cell surface changes that induce this response, the host receptors recognizing *rim101*Δ cells are still unknown. We found that both the TLR and C-type lectin receptor families are involved in *rim101*Δ detection, indicating this is a complex immune response involving multiple receptors. Fortunately, TLR and C-type lectin receptors have been studied extensively in the context of fungal infection, and mouse lines deficient for most individual members of these receptor families are already

available. To pursue the exact immune sensors and effectors responsible for the *rim101*Δ-mediated hyper-inflammatory response, future studies will initially focus on TLR and C-type lectin receptors shown to detect chitin or *C. neoformans* in previous studies. These include TLR2, TLR4, TLR9, and Dectin-2 [99,102,104,105]. This would most readily be accomplished by first using bone marrow derived macrophages from mouse strains deficient in individual receptors to determine which are required for TNF-α production (macrophage activation) in response to *rim101*Δ. This would be the first study to explore innate immune receptors involved in a damaging immune response to *C. neoformans* and may identify host factor that contribute to the development of IRIS in humans.

5.1.5 Determine whether the *rim101*Δ-induced immune response is protective.

Natural infection with *C. neoformans* does not necessarily induce a protective immune response. For example, mice infected with a sub-lethal dose of *C. neoformans* remains susceptible to a rechallenge with this organism. However, recent studies from several investigators have begun to identify strains that are protective; after an experimental infection with selected mutant strains, the animals are able to survive in infectious challenge with a typically lethal dose of wild type *C neoformans* cells. These strains include chitosan-deficient mutants and a strain engineered to secreted murine INF-gamma. These strains have in common the ability to induce a strong Th1 immune response during the early period of infection. Even though the *rim101*Δ-induced immune response is damaging to the infected host, the response is also primarily characterized by Th1 cytokine production. Therefore, the *rim101*Δ immune response may be protective

if it was induced in a measured way to prevent host damage. Similar to recent studies of chitosan mutants from the Lodge laboratory (J. Lodge, personal communication), I propose new studies in which a high dose of heat-killed *rim101*Δ cells would be used to infect mice. I anticipate that the heat-killed cells will induce a robust Th1-weighted immune response, but that these inviable cells would be rapidly cleared after inoculation. I hypothesize that rechallenging these “immunized” mice with a virulent, wild type *C. neoformans* strain would demonstrate a degree of protective immunity not induced by a similar inoculum of heat-killed wild type cells. These types of exciting studies are currently being performed by other investigators with other strains with various cell wall changes, indicating the importance of intact cell wall homeostasis in the process of immune evasion by this pathogen. Such studies will also demonstrate a significant translational potential for protecting future patients from cryptococcosis.

These studies began by identifying intracellular signaling pathways involved in microbial sensing of the external environment. Building upon this foundation, I have explored the ways in which environmental sensing actually shaped the adaptive response of *C. neoformans* to survive cell stresses. These principles are very important in the adaptation of this opportunistic pathogen to the infected host, and ultimately on the process of cryptococcal pathogenesis. I envision that further exploration of these cellular pathways in microorganisms will directly inform our growing understanding of basic eukaryotic cell physiology, host-microbe interactions, and cellular stress response.

References

1. Maziarz EK, Perfect JR (2016) Cryptococcosis. Infect Dis Clin North Am 30: 179–206. doi:10.1016/j.idc.2015.10.006.
2. Park BJ, Wannemuehler KA, Marston BJ, Govender N, Pappas PG, et al. (2009) Estimation of the current global burden of cryptococcal meningitis among persons living with HIV/AIDS. AIDS 23: 525–530 10.1097/QAD.0b013e328322ffac.
3. Kwon-Chung KJ, Fraser JA, Doering TL, Wang Z, Janbon G, et al. (2014) Cryptococcus neoformans and Cryptococcus gattii, the etiologic agents of cryptococcosis. Cold Spring Harb Perspect Med 4: a019760. doi:10.1101/cshperspect.a019760.
4. Emmons CW (1955) Saprophytic sources of Cryptococcus neoformans associated with the pigeon (Columba livia). Am J Hyg 62: 227–232.
5. Goldman DL, Khine H, Abadi J, Lindenberg DJ, Pirofski L, et al. (2001) Serologic evidence for Cryptococcus neoformans infection in early childhood. Pediatrics 107: E66.
6. Wang L, Zhai B, Lin X (2012) The link between morphotype transition and virulence in Cryptococcus neoformans. PLoS Pathog 8: e1002765. doi:10.1371/journal.ppat.1002765.
7. Wang L, Lin X (2015) The morphotype heterogeneity in Cryptococcus neoformans. Curr Opin Microbiol 26: 60–64. doi:10.1016/j.mib.2015.06.003.
8. Velagapudi R, Hsueh Y-P, Geunes-Boyer S, Wright JR, Heitman J (2009) Spores as infectious propagules of Cryptococcus neoformans. Infect Immun 77: 4345–4355. doi:10.1128/IAI.00542-09.
9. Salyer WR, Salyer DC, Baker RD (1974) Primary complex of Cryptococcus and pulmonary lymph nodes. J Infect Dis 130: 74–77.
10. Garcia-Hermoso D, Janbon G, Dromer F (1999) Epidemiological evidence for dormant Cryptococcus neoformans infection. J Clin Microbiol 37: 3204–3209.
11. Liu TB, Kim JC, Wang Y, Toffaletti DL, Eugenin E, et al. (2013) Brain inositol is a novel stimulator for promoting cryptococcus penetration of the blood-brain barrier. PLoS Pathog 9: e1003247. doi:10.1371/journal.ppat.1003247.
12. Brizendine KD, Baddley JW, Pappas PG (2011) Pulmonary cryptococcosis. Semin Respir Crit Care Med 32: 727–734. doi:10.1055/s-0031-1295720.
13. Wiesner DL, Boulware DR (2011) Cryptococcus-Related Immune Reconstitution Inflammatory Syndrome(IRIS): Pathogenesis and Its Clinical Implications. Curr Fungal Infect Rep 5: 252–261. doi:10.1007/s12281-011-0064-8.
14. Perfect JR (2012) The impact of the host on fungal infections. Am J Med 125: S39–S51. doi:10.1016/j.amjmed.2011.10.010.

15. McFadden DC, De Jesus M, Casadevall A (2006) The physical properties of the capsular polysaccharides from Cryptococcus neoformans suggest features for capsule construction. J Biol Chem 281: 1868–1875. doi:10.1074/jbc.M509465200.

16. Heiss C, Klutts JS, Wang Z, Doering TL, Azadi P (2009) The structure of Cryptococcus neoformans galactoxylomannan contains beta-D-glucuronic acid. Carbohydr Res 344: 915–920. doi:10.1016/j.carres.2009.03.003.

17. Retini C, Vecchiarelli A, Monari C, Bistoni F, Kozel TR (1998) Encapsulation of Cryptococcus neoformans with glucuronoxylomannan inhibits the antigen-presenting capacity of monocytes. Infect Immun 66: 664–669.

18. Vecchiarelli A, Pietrella D, Lupo P, Bistoni F, McFadden DC, et al. (2003) The polysaccharide capsule of Cryptococcus neoformans interferes with human dendritic cell maturation and activation. J Leukoc Biol 74: 370–378.

19. Piccioni M, Monari C, Kenno S, Pericolini E, Gabrielli E, et al. (2013) A purified capsular polysaccharide markedly inhibits inflammatory response during endotoxic shock. Infect Immun 81: 90–98. doi:10.1128/IAI.00553-12.

20. Kozel TR, Gotschlich EC (1982) The capsule of cryptococcus neoformans passively inhibits phagocytosis of the yeast by macrophages. J Immunol 129: 1675–1680.

21. Guo C, Chen M, Fa Z, Lu A, Fang W, et al. (2014) Acapsular Cryptococcus neoformans activates the NLRP3 inflammasome. Microbes Infect 16: 845–854. doi:10.1016/j.micinf.2014.08.013.

22. Zaragoza O, Chrisman CJ, Castelli M V, Frases S, Cuenca-Estrella M, et al. (2008) Capsule enlargement in Cryptococcus neoformans confers resistance to oxidative stress suggesting a mechanism for intracellular survival. Cell Microbiol 10: 2043–2057. doi:10.1111/j.1462-5822.2008.01186.x.

23. Vartivarian SE, Anaissie EJ, Cowart RE, Sprigg HA, Tingler MJ., et al. (1993) Regulation of Cryptococcal Capsular Polysaccharide by Iron. J Infect Dis 167: 186–190. doi:10.1093/infdis/167.1.186.

24. Granger DL, Perfect JR, Durack DT (1985) Virulence of Cryptococcus neoformans. Regulation of capsule synthesis by carbon dioxide. J Clin Invest 76: 508–516. doi:10.1172/JCI112000.

25. O'Meara TR, Alspaugh JA (2012) The Cryptococcus neoformans capsule: a sword and a shield. Clin Microbiol Rev 25: 387–408. doi:10.1128/CMR.00001-12.

26. Rhodes JC, Polacheck I, Kwon-Chung KJ (1982) Phenoloxidase activity and virulence in isogenic strains of Cryptococcus neoformans. Infect Immun 36: 1175–1184.

27. Leopold Wager CM, Hole CR, Wozniak KL, Wormley FL (2016) Cryptococcus and Phagocytes: Complex Interactions that Influence Disease Outcome. Front Microbiol 7: 105. doi:10.3389/fmicb.2016.00105.

28. Zaragoza O, García-Rodas R, Nosanchuk JD, Cuenca-Estrella M, Rodríguez-Tudela JL, et al. (2010) Fungal Cell Gigantism during Mammalian Infection. PLoS Pathog 6: e1000945. doi:10.1371/journal.ppat.1000945.

29. Okagaki LH, Strain AK, Nielsen JN, Charlier C, Baltes NJ, et al. (2010) Cryptococcal Cell Morphology Affects Host Cell Interactions and Pathogenicity. PLoS Pathog 6: e1000953. doi:10.1371/journal.ppat.1000953.

30. Gerstein AC, Fu MS, Mukaremera L, Li Z, Ormerod KL, et al. (2015) Polyploid titan cells produce haploid and aneuploid progeny to promote stress adaptation. MBio 6: e01340–15. doi:10.1128/mBio.01340-15.

31. García-Barbazán I, Trevijano-Contador N, Rueda C, de Andrés B, Pérez-Tavárez R, et al. (2016) The formation of titan cells in Cryptococcus neoformans depends on the mouse strain and correlates with induction of Th2-type responses. Cell Microbiol 18: 111–124. doi:10.1111/cmi.12488.

32. McDonald T, Wiesner DL, Nielsen K (2012) Cryptococcus. Curr Biol 22: R554–R555. doi:10.1016/j.cub.2012.05.040.

33. Alspaugh JA, Cavallo LM, Perfect JR, Heitman J (2000) RAS1 regulates filamentation, mating and growth at high temperature of Cryptococcus neoformans. Mol Microbiol 36: 352–365.

34. Ballou ER, Kozubowski L, Nichols CB, Alspaugh JA (2013) Ras1 Acts through Duplicated Cdc42 and Rac Proteins to Regulate Morphogenesis and Pathogenesis in the Human Fungal Pathogen Cryptococcus neoformans. PLoS Genet 9: e1003687. doi:10.1371/journal.pgen.1003687.

35. Ballou ER, Selvig K, Narloch JL, Nichols CB, Alspaugh JA (2013) Two Rac paralogs regulate polarized growth in the human fungal pathogen Cryptococcus neoformans. Fungal Genet Biol 57: 58–75. doi:10.1016/j.fgb.2013.05.006.

36. Vallim MA, Nichols CB, Fernandes L, Cramer KL, Alspaugh JA (2005) A Rac homolog functions downstream of Ras1 to control hyphal differentiation and high-temperature growth in the pathogenic fungus Cryptococcus neoformans. Eukaryot Cell 4: 1066–1078. doi:10.1128/EC.4.6.1066-1078.2005.

37. Ballou ER, Nichols CB, Miglia KJ, Kozubowski L, Alspaugh JA (2010) Two CDC42 paralogues modulate Cryptococcus neoformans thermotolerance and morphogenesis under host physiological conditions. Mol Microbiol 75: 763–780. doi:10.1111/j.1365-2958.2009.07019.x.

38. Chang YC, Penoyer LA (2000) Properties of various Rho1 mutant alleles of Cryptococcus neoformans. J Bacteriol 182: 4987–4991.

39. Lam WC, Gerik KJ, Lodge JK (2013) Role of Cryptococcus neoformans Rho1 GTPases in the PKC1 Signaling Pathway in Response to Thermal Stress. Eukaryot Cell 12: 118–131. doi:10.1128/ec.05305-11.

40. Schafer WR, Rine J (1992) Protein prenylation: genes, enzymes, targets, and

functions. Annu Rev Genet 26: 209–237. doi:10.1146/annurev.ge.26.120192.001233.

41. Basso AD, Kirschmeier P, Bishop WR (2006) Thematic review series: Lipid Posttranslational Modifications. Farnesyl transferase inhibitors. J Lipid Res 47: 15–31. doi:10.1194/jlr.R500012-JLR200.

42. Casey PJ, Seabra MC (1996) Protein prenyltransferases. J Biol Chem 271: 5289–5292.

43. Obara K, Kihara A (2014) Signaling Events of the Rim101 Pathway Occur at the Plasma Membrane in a Ubiquitination-Dependent Manner. Mol Cell Biol 34 : 3525–3534. doi:10.1128/MCB.00408-14.

44. Peñalva MA, Lucena-Agell D, Arst HN (2014) Liaison alcaline: Pals entice non-endosomal ESCRTs to the plasma membrane for pH signaling. Curr Opin Microbiol 22C: 49–59. doi:10.1016/j.mib.2014.09.005.

45. Galindo A, Calcagno-Pizarelli AM, Arst HN, Peñalva MÁ (2012) An ordered pathway for the assembly of fungal ESCRT-containing ambient pH signalling complexes at the plasma membrane. J Cell Sci 125: 1784–1795. doi:10.1242/jcs.098897.

46. Calcagno-Pizarelli AM, Negrete-Urtasun S, Denison SH, Rudnicka JD, Bussink H-J, et al. (2007) Establishment of the ambient pH signaling complex in Aspergillus nidulans: PalI assists plasma membrane localization of PalH. Eukaryot Cell 6: 2365–2375. doi:10.1128/EC.00275-07.

47. Obara K, Yamamoto H, Kihara A (2012) Membrane protein Rim21 plays a central role in sensing ambient pH in Saccharomyces cerevisiae. J Biol Chem 287: 38473–38481. doi:10.1074/jbc.M112.394205.

48. Shenoy SK, Lefkowitz RJ (2011) β-Arrestin-mediated receptor trafficking and signal transduction. Trends Pharmacol Sci 32: 521–533. doi:10.1016/j.tips.2011.05.002.

49. Herranz S, Rodríguez JM, Bussink H-J, Sánchez-Ferrero JC, Arst HN, et al. (2005) Arrestin-related proteins mediate pH signaling in fungi. Proc Natl Acad Sci U S A 102: 12141–12146. doi:10.1073/pnas.0504776102.

50. Herrador A, Herranz S, Lara D, Vincent O (2010) Recruitment of the ESCRT machinery to a putative seven-transmembrane-domain receptor is mediated by an arrestin-related protein. Mol Cell Biol 30: 897–907. doi:10.1128/MCB.00132-09.

51. Hervás-Aguilar A, Galindo A, Peñalva MA (2010) Receptor-independent Ambient pH signaling by ubiquitin attachment to fungal arrestin-like PalF. J Biol Chem 285: 18095–18102. doi:10.1074/jbc.M110.114371.

52. Barwell KJ, Boysen JH, Xu W, Aaron P, Mitchell AP (2005) Relationship of DFG16 to the Rim101p pH Response Pathway in Saccharomyces cerevisiae and Candida albicans Relationship of DFG16 to the Rim101p pH Response Pathway

in Saccharomyces cerevisiae and Candida albicans †. doi:10.1128/EC.4.5.890.

53. Rothfels K, Tanny JC, Molnar EE, Friesen H, Commisso C, et al. (2005) Components of the ESCRT Pathway, DFG16, and YGR122w Are Required for Rim101 To Act as a Corepressor with Nrg1 at the Negative Regulatory Element of the DIT1 Gene of Saccharomyces cerevisiae. Mol Cell Biol 25: 6772–6788. doi:10.1128/mcb.25.15.6772-6788.2005.

54. Henne WM, Buchkovich NJ, Emr SD (2011) The ESCRT pathway. Dev Cell 21: 77–91. doi:10.1016/j.devcel.2011.05.015.

55. Xu W, Smith FJ, Subaran R, Mitchell AP (2004) Multivesicular body-ESCRT components function in pH response regulation in Saccharomyces cerevisiae and Candida albicans. Mol Biol Cell 15: 5528–5537. doi:10.1091/mbc.E04-08-0666.

56. Galindo A, Hervás-Aguilar A, Rodríguez-Galán O, Vincent O, Arst HN, et al. (2007) PalC, one of two Bro1 domain proteins in the fungal pH signalling pathway, localizes to cortical structures and binds Vps32. Traffic 8: 1346–1364. doi:10.1111/j.1600-0854.2007.00620.x.

57. Vincent O, Rainbow L, Tilburn J, Arst HN, Penalva MA (2003) YPXL/I Is a Protein Interaction Motif Recognized by Aspergillus PalA and Its Human Homologue, AIP1/Alix. Mol Cell Biol 23: 1647–1655. doi:10.1128/MCB.23.5.1647-1655.2003.

58. Li W, Mitchell AP (1997) Proteolytic Activation of Rim1p, a Positive Regulator of Yeast Sporulation and Invasive Growth. Genetics 145: 63–73.

59. Lamb TM, Mitchell AP (2003) The Transcription Factor Rim101p Governs Ion Tolerance and Cell Differentiation by Direct Repression of the Regulatory Genes NRG1 and SMP1 in Saccharomyces cerevisiae The Transcription Factor Rim101p Governs Ion Tolerance and Cell Differentiation by Direc. doi:10.1128/MCB.23.2.677.

60. Díez E, Alvaro JJ, Espeso E a, Rainbow L, Suárez T, et al. (2002) Activation of the Aspergillus PacC zinc finger transcription factor requires two proteolytic steps. EMBO J 21: 1350–1359. doi:10.1093/emboj/21.6.1350.

61. Caddick MX, Brownlee AG, Arst HN, Building R (1986) OIG ' G of the growth medium in Aspergillus nidulans. 1: 346–353.

62. Penalva MA, Tilburn J, Bignell E, Arst Jr. HN (2008) Ambient pH gene regulation in fungi: making connections. Trends Microbiol 16: 291–300. doi:S0966-842X(08)00090-5 [pii]10.1016/j.tim.2008.03.006.

63. Lamb TM, Xu W, Diamond A, Mitchell AP (2001) Alkaline Response Genes of Saccharomyces cerevisiaeand Their Relationship to the RIM101 Pathway. J Biol Chem 276: 1850–1856. doi:10.1074/jbc.M008381200.

64. Davis D, Edwards JE, Mitchell AP, Ibrahim AS (2000) Candida albicans RIM101 pH response pathway is required for host-pathogen interactions. Infect Immun 68: 5953–5959. doi:10.1128/IAI.68.10.5953-5959.2000.Updated.

65. Davis D, Wilson RB, Mitchell AP (2000) Pathways Govern pH Responses in Candida albicans RIM101 -Dependent and -Independent Pathways Govern pH Responses in Candida albicans. 20. doi:10.1128/MCB.20.3.971-978.2000.Updated.

66. Davis D (2003) Adaptation to environmental pH in Candida albicans and its relation to pathogenesis. Curr Genet 44: 1–7. doi:10.1007/s00294-003-0415-2.

67. Davis DA (2009) How human pathogenic fungi sense and adapt to pH: the link to virulence. Curr Opin Microbiol 12: 365–370. doi:10.1016/j.mib.2009.05.006.

68. De Bernardis F, Mühlschlegel FA, Cassone A, Fonzi WA (1998) The pH of the host niche controls gene expression in and virulence of Candida albicans. Infect Immun 66: 3317–3325.

69. Li M, Martin SJ, Bruno VM, Davis DA, Mitchell AP (2004) Candida albicans Rim13p, a Protease Required for Rim101p Processing at Acidic and Alkaline pHs. Eukaryot Cell 3: 741–751. doi:10.1128/ec.3.3.741-751.2004.

70. Cornet M, Richard ML, Gaillardin C (2009) The homologue of the Saccharomyces cerevisiae RIM9 gene is required for ambient pH signalling in Candida albicans. Res Microbiol 160: 219–223. doi:10.1016/j.resmic.2009.02.002.

71. Baek Y-U, Li M, Davis DA (2008) Candida albicans Ferric Reductases Are Differentially Regulated in Response to Distinct Forms of Iron Limitation by the Rim101 and CBF Transcription Factors. Eukaryot Cell 7: 1168–1179. doi:10.1128/ec.00108-08.

72. Bensen ES, Martin SJ, Li M, Berman J, Davis DA (2004) Transcriptional profiling in Candida albicans reveals new adaptive responses to extracellular pH and functions for Rim101p. Mol Microbiol 54: 1335–1351. doi:10.1111/j.1365-2958.2004.04350.x.

73. Thewes S, Kretschmar M, Park H, Schaller M, Filler SG, et al. (2007) In vivo and ex vivo comparative transcriptional profiling of invasive and non-invasive Candida albicans isolates identifies genes associated with tissue invasion. Mol Microbiol 63: 1606–1628. doi:10.1111/j.1365-2958.2007.05614.x.

74. Nobile CJ, Solis N, Myers CL, Fay AJ, Deneault J-S, et al. (2008) Candida albicans transcription factor Rim101 mediates pathogenic interactions through cell wall functions. Cell Microbiol 10: 2180–2196. doi:10.1111/j.1462-5822.2008.01198.x.

75. Baek Y-U, Martin SJ, Davis D a (2006) Evidence for novel pH-dependent regulation of Candida albicans Rim101, a direct transcriptional repressor of the cell wall beta-glycosidase Phr2. Eukaryot Cell 5: 1550–1559. doi:10.1128/EC.00088-06.

76. Heitman J (2010) Evolution of eukaryotic microbial pathogens via covert sexual reproduction. Cell Host Microbe 8: 86–99. doi:10.1016/j.chom.2010.06.011.

77. Nyberg K, Johansson U, Johansson A, Camner P (1992) Phagolysosomal pH in alveolar macrophages. Env Heal Perspect 97: 149–152.

78. Cox GM, Harrison TS, McDade HC, Taborda CP, Heinrich G, et al. (2003) Superoxide Dismutase Influences the Virulence of Cryptococcus neoformans by Affecting Growth within Macrophages. Infect Immun 71: 173–180. doi:10.1128/iai.71.1.173-180.2003.

79. Liu OW, Chun CD, Chow ED, Chen C, Madhani HD, et al. (2008) Systematic Genetic Analysis of Virulence in the Human Fungal Pathogen Cryptococcus neoformans. Cell 135: 174–188. doi:10.1016/j.cell.2008.07.046.

80. Hong MP, Vu K, Bautos JM, Tham R, Jamklang M, et al. (2013) Activity of the calcium channel pore Cch1 is dependent on a modulatory region of the subunit Mid1 in Cryptococcus neoformans. Eukaryot Cell 12: 142–150. doi:10.1128/EC.00130-12.

81. O'Meara TR, Norton D, Price MS, Hay C, Clements MF, et al. (2010) Interaction of Cryptococcus neoformans Rim101 and protein kinase A regulates capsule. PLoS Pathog 6: e1000776. doi:10.1371/journal.ppat.1000776.

82. Okagaki LH, Wang Y, Ballou ER, O'Meara TR, Bahn Y-SS, et al. (2011) Cryptococcal Titan Cell Formation Is Regulated by G-Protein Signaling in Response to Multiple Stimuli. Eukaryot Cell 10: 1306–1316. doi:10.1128/EC.05179-11.

83. Chun CD, Madhani HD (2010) Ctr2 Links Copper Homeostasis to Polysaccharide Capsule Formation and Phagocytosis Inhibition in the Human Fungal Pathogen <italic>Cryptococcus neoformans</italic>. PLoS One 5: e12503. doi:10.1371/journal.pone.0012503.

84. Aréchiga-Carvajal ET, Ruiz-Herrera J (2005) The RIM101/pacC Homologue from the Basidiomycete Ustilago maydis Is Functional in Multiple pH-Sensitive Phenomena. Eukaryot Cell 4: 999–1008. doi:10.1128/ec.4.6.999-1008.2005.

85. Antonio C-CJ, Lucila O-C, Miriam T-S, Scott G, José R-H (2010) Functional analysis of the pH responsive pathway Pal/Rim in the phytopathogenic basidiomycete Ustilago maydis. Fungal Genet Biol 47: 446–457. doi:10.1016/j.fgb.2010.02.004.

86. Kullas AL, Martin SJ, Davis D (2007) Adaptation to environmental pH: integrating the Rim101 and calcineurin signal transduction pathways. Mol Microbiol 66: 858–871. doi:10.1111/j.1365-2958.2007.05929.x.

87. Wang H, Liang Y, Zhang B, Zheng W, Xing L, et al. (2011) Alkaline stress triggers an immediate calcium fluctuation in Candida albicans mediated by Rim101p and Crz1p transcription factors. FEMS Yeast Res 11: 430–439. doi:10.1111/j.1567-1364.2011.00730.x.

88. Ariño J (2010) Integrative responses to high pH stress in S. cerevisiae. OMICS 14: 517–523. doi:10.1089/omi.2010.0044.

89. Casado C, González A, Platara M, Ruiz A, Ariño J (2011) The role of the protein kinase A pathway in the response to alkaline pH stress in yeast. Biochem J 438: 523–533. doi:10.1042/BJ20110607.

90. Bahn Y-S, Mühlschlegel FA (2006) CO2 sensing in fungi and beyond. Curr Opin Microbiol 9: 572–578. doi:10.1016/j.mib.2006.09.003.

91. Mogensen EG, Janbon G, Chaloupka J, Steegborn C, Fu MS, et al. (2006) Cryptococcus neoformans Senses CO2 through the Carbonic Anhydrase Can2 and the Adenylyl Cyclase Cac1. Eukaryot Cell 5: 103–111. doi:10.1128/EC.5.1.103-111.2006.

92. Zacchi LF, Gomez-Raja J, Davis DA (2010) Mds3 Regulates Morphogenesis in Candida albicans through the TOR Pathway. Mol Cell Biol 30: 3695–3710. doi:10.1128/mcb.01540-09.

93. Vylkova S, Carman AJ, Danhof HA, Collette JR, Zhou H, et al. (2011) The Fungal Pathogen Candida albicans Autoinduces Hyphal Morphogenesis by Raising Extracellular pH. MBio 2. doi:10.1128/mBio.00055-11.

94. Free SJ (2013) Fungal cell wall organization and biosynthesis. 1st ed. Elsevier Inc. 33-82 p. doi:10.1016/B978-0-12-407677-8.00002-6.

95. Heitman Joseph Kwon-Chung Kyung J, Perfect John R, Casadevall Arturo KTR (2010) Cryptococcus: from human pathogen to model yeast. ASM Press.

96. Lee MJ, Sheppard DC (2016) Recent advances in the understanding of the Aspergillus fumigatus cell wall. J Microbiol 54: 232–242. doi:10.1007/s12275-016-6045-4.

97. Ene I V, Adya AK, Wehmeier S, Brand AC, MacCallum DM, et al. (2012) Host carbon sources modulate cell wall architecture, drug resistance and virulence in a fungal pathogen. Cell Microbiol 14: 1319–1335. doi:10.1111/j.1462-5822.2012.01813.x.

98. Brown GD, Herre J, Williams DL, Willment J a, Marshall ASJ, et al. (2003) Dectin-1 mediates the biological effects of beta-glucans. J Exp Med 197: 1119–1124. doi:10.1084/jem.20021890.

99. Plato A, Hardison SE, Brown GD (2015) Pattern recognition receptors in antifungal immunity. Semin Immunopathol 37: 97–106. doi:10.1007/s00281-014-0462-4.

100. Kottom TJ, Hebrink DM, Jenson PE, Gudmundsson G, Limper AH (2015) Evidence for Proinflammatory β-1,6 Glucans in the Pneumocystis carinii Cell Wall. Infect Immun 83: 2816–2826. doi:10.1128/IAI.00196-15.

101. Bueter CL, Specht CA, Levitz SM (2013) Innate sensing of chitin and chitosan. PLoS Pathog 9: e1003080. doi:10.1371/journal.ppat.1003080.

102. Wagener J, Malireddi RKS, Lenardon MD, Köberle M, Vautier S, et al. (2014) Fungal chitin dampens inflammation through IL-10 induction mediated by NOD2

and TLR9 activation. PLoS Pathog 10: e1004050. doi:10.1371/journal.ppat.1004050.

103. Wiesner DL, Specht CA, Lee CK, Smith KD, Mukaremera L, et al. (2015) Chitin recognition via chitotriosidase promotes pathologic type-2 helper T cell responses to cryptococcal infection. PLoS Pathog 11: e1004701. doi:10.1371/journal.ppat.1004701.

104. Da Silva C a, Hartl D, Liu W, Lee CG, Elias J a (2008) TLR-2 and IL-17A in chitin-induced macrophage activation and acute inflammation. J Immunol 181: 4279–4286.

105. Mora-Montes HM, Netea MG, Ferwerda G, Lenardon MD, Brown GD, et al. (2011) Recognition and blocking of innate immunity cells by Candida albicans chitin. Infect Immun 79: 1961–1970. doi:10.1128/IAI.01282-10.

106. Rappleye C a, Goldman WE (2008) Fungal stealth technology. Trends Immunol 29: 18–24. doi:10.1016/j.it.2007.10.001.

107. Rappleye CA, Eissenberg LG, Goldman WE (2007) Histoplasma capsulatum α-(1,3)-Glucan Blocks Innate Immune Recognition by the β-Glucan Receptor. Proc Natl Acad Sci U S A 104: 1366–1370.

108. Aimanianda V, Bayry J, Bozza S, Kniemeyer O, Perruccio K, et al. (2009) Surface hydrophobin prevents immune recognition of airborne fungal spores. Nature 460: 1117–1121. doi:10.1038/nature08264.

109. Bain JM, Louw J, Lewis LE, Okai B, Walls CA, et al. (2014) Candida albicans hypha formation and mannan masking of β-glucan inhibit macrophage phagosome maturation. MBio 5: e01874. doi:10.1128/mBio.01874-14.

110. Davis SE, Hopke A, Minkin SC, Montedonico AE, Wheeler RT, et al. (2014) Masking of β(1-3)-glucan in the cell wall of Candida albicans from detection by innate immune cells depends on phosphatidylserine. Infect Immun 82: 4405–4413. doi:10.1128/IAI.01612-14.

111. Fleuridor R, Lees A, Pirofski L (2001) A cryptococcal capsular polysaccharide mimotope prolongs the survival of mice with Cryptococcus neoformans infection. J Immunol 166: 1087–1096.

112. Nichols CB, Ferreyra J, Ballou ER, Alspaugh JA (2009) Subcellular localization directs signaling specificity of the Cryptococcus neoformans Ras1 protein. Eukaryot Cell 8: 181–189. doi:10.1128/EC.00351-08.

113. Vallim MA, Fernandes L, Alspaugh JA (2004) The RAM1 gene encoding a protein-farnesyltransferase beta-subunit homologue is essential in Cryptococcus neoformans. Microbiology 150: 1925–1935. doi:10.1099/mic.0.27030-0.

114. O'Meara TR, Xu W, Selvig KM, O'Meara MJ, Mitchell AP, et al. (2014) The Cryptococcus neoformans Rim101 transcription factor directly regulates genes required for adaptation to the host. Mol Cell Biol 34: 673–684.

doi:10.1128/MCB.01359-13.

115. Hu G, Caza M, Cadieux B, Chan V, Liu V, et al. (2013) Cryptococcus neoformans requires the ESCRT protein Vps23 for iron acquisition from heme, for capsule formation, and for virulence. Infect Immun 81: 292–302. doi:10.1128/IAI.01037-12.

116. Hu G, Caza M, Cadieux B, Bakkeren E, Do E, et al. (2015) The ESCRT machinery influences haem uptake and capsule elaboration in Cryptococcus neoformans. Mol Microbiol. doi:10.1111/mmi.12985.

117. O'Meara TR, Holmer SM, Selvig K, Dietrich F, Alspaugh JA (2013) Cryptococcus neoformans Rim101 is associated with cell wall remodeling and evasion of the host immune responses. MBio 4. doi:10.1128/mBio.00522-12.

118. Nguyen UT, Goody RS, Alexandrov K (2010) Understanding and exploiting protein prenyltransferases. Chembiochem 11: 1194–1201. doi:10.1002/cbic.200900727.

119. Reid TS, Terry KL, Casey PJ, Beese LS (2004) Crystallographic analysis of CaaX prenyltransferases complexed with substrates defines rules of protein substrate selectivity. J Mol Biol 343: 417–433. doi:10.1016/j.jmb.2004.08.056.

120. Finegold AA, Johnson DI, Farnsworth CC, Gelb MH, Judd SR, et al. (1991) Protein geranylgeranyltransferase of Saccharomyces cerevisiae is specific for Cys-Xaa-Xaa-Leu motif proteins and requires the CDC43 gene product but not the DPR1 gene product. Proc Natl Acad Sci 88: 4448–4452. doi:10.1073/pnas.88.10.4448.

121. Moores SL, Schaber MD, Mosser SD, Rands E, O'Hara MB, et al. (1991) Sequence dependence of protein isoprenylation. J Biol Chem 266: 14603–14610.

122. Ashby MN, King DS, Rine J (1992) Endoproteolytic processing of a farnesylated peptide in vitro. Proc Natl Acad Sci 89: 4613–4617. doi:10.1073/pnas.89.10.4613.

123. Hrycyna CA, Clarke S (1992) Maturation of isoprenylated proteins in Saccharomyces cerevisiae. Multiple activities catalyze the cleavage of the three carboxyl-terminal amino acids from farnesylated substrates in vitro. J Biol Chem 267: 10457–10464.

124. Ashby MN, Errada PR, Boyartchuk VL, Rine J (1993) Isolation and DNA sequence of the STE14 gene encoding farnesyl cysteine: carboxyl methyltransferase. Yeast 9: 907–913. doi:10.1002/yea.320090810.

125. Boyartchuk VL, Ashby MN, Rine J (1997) Modulation of Ras and a-Factor Function by Carboxyl-Terminal Proteolysis. Science (80-) 275: 1796–1800. doi:10.1126/science.275.5307.1796.

126. Hrycyna CA, Sapperstein SK, Clarke S, Michaelis S (1991) The Saccharomyces-Cerevisiae Ste14 Gene Encodes a Methyltransferase That Mediates C-Terminal Methylation of a-Factor and Ras Proteins. Embo J 10: 1699–1709.

127. Chakrabarti D, Da Silva T, Barger J, Paquette S, Patel H, et al. (2002) Protein

farnesyltransferase and protein prenylation in Plasmodium falciparum. J Biol Chem 277: 42066–42073. doi:10.1074/jbc.M202860200.

128. Eastman RT, Buckner FS, Yokoyama K, Gelb MH, Van Voorhis WC (2006) Thematic review series: lipid posttranslational modifications. Fighting parasitic disease by blocking protein farnesylation. J Lipid Res 47: 233–240. doi:10.1194/jlr.R500016-JLR200.

129. No JH, de Macedo Dossin F, Zhang Y, Liu YL, Zhu W, et al. (2012) Lipophilic analogs of zoledronate and risedronate inhibit Plasmodium geranylgeranyl diphosphate synthase (GGPPS) and exhibit potent antimalarial activity. Proc Natl Acad Sci U S A 109: 4058–4063. doi:10.1073/pnas.1118215109.

130. Song JL, White TC (2003) RAM2: an essential gene in the prenylation pathway of Candida albicans. Microbiology 149: 249–259. doi:10.1099/mic.0.25887-0.

131. Piispanen AE, Bonnefoi O, Carden S, Deveau A, Bassilana M, et al. (2011) Roles of Ras1 Membrane Localization during Candida albicans Hyphal Growth and Farnesol Response. Eukaryot Cell 10: 1473–1484. doi:10.1128/ec.05153-11.

132. Ohya Y, Qadota H, Anraku Y, Pringle JR, Botstein D (1993) Suppression of yeast geranylgeranyl transferase I defect by alternative prenylation of two target GTPases, Rho1p and Cdc42p. Mol Biol Cell 4: 1017–1025.

133. Shen G, Zhou E, Alspaugh JA, Wang P (2012) Wsp1 is downstream of Cin1 and regulates vesicle transport and actin cytoskeleton as an effector of Cdc42 and Rac1 in Cryptococcus neoformans. Eukaryot Cell 11: 471–481. doi:10.1128/EC.00011-12.

134. Sherman F (1991) Getting started with yeast. Methods Enzym 194: 3–41.

135. Murashige T, Skoog F (1962) A Revised Medium for Rapid Growth and Bio Assays with Tobacco Tissue Cultures. Physiol Plant 15: 473–497. doi:10.1111/j.1399-3054.1962.tb08052.x.

136. McDade HC, Cox GM, McDade G. M. HC. C (2001) A new dominant selectable marker for use in Cryptococcus neoformans. Med Mycol 39: 151–154. doi:doi:10.1080/mmy.39.1.151.154.

137. Fraser JA, Subaran RL, Nichols CB, Heitman J (2003) Recapitulation of the Sexual Cycle of the Primary Fungal Pathogen Cryptococcus neoformans var. gattii: Implications for an Outbreak on Vancouver Island, Canada. Eukaryot Cell 2: 1036–1045. doi:10.1128/ec.2.5.1036-1045.2003.

138. Toffaletti DL, Rude TH, Johnston SA, Durack DT, Perfect JR (1993) Gene transfer in Cryptococcus neoformans by use of biolistic delivery of DNA. J Bacteriol 175: 1405–1411.

139. Wormley Jr. FL, Perfect JR (2005) Immunology of infection caused by Cryptococcus neoformans. Methods Mol Med 118: 193–198. doi:10.1385/1-59259-943-5:193.

140. Mukherjee S, Lee S, Mukherjee J, Scharff MD, Casadevall A (1994) Monoclonal antibodies to Cryptococcus neoformans capsular polysaccharide modify the course of intravenous infection in mice. Infect Immun 62: 1079–1088.

141. Casadevall A, Cleare W, Feldmesser M, Glatman-Freedman A, Goldman DL, et al. (1998) Characterization of a Murine Monoclonal Antibody toCryptococcus neoformans Polysaccharide That Is a Candidate for Human Therapeutic Studies. Antimicrob Agents Chemother 42: 1437–1446.

142. Cox GM, Mukherjee J, Cole GT, Casadevall A, Perfect JR (2000) Urease as a Virulence Factor in Experimental Cryptococcosis. Infect Immun 68: 443–448. doi:10.1128/iai.68.2.443-448.2000.

143. Adams AE, Johnson DI, Longnecker RM, Sloat BF, Pringle JR (1990) CDC42 and CDC43, two additional genes involved in budding and the establishment of cell polarity in the yeast Saccharomyces cerevisiae. J Cell Biol 111: 131–142. doi:10.1083/jcb.111.1.131.

144. Diaz M, Sanchez Y, Bennett T, Sun CR, Godoy C, et al. (1993) The Schizosaccharomyces pombe cwg2+ gene codes for the beta subunit of a geranylgeranyltransferase type I required for beta-glucan synthesis. EMBO J 12: 5245–5254.

145. Arellano M, Coll PM, Yang W, Duran A, Tamanoi F, et al. (1998) Characterization of the geranylgeranyl transferase type I from Schizosaccharomyces pombe. Mol Microbiol 29: 1357–1367. doi:10.1046/j.1365-2958.1998.01009.x.

146. Kelly R, Card D, Register E, Mazur P, Kelly T, et al. (2000) Geranylgeranyltransferase I of Candida albicans: Null Mutants or Enzyme Inhibitors Produce Unexpected Phenotypes. J Bacteriol 182: 704–713. doi:10.1128/jb.182.3.704-713.2000.

147. Waugh MS, Nichols CB, DeCesare CM, Cox GM, Heitman J, et al. (2002) Ras1 and Ras2 contribute shared and unique roles in physiology and virulence of Cryptococcus neoformans. Microbiology 148: 191–201.

148. Nichols CB, Perfect ZH, Alspaugh JA (2007) A Ras1-Cdc24 signal transduction pathway mediates thermotolerance in the fungal pathogen Cryptococcus neoformans. Mol Microbiol 63: 1118–1130. doi:10.1111/j.1365-2958.2006.05566.x.

149. Johnston SA, May RC (2013) Cryptococcus interactions with macrophages: evasion and manipulation of the phagosome by a fungal pathogen. Cell Microbiol 15: 403–411. doi:10.1111/cmi.12067.

150. Lane KT, Beese LS (2006) Thematic review series: Lipid Posttranslational Modifications. Structural biology of protein farnesyltransferase and geranylgeranyltransferase type I. J Lipid Res 47: 681–699. doi:10.1194/jlr.R600002-JLR200.

151. Hast MA, Nichols CB, Armstrong SM, Kelly SM, Hellinga HW, et al. (2011)

Structures of Cryptococcus neoformans protein farnesyltransferase reveal strategies for developing inhibitors that target fungal pathogens. J Biol Chem 286: 35149–35162. doi:10.1074/jbc.M111.250506.

152. Ohya Y, Goebl M, Goodman LE, Petersen-Bjørn S, Friesen JD, et al. (1991) Yeast CAL1 is a structural and functional homologue to the DPR1 (RAM) gene involved in ras processing. J Biol Chem 266: 12356–12360.

153. Roberts PJ, Mitin N, Keller PJ, Chenette EJ, Madigan JP, et al. (2008) Rho Family GTPase Modification and Dependence on CAAX Motif-signaled Posttranslational Modification. J Biol Chem 283: 25150–25163. doi:10.1074/jbc.M800882200.

154. Price MS, Nichols CB, Alspaugh JA (2008) The Cryptococcus neoformans Rho-GDP Dissociation Inhibitor Mediates Intracellular Survival and Virulence. Infect Immun 76: 5729–5737. doi:10.1128/iai.00896-08.

155. Hancock JF, Paterson H, Marshall CJ (1990) A polybasic domain or palmitoylation is required in addition to the CAAX motif to localize p21ras to the plasma membrane. Cell 63: 133–139.

156. Hancock JF, Cadwallader K, Paterson H, Marshall CJ (1991) A CAAX or a CAAL motif and a second signal are sufficient for plasma membrane targeting of ras proteins. EMBO J 10: 4033–4039.

157. Banks IR, Specht CA, Donlin MJ, Gerik KJ, Levitz SM, et al. (2005) A chitin synthase and its regulator protein are critical for chitosan production and growth of the fungal pathogen Cryptococcus neoformans. Eukaryot Cell 4: 1902–1912. doi:10.1128/ec.4.11.1902-1912.2005.

158. Bertuzzi M, Schrettl M, Alcazar-Fuoli L, Cairns TC, Muñoz A, et al. (2014) The pH-responsive PacC transcription factor of Aspergillus fumigatus governs epithelial entry and tissue invasion during pulmonary aspergillosis. PLoS Pathog 10: e1004413. doi:10.1371/journal.ppat.1004413.

159. Huang W, Shang Y, Chen P, Gao Q, Wang C (2014) MrpacC regulates sporulation, insect cuticle penetration and immune evasion in Metarhizium robertsii. Environ Microbiol. doi:10.1111/1462-2920.12451.

160. Narayan S, Batta K, Colloby P, Tan CY (2000) Cutaneous cryptococcus infection due to C. albidus associated with Sezary syndrome. Br J Dermatol 143: 632–634.

161. You B-J, Choquer M, Chung K-R (2007) The Colletotrichum acutatum gene encoding a putative pH-responsive transcription regulator is a key virulence determinant during fungal pathogenesis on citrus. Mol Plant Microbe Interact 20: 1149–1160. doi:10.1094/MPMI-20-9-1149.

162. Landraud P, Chuzeville S, Billon-Grande G, Poussereau N, Bruel C (2013) Adaptation to pH and role of PacC in the rice blast fungus Magnaporthe oryzae. PLoS One 8: e69236. doi:10.1371/journal.pone.0069236.

163. Chun CD, Madhani HD (2010) Ctr2 links copper homeostasis to polysaccharide

capsule formation and phagocytosis inhibition in the human fungal pathogen Cryptococcus neoformans. PLoS One 5: e12503. doi:10.1371/journal.pone.0012503.

164. Xu W, Mitchell AP (2001) Yeast PalA / AIP1 / Alix Homolog Rim20p Associates with a PEST-Like Region and Is Required for Its Proteolytic Cleavage Yeast PalA / AIP1 / Alix Homolog Rim20p Associates with a PEST-Like Region and Is Required for Its Proteolytic Cleavage. 183. doi:10.1128/JB.183.23.6917.

165. Díez E, Alvaro J, Espeso E a, Rainbow L, Suárez T, et al. (2002) Activation of the Aspergillus PacC zinc finger transcription factor requires two proteolytic steps. EMBO J 21: 1350–1359. doi:10.1093/emboj/21.6.1350.

166. Kosman DJ (2013) Iron metabolism in aerobes: Managing ferric iron hydrolysis and ferrous iron autoxidation. Coord Chem Rev 257: 210–217. doi:10.1016/j.ccr.2012.06.030.

167. Orejas M, Espeso EA, Tilburn J, Sarkar S, Arst Jr. HN, et al. (1995) Activation of the Aspergillus PacC transcription factor in response to alkaline ambient pH requires proteolysis of the carboxy-terminal moiety. Genes Dev 9: 1622–1632.

168. Kullas AL, Li M, Davis DA (2004) Snf7p, a component of the ESCRT-III protein complex, is an upstream member of the RIM101 pathway in Candida albicans. Eukaryot Cell 3: 1609–1618. doi:10.1128/EC.3.6.1609-1618.2004.

169. Blanchin-Roland S, Da Costa G, Gaillardin C (2005) ESCRT-I components of the endocytic machinery are required for Rim101-dependent ambient pH regulation in the yeast Yarrowia lipolytica. Microbiology 151: 3627–3637. doi:10.1099/mic.0.28196-0.

170. Rodríguez-Galán O, Galindo A, Hervás-Aguilar A, Arst HN, Peñalva MA (2009) Physiological involvement in pH signaling of Vps24-mediated recruitment of Aspergillus PalB cysteine protease to ESCRT-III. J Biol Chem 284: 4404–4412. doi:10.1074/jbc.M808645200.

171. Calcagno-Pizarelli AM, Hervás-Aguilar A, Galindo A, Abenza JF, Peñalva MA, et al. (2011) Rescue of Aspergillus nidulans severely debilitating null mutations in ESCRT-0, I, II and III genes by inactivation of a salt-tolerance pathway allows examination of ESCRT gene roles in pH signalling. J Cell Sci 124: 4064–4076. doi:10.1242/jcs.088344.

172. Godinho RM da C, Crestani J, Kmetzsch LL, Araujo G de S, Frases S, et al. (2014) The vacuolar-sorting protein Snf7 is required for export of virulence determinants in members of the Cryptococcus neoformans complex. Sci Rep 4: 6198. doi:10.1038/srep06198.

173. Jung WH, Saikia S, Hu G, Wang J, Fung CK, et al. (2010) HapX positively and negatively regulates the transcriptional response to iron deprivation in Cryptococcus neoformans. PLoS Pathog 6: e1001209. doi:10.1371/journal.ppat.1001209.

174. Hofmann K, Stoffel W (1993) TMBASE - a database of membrane spanning protein segments. Biol Chem HoppeSeyler 374: 166.

175. Notredame C, Higgins DG, Heringa J (2000) T-Coffee: A novel method for fast and accurate multiple sequence alignment. J Mol Biol 302: 205–217. doi:10.1006/jmbi.2000.4042.

176. Alspaugh JA, Perfect JR, Heitman J (1997) Cryptococcus neoformans mating and virulence are regulated by the G-protein α subunit GPA1 and cAMP. Genes Dev 11: 3206–3217. doi:10.1101/gad.11.23.3206.

177. Hsueh Y-PP, Xue C, Heitman J (2007) G protein signaling governing cell fate decisions involves opposing Galpha subunits in Cryptococcus neoformans. Mol Biol Cell 18: 3237–3249. doi:10.1091/mbc.E07-02-0133.

178. Nishino K, Obara K, Kihara A (2015) The C-terminal Cytosolic Region of Rim21 Senses Alterations in Plasma Membrane Lipid Composition: Insights into Sensing Mechanisms for Plasma Membrane Lipid Asymmetry. J Biol Chem. doi:10.1074/jbc.M115.674382.

179. Ikeda M, Kihara A, Denpoh A, Igarashi Y (2008) The Rim101 Pathway Is Involved in Rsb1 Expression Induced by Altered Lipid Asymmetry. 19: 1922–1931. doi:10.1091/mbc.E07.

180. Chun CD, Madhani HD (2010) Ctr2 links copper homeostasis to polysaccharide capsule formation and phagocytosis inhibition in the human fungal pathogen Cryptococcus neoformans. PLoS One 5. doi:10.1371/journal.pone.0012503.

181. Heath VL, Shaw SL, Roy S, Cyert S, Heath VL, et al. (2004) Hph1p and Hph2p , Novel Components of Calcineurin-Mediated Stress Responses in Saccharomyces cerevisiae Hph1p and Hph2p , Novel Components of Calcineurin-Mediated Stress Responses in Saccharomyces cerevisiae. doi:10.1128/EC.3.3.695.

182. Dechant R, Saad S, Ibáñez AJ, Peter M (2014) Cytosolic pH regulates cell growth through distinct GTPases, Arf1 and Gtr1, to promote Ras/PKA and TORC1 activity. Mol Cell 55: 409–421. doi:10.1016/j.molcel.2014.06.002.

183. Chen Y, Toffaletti DL, Tenor JL (2014) The Cryptococcus neoformans Transcriptome at the Site of Human. doi:10.1128/mBio.01087-13.Editor.

184. Janbon G, Ormerod KL, Paulet D, Byrnes EJ, Yadav V, et al. (2014) Analysis of the Genome and Transcriptome of Cryptococcus neoformans var. grubii Reveals Complex RNA Expression and Microevolution Leading to Virulence Attenuation. PLoS Genet 10: e1004261. doi:10.1371/journal.pgen.1004261.

185. Perfect JR, Lang SD, Durack DT (1980) Chronic cryptococcal meningitis: a new experimental model in rabbits. Am J Pathol 101: 177–194.

186. Nielsen K, Cox GM, Wang P, Toffaletti DL, Perfect JR, et al. (2003) Sexual cycle of Cryptococcus neoformans var. grubii and Virulence of congenic a and α isolates. Infect Immun 71: 4831–4841. doi:10.1128/IAI.71.9.4831-4841.2003.

187. Xue C, Bahn Y-SS, Cox GM, Heitman J (2006) G Protein-coupled Receptor Gpr4 Senses Amino Acids and Activates the cAMP-PKA Pathway in Cryptococcus neoformans. Mol Biol Cell 17: 667–679. doi:10.1091/mbc.E05-07-0699.

188. Kidd SE, Hagen F, Tscharke RL, Huynh M, Bartlett KH, et al. (2004) A rare genotype of Cryptococcus gattii caused the cryptococcosis outbreak on Vancouver Island (British Columbia, Canada). Proc Natl Acad Sci U S A 101: 17258–17263. doi:10.1073/pnas.0402981101.

189. Kim MS, Kim SY, Jung KW, Bahn YS (2012) Targeted gene disruption in Cryptococcus neoformans using double-joint PCR with split dominant selectable markers. Methods Mol Biol 845: 67–84. doi:10.1007/978-1-61779-539-8_5.

190. Idnurm A, Reedy JL, Nussbaum JC, Heitman J (2004) Cryptococcus neoformans virulence gene discovery through insertional mutagenesis. Eukaryot Cell 3: 420–429. doi:10.1128/EC.3.2.420-429.2004.

191. Doering TL (2009) How sweet it is! Cell wall biogenesis and polysaccharide capsule formation in Cryptococcus neoformans. Annu Rev Microbiol 63: 223–247. doi:10.1146/annurev.micro.62.081307.162753.

192. Baker LG, Specht C a, Lodge JK (2011) Cell wall chitosan is necessary for virulence in the opportunistic pathogen Cryptococcus neoformans. Eukaryot Cell 10: 1264–1268. doi:10.1128/EC.05138-11.

193. Feldmesser M, Kress Y, Casadevall A (2001) Dynamic changes in the morphology of Cryptococcus neoformans during murine pulmonary infection. Microbiology 147: 2355–2365.

194. Allen a K, Neuberger a, Sharon N (1973) The purification, composition and specificity of wheat-germ agglutinin. Biochem J 131: 155–162.

195. Roncero C, Valdivieso MH, Ribas JC, Duran A (1988) Isolation and characterization of Saccharomyces cerevisiae mutants resistant to Calcofluor white. J Bacteriol 170: 1950–1954.

196. Esher SK, Granek JA, Alspaugh JA (2015) Rapid mapping of insertional mutations to probe cell wall regulation in Cryptococcus neoformans. Fungal Genet Biol 82: 9–21. doi:10.1016/j.fgb.2015.06.003.

197. Vecchiarelli A, Pericolini E, Gabrielli E, Kenno S, Perito S, et al. (2013) Elucidating the immunological function of the Cryptococcus neoformans capsule. Future Microbiol 8: 1107–1116. doi:10.2217/fmb.13.84.

198. Reese TA, Liang H, Tager AM, Luster AD, Van Rooijen N, et al. (2007) Chitin induces accumulation in tissue of innate immune cells associated with allergy. Nature 447: 92–96. doi:10.1038/nature05746.

199. Strong P, Clark H, Reid K (2002) Intranasal application of chitin microparticles down-regulates symptoms of allergic hypersensitivity to Dermatophagoides pteronyssinus and Aspergillus fumigatus in murine models of allergy. Clin Exp

Allergy 32: 1794–1800. doi:10.1046/j.1365-2222.2002.01551.x.

200. Shibata Y, Foster L a, Bradfield JF, Myrvik QN (2000) Oral administration of chitin down-regulates serum IgE levels and lung eosinophilia in the allergic mouse. J Immunol 164: 1314–1321.

201. Leao CA, Ferreira-Paim K, Andrade-Silva L, Mora DJ, da Silva PR, et al. (2011) Primary cutaneous cryptococcosis caused by Cryptococcus gattii in an immunocompetent host. Med Mycol 49: 352–355. doi:10.3109/13693786.2010.530697.

202. Kim LK, Morita R, Kobayashi Y, Eisenbarth SC, Lee CG, et al. (2015) AMCase is a crucial regulator of type 2 immune responses to inhaled house dust mites. Proc Natl Acad Sci U S A 112: E2891–E2899. doi:10.1073/pnas.1507393112.

203. Bueter CL, Lee CK, Rathinam VAK, Healy GJ, Taron CH, et al. (2011) Chitosan but not chitin activates the inflammasome by a mechanism dependent upon phagocytosis. J Biol Chem 286: 35447–35455. doi:10.1074/jbc.M111.274936.

204. Bueter CL, Lee CK, Wang JP, Ostroff GR, Specht CA, et al. (2014) Spectrum and Mechanisms of Inflammasome Activation by Chitosan. J Immunol 192: 5943–5951. doi:10.4049/jimmunol.1301695.

205. Na H, Cho M, Chung Y (2016) Regulation of Th2 Cell Immunity by Dendritic Cells. Immune Netw 16: 1–12. doi:10.4110/in.2016.16.1.1.

206. Plaine A, Walker L, Da Costa G, Mora-Montes HM, McKinnon A, et al. (2008) Functional analysis of Candida albicans GPI-anchored proteins: roles in cell wall integrity and caspofungin sensitivity. Fungal Genet Biol 45: 1404–1414. doi:10.1016/j.fgb.2008.08.003.

207. Chen M, Xing Y, Lu A, Fang W, Sun B, et al. (2015) Internalized Cryptococcus neoformans Activates the Canonical Caspase-1 and the Noncanonical Caspase-8 Inflammasomes. J Immunol: jimmunol.1500865 – . doi:10.4049/jimmunol.1500865.

208. Johnson CR, Kitz D, Little JR (1983) A method for the derivation and continuous propagation of cloned murine bone marrow macrophages. J Immunol Methods 65: 319–332. doi:10.1016/0022-1759(83)90127-8.

209. Zhai B, Wozniak KL, Masso-Silva J, Upadhyay S, Hole C, et al. (2015) Development of protective inflammation and cell-mediated immunity against Cryptococcus neoformans after exposure to hyphal mutants. MBio 6: e01433–15. doi:10.1128/mBio.01433-15.

210. Krulwich TA, Sachs G, Padan E (2011) Molecular aspects of bacterial pH sensing and homeostasis. Nat Rev Microbiol 9: 330–343. doi:10.1038/nrmicro2549.

211. Ludwig M-G, Vanek M, Guerini D, Gasser JA, Jones CE, et al. (2003) Proton-sensing G-protein-coupled receptors. Nature 425: 93–98. doi:10.1038/nature01905.

212. Bussink H-J, Bignell EM, Múnera-Huertas T, Lucena-Agell D, Scazzocchio C, et al. (2015) Refining the pH response in Aspergillus nidulans: a modulatory triad involving PacX, a novel zinc binuclear cluster protein. Mol Microbiol 98: 1051–1072. doi:10.1111/mmi.13173.

213. Reese AJ, Doering TL (2003) Cell wall alpha-1,3-glucan is required to anchor the Cryptococcus neoformans capsule. Mol Microbiol 50: 1401–1409.

214. Ramos CL, Fonseca FL, Rodrigues J, Guimaraes AJ, Cinelli LP, et al. (2012) Chitin-like molecules associate with Cryptococcus neoformans glucuronoxylomannan to form a glycan complex with previously unknown properties. Eukaryot Cell 11: 1086–1094. doi:10.1128/EC.00001-12.

215. Fonseca FL, Nimrichter L, Cordero RJB, Frases S, Rodrigues J, et al. (2009) Role for chitin and chitooligomers in the capsular architecture of Cryptococcus neoformans. Eukaryot Cell 8: 1543–1553. doi:10.1128/EC.00142-09.

Biography

Kyla Selvig Ost was born in Plentywood Montana on February 11th 1988. She received a BS in Biochemistry from Montana State University. In 2010, she began her graduate work in the Cell and Molecular Biology program at Duke University where she later joined the University Program of Genetics and Genomics and joined the Alspaugh Lab.

In the Alspaugh lab, Kyla was the first author of the publications "The *Cryptococcus neoformans* Alkaline Response Pathway: Identification of a Novel Rim pathway Activator." in PLOS Genetics, "Restricted substrate specificity for the geranylgeranyltransferase-I enzyme in *Cryptococcus neoformans*: implications for virulence." in Eukaryotic Cell, and "pH Response Pathways in Fungi: Adapting to Host-derived and Environmental Signals." in Mycobiology. She has also collaborated on the publications "*Cryptococcus neoformans* Rim101 is required for cell wall remodeling and evasion of the host immune responses" in MBio, "The *Cryptococcus neoformans* Rim101 Transcription Factor Directly Regulates Genes Required for Adaptation to the Host" in Molecular and Cellular Biology, "Impact of protein palmitoylation of the virulence potential of *Cryptococcus neoformans.*" in Eukaryotic Cell, and "Relative contributions of prenylation and post-prenylation processing in *Cryptococcus neoformans* pathogenesis" in mSphere.

Kyla received the MGM Chairman's Travel Award (2014), and the Mycology Meritorious Research Travel Award (2013) to attend conferences. She also received a Poster Award at the 2015 Fungal Genetics Conference.